Revised Draft Environmental Impact Statement/
Environmental Impact Report

Truckee River Operating Agreement

Sedimentation and Erosion Appendix

California and Nevada

August 2004

United States Department of the Interior
Bureau of Reclamation
Fish and Wildlife Service
Bureau of Indian Affairs

State of California
Department of Water Resources

Contents

Page

SEDIMENTATION AND EROSION APPENDIX

This appendix consists of four parts: (1) a summary table of the effects of the alternatives on sedimentation and erosion, (2) discussion of erosion at Lake Tahoe, (3) discussion of stream channel erosion and sediment transport, and (4) discussion of Truckee River delta formation at Pyramid Lake.

I. SUMMARY OF EFFECTS OF ALTERNATIVES ON SEDIMENTATION AND EROSION

Table SED-A.1 summarizes the effects of the alternatives on sedimentation and erosion.

Table SED-A.1—Summary of effects on sedimentation and erosion

Indicator	No Action	LWSA	TROA
Shoreline erosion at Lake Tahoe	No manmade induced degradation of any water quality parameters	Same as No Action	Same as No Action
Stream channel erosion and sediment transport capacity change	Truckee River from Donner Creek to the Little Truckee River confluence: Same as under current conditions. Little Truckee River from Stampede Dam to Boca Reservoir: potentially more erosion but since located downstream from dam little effect is expected Spice and Lockwood reaches. Potential for more deposition exists. Spice does not seem to have large sediment source upstream. Lockwood could see more deposition because Steamboat Creek, a large sediment source is located within this reach	Truckee River from Donner Creek to the Little Truckee River confluence: Same as under current conditions. Little Truckee River from Stampede Dam to Boca Reservoir: Same as No Action Spice and Lockwood reaches: Same as No Action.	Truckee River from Donner Creek to the Little Truckee River confluence: Same as under current conditions. Little Truckee River from Stampede Dam to Boca Reservoir: potentially more deposition but since located downstream from dam little effect is expected Spice and Lockwood reaches: Some deposition could occur in Spice reach, but large sediment source not available upstream. No effect in Lockwood reach.

Table SED-A.1—Summary of effects on sedimentation and erosion

Indicator	No Action	LWSA	TROA
Stream channel erosion and sediment transport capacity change (continued)	Nixon reach: Less erosion and some deposition but no large sediment source located upstream that enters this reach	Nixon reach: Same as No Action.	Nixon reach: No effect
Truckee River delta formation at Pyramid Lake	No effect.	No effect.	No effect.

II. SHORELINE EROSION AT LAKE TAHOE

Lake Tahoe has a surface area of 192 square miles (120,000 acres), and its watershed area is 314 square miles. The lake has an average water depth of 1027 feet, a maximum depth of 1646 feet, and 72 miles of shoreline. The Federal Clean Water Act of 1972 designated Lake Tahoe as an "Outstanding Natural Resource." As such, no man-induced degradation of its water quality is allowed. The California State Water Resources Control Board also adopted Resolution 68-16 that establishes a nondegradation policy for the protection of water quality, where waters are designated as high quality water, including Lake Tahoe (SWRCB, 1994). Lake Tahoe is identified as impaired under the Clean Water Act for nitrogen, phosphorus, and sedimentation/siltation. Total maximum daily load limits are being studied to identify load limits for the lake. It is considered an oligotrophic (low productivity) lake; that is, it still has relatively low concentrations of nitrogen and phosphorus.

The geologic history and setting directly relates to the shorezone of the lake and effects of shorezone erosion. The general geology of the shorezone has a wide range of geologic formations (Adams, 2003). The eastern shorezone is predominantly granite bedrock and is not erodible. The southern zone is composed of glacial outwash deposits and lake deposits. The western shore is composed of glacial moraine material, outwash and lake deposits. The northern shore is composed of Tertiary volcanic rocks and alluvial and lake deposits.

Lake Tahoe shoreline erosion is directly related to the material properties of the shorezone, wave activity, and fluctuating water levels (Adams and Minor, 2002). More specifically, shorezone erosion is typically caused by waves breaking at the bases of easily eroded bluffs when lake level is high. Both the direct impact of waves on the bluffs and the onrush of wave swash up the beach are capable of erosion and sediment transport. When lake level is low, wave energy is expended on the beaches and does not impact long-term shore erosion.

Ken Adams of the Desert Research Institute performed studies of Lake Tahoe including a background review of existing references. In addition he tried to establish some estimate of shoreline erosion by using Geographical Information System analysis of maps to determine the shoreline change based on several aerial photos between 1939 and the present time.

To further study Lake Tahoe, Adams (2003) also estimated shoreline angles at 90 locations to determine the maximum elevation for historical shoreline erosion or potential new erosion. Shoreline angles are either abrupt changes in slope found at the top of the beach or the crest of beach ridges. These locations and elevations are shown in table SED-A.2. Lake Tahoe fluctuates between elevation 6223 and 6229.1 feet. The potential for shoreline erosion would only occur when lake levels are high. To estimate the potential for shoreline erosion, Adams (2003) looked at shoreline angles as compared to a potential range of wave conditions. Adams also set up wave-recording stations at three locations: Incline Village, Meeks Bay and the Thunderbird Lodge. These stations recorded data for more than 1 year, and the recorded data was analyzed according to technical standards.

Until recently, existing quantitative wave information for Lake Tahoe was quite sparse. Orme (1971) reported that waves could reach up to 2 to 3meters, but waves of this height were not observed. Instead, this range in heights was probably derived from maximum fetch distances and theoretical considerations using the wave growth formulae suggested by the U.S. Army Corps of Engineers (CERC, 1984). Engstrom (1978) also used the wave hindcasting procedures outlined in the Shore Protection Manual (CERC, 1984) combined with wind data reported by TRPA for Tahoe City (Agency, 1971) to hindcast waves at Lake Tahoe. Again, because winds specified by both velocity and duration were not available, this meant that the wind data is not as accurate as it could be.

Very little quantitative data exist for winds in the basin and the effects of the wind on shoreline erosion. The Western Regional Climate Center at DRI archived climate data at from the South Lake Tahoe airport from 1992. These data are limited because winds are only measured in the daytime and far from lake. Other data were collected at the South Lake Tahoe airport from 1965 to 1967. These data were limited to only daylight hours. Air Resource Specialists, Inc. (ARS) has been collecting wind data from at least three different sites at Lake Tahoe. These include sites at D.L. Bliss State Park in the southwest part of the basin, Thunderbird Lodge on the northeast shore, and South Lake Tahoe Boulevard at South Shore. Other researchers have tried to tie wind data to wave propagation but this was difficult with limited data and duration of winds.

Adams (2003) suggested that wave energy is the main force behind shoreline erosion. To date, it has not been determined whether large infrequent storms or frequent daily storm events with small waves provide the majority of the shore erosion. For extreme events, Adams (2003) explored the idea of an extreme wind event as defined by the Tahoe Regional Planning Agency (TRPA) Code. This wind was a wind of 80 miles per hour for 1 hour, because of the fetch-limited conditions at Lake Tahoe. Using TRPA's definition of an extreme wind event in comparison to small waves generated on a daily basis, Adams determined the amount of energy associated with the extreme wind event vs. the amount of energy associated with the small waves that occur on a daily basis for a year. His conclusion was that there was greater energy associated with the small frequent waves that occur on a daily basis.

Lake Tahoe is subject to seiches, which are periodic oscillations of a body of water whose period is determined by the resonant characteristics of the basin. Seiches can temporarily raise water levels along a shore. The importance of seiches to shorezone erosion is that they

Table SED-A.2

Lake Tahoe. SL angle = shoreline angle. Normalized height is the height of the feature minus the legal high limit of Lake Tahoe (6229.1 ft). Coordinate system is UTM Zone 10, NAD 27.

	Easting	Northing	Feature	Height of featu	normalized height (ft)
1	749818	4325595	beach ridge	6229.88	1.73
2	749692	4327507	SL angle	6229.72	1.57
3	749729	4327475	SL angle	6229.06	0.91
4	749765	4327442	SL angle	6228.08	-0.07
5	749834	4327167	SL angle	6228.57	0.42
6	749836	4327140	SL angle	6227.75	-0.40
7	749819	4327096	SL angle	6228.40	0.26
8	749821	4327056	SL angle	6227.09	-1.05
9	749815	4326989	SL angle	6227.26	-0.89
10	749810	4326951	SL angle	6227.58	-0.56
11	749809	4326922	SL angle	6229.22	1.08
12	749810	4326874	SL angle	6229.22	1.08
13	749957	4326279	SL angle	6228.73	0.59
14	749981	4326228	SL angle	6228.73	0.59
15	750001	4326195	SL angle	6228.90	0.75
16	750013	4326153	SL angle	6228.73	0.59
17	750034	4326096	SL angle	6229.22	1.08
18	750073	4326030	SL angle	6229.22	1.08
19	750095	4326006	SL angle	6229.22	1.08
20	749926	4325665	SL angle	6228.90	0.75
21	753637	4314771	SL angle	6227.75	-0.39
22	753793	4314630	beach ridge	6230.37	2.24
23	753975	4314530	beach ridge	6229.06	0.92
24	754320	4314359	beach ridge	6230.21	2.07
25	754809	4314188	beach ridge	6229.72	1.58
26	754946	4314156	beach ridge	6229.39	1.25
27	755380	4314218	SL angle	6227.91	-0.22
28	755651	4314171	SL angle	6228.90	0.76
29	755806	4314131	SL angle	6229.22	1.09
30	756148	4314042	SL angle	6229.06	0.92
31	756383	4314003	SL angle	6228.57	0.43
32	759651	4314232	SL angle	6228.73	0.60
33	759996	4314378	SL angle	6227.91	-0.22
34	760363	4314440	beach ridge	6228.73	0.60
35	760578	4314526	beach ridge	6228.57	0.43
36	760687	4314541	beach ridge	6229.39	1.25
37	760902	4314633	SL angle	6226.44	-1.70
38	761200	4314707	SL angle	6227.58	-0.55
39	761833	4314795	SL angle	6228.08	-0.06
40	762209	4314854	SL angle	6228.24	0.10
41	762699	4315017	SL angle	6228.24	0.10
42	762796	4315054	SL angle	6228.08	-0.06
43	764234	4318118	beach ridge	6229.72	1.57
44	764378	4316957	SL angle	6229.06	0.91
45	764010	4315990	SL angle	6228.73	0.59
46	763710	4319290	SL angle	6228.73	0.59
47	745841	4333076	SL angle	6228.76	0.60
48	745431	4331603	SL angle	6228.27	0.11
49	745378	4331073	SL angle	6228.60	0.44
50	745666	4330290	SL angle	6228.44	0.27
51	745920	4329647	SL angle	6229.75	1.59
52	746441	4328952	SL angle	6228.76	0.60
53	746631	4328787	SL angle	6228.76	0.60
54	749259	4327770	SL angle	6228.27	0.11
55	749693	4327516	SL angle	6229.42	1.26
56	746000	4334744	beach ridge	6229.26	1.09
57	746273	4335259	SL angle	6227.94	-0.22
58	746273	4335413	SL angle	6228.11	-0.05
59	746200	4336210	SL angle	6228.93	0.77
60	746656	4336629	SL angle	6228.44	0.27
61	746949	4337495	SL angle	6228.27	0.11
62	747133	4338565	SL angle	6228.27	0.11
63	748166	4340504	SL angle	6228.44	0.27
64	749458	4323365	SL angle	6228.57	0.41
65	749726	4322339	SL angle	6228.90	0.74
66	751248	4320567	SL angle	6227.91	-0.24
67	750243	4321404	SL angle	6228.57	0.41
68	764477	4327693	SL angle	6228.54	0.37
69	764529	4327899	SL angle	6228.21	0.04
70	764574	4328969	SL angle	6228.37	0.21
71	764376	4329197	SL angle	6228.21	0.04
72	764222	4325661	SL angle	6228.54	0.37
73	749161	4340634	SL angle	6227.81	-0.33
74	749436	4340744	SL angle	6228.80	0.65
75	749774	4340910	SL angle	6227.81	-0.33
76	750360	4341034	SL angle	6228.96	0.81
77	750923	4341830	SL angle	6227.98	-0.17
78	751657	4345319	SL angle	6228.47	0.32
79	752272	4345755	beach ridge	6231.09	2.95
80	754565	4347239	SL angle	6228.73	0.57
81	754952	4347210	SL angle	6228.90	0.74
82	756345	4347036	SL angle	6228.57	0.41
83	758514	4345579	SL angle	6229.55	1.39
84	761495	4348327	SL angle	6229.22	1.07
85	764297	4322109	SL angle	6228.70	0.54
86	764262	4322179	SL angle	6228.37	0.21
87	764247	4322214	SL angle	6228.37	0.21
88	764221	4322240	SL angle	6228.37	0.21
89	764205	4322375	SL angle	6228.37	0.21
90	764082	4322615	SL angle	6229.03	0.87

can temporarily raise water level along a shore, allowing waves to travel further inland and increasing shoreline erosion. Budlong (1971) personally observed seiches ranging in amplitude from 0.4 to 0.8 foot. On a moderately sloping beach along the south shore, the lateral distance in wave runup appeared to change by as much as several feet with a seiche of about 0.4 foot (Budlong, 1971).

Adams (2003) describes the studies of Budlong (1971) who studied processes and rates of shore erosion. In this work, rapid erosion occurred immediately west of the Keys East channel because of the effect of a pair of jetties protecting the channel. During a single 10-month period (6/01/69 – 3/31/70), the shoreline retreated up to 52 feet over a distance of about 492 ft. In this case, Budlong surmised that the reason for this extensive retreat was due to the extensive willow clearing activities by Tahoe Keys personnel had contributed to the rapid shoreline retreat.

Orme (1971) describes the natural processes of Lake Tahoe. Orme's work was also the basis of the TRPA shorezone plan that was finalized in 1976. Orme (1972) stated that eroding shorelines comprise 16.3 percent of the Lake Tahoe shoreline. Orme (1971) also described the currents and littoral drift patterns of the lake. Adams (2003) made refinement to Orme description of currents and littoral drift.

Monthly water elevations at Lake Tahoe under current conditions, No Action, LWSA, and TROA are shown in table SED-A.3 for median hydrologic conditions and very wet hydrologic conditions. With the use of this data and the stochastic model formulated by Adams (2003), a determination was made that none of the alternatives had a significant effect on shoreline erosion and did not cause any degradation of long term water quality. This study is explained in the following paragraphs.

Lake Tahoe typically fluctuates between its maximum lake elevation of 1898.65 (6229.1 feet) and its natural rim elevation of about 1896.8 meters (6223 feet) (figure 1), although sometimes the lake drops below its natural rim, as at present (December 2003). It is reasonable to assume that shorezone erosion only occurs when lake level is high.

The question then becomes: At what lake surface elevation does shorezone erosion potentially become significant? To address this question, we use the observations of the elevations of the shoreline angles and compare it to the estimates of different wave heights added on to the water surface elevations projected for different alternatives at median and very wet conditions (table SED-A.3).

Ken Adams (2003) addressed the question of whether TROA or any other alternative would potentially have a greater effect on shorezone erosion and at what elevations would erosion occur. He used the assessment that he performed of shoreline elevation and angles (table SED-A.2), and compared elevations of wave run above the lake water surface elevation observed for the shoreline angle. If the lake elevation plus the maximum wave height was greater than the shoreline angle elevation, then erosion could potentially occur.

Table SED-A.3.—Median hydrologic conditions

Median Conditions												
Current	6226.98	6226.98	6226.96	6227.31	6227.32	6227.37	6227.42	6228.07	6228.55	6228.34	6227.98	6227.57
No Action	6226.99	6226.94	6226.91	6227.21	6227.25	6227.34	6227.40	6228.07	6228.49	6228.30	6227.94	6227.52
Difference	0.01	-0.04	-0.05	-0.10	-0.07	-0.03	-0.02	0.00	-0.06	-0.03	-0.04	-0.05
Current	6226.98	6226.98	6226.96	6227.31	6227.32	6227.37	6227.42	6228.07	6228.55	6228.34	6227.98	6227.57
LWSA	6226.98	6226.94	6226.91	6227.21	6227.25	6227.33	6227.40	6228.07	6228.48	6228.30	6227.94	6227.52
Difference	0.00	-0.04	-0.05	-0.10	-0.07	-0.04	-0.02	0.00	-0.07	-0.03	-0.04	-0.05
Current	6226.98	6226.98	6226.96	6227.31	6227.32	6227.37	6227.42	6228.07	6228.55	6228.34	6227.98	6227.57
TROA	6227.16	6227.15	6227.12	6227.31	6227.39	6227.41	6227.52	6228.11	6228.52	6228.33	6227.96	6227.61
Difference	0.18	0.17	0.16	0.00	0.07	0.04	0.11	0.04	-0.02	-0.01	-0.02	0.04
No Action	6226.99	6226.94	6226.91	6227.21	6227.25	6227.34	6227.40	6228.07	6228.49	6228.30	6227.94	6227.52
LWSA	6226.98	6226.94	6226.91	6227.21	6227.25	6227.33	6227.40	6228.07	6228.48	6228.30	6227.94	6227.52
Difference	0.01	0.00	0.00	0.00	0.00	0.01	0.00	0.00	0.01	0.00	0.00	0.00
No Action	6226.99	6226.94	6226.91	6227.21	6227.25	6227.34	6227.40	6228.07	6228.49	6228.30	6227.94	6227.52
TROA	6227.16	6227.15	6227.12	6227.31	6227.39	6227.41	6227.52	6228.11	6228.52	6228.33	6227.96	6227.61
Difference	0.17	0.21	0.21	0.10	0.14	0.07	0.12	0.04	0.03	0.03	0.02	0.09
Very wet conditions												
Current	6228.40	6228.22	6228.30	6228.41	6228.49	6228.65	6228.75	6229.00	6229.00	6229.00	6228.78	6228.50
No Action	6228.37	6228.30	6228.34	6228.44	6228.49	6228.65	6228.75	6229.00	6229.00	6229.00	6228.79	6228.51
Difference	-0.03	0.09	0.04	0.03	0.00	0.00	0.00	0.00	0.00	0.00	0.01	0.01
Current	6228.40	6228.22	6228.30	6228.41	6228.49	6228.65	6228.75	6229.00	6229.00	6229.00	6228.78	6228.50
LWSA	6228.37	6228.30	6228.34	6228.44	6228.49	6228.65	6228.75	6229.00	6229.00	6229.00	6228.79	6228.51
Difference	-0.03	0.09	0.04	0.03	0.00	0.00	0.00	0.00	0.00	0.00	0.01	0.01
Current	6228.40	6228.22	6228.30	6228.41	6228.49	6228.65	6228.75	6229.00	6229.00	6229.00	6228.78	6228.50
TROA	6228.36	6228.28	6228.34	6228.45	6228.51	6228.69	6228.75	6229.00	6229.00	6229.00	6228.77	6228.50
Difference	-0.04	0.06	0.04	0.04	0.02	0.04	0.00	0.00	0.00	0.00	-0.01	0.00
No Action	6228.37	6228.30	6228.34	6228.44	6228.49	6228.65	6228.75	6229.00	6229.00	6229.00	6228.79	6228.51
LWSA	6228.37	6228.30	6228.34	6228.44	6228.49	6228.65	6228.75	6229.00	6229.00	6229.00	6228.79	6228.51
Difference	0.00	0.00	0.00	0.00	0.00	0.00	0.00	0.00	0.00	0.00	0.00	0.00
No Action	6228.37	6228.30	6228.34	6228.44	6228.49	6228.65	6228.75	6229.00	6229.00	6229.00	6228.79	6228.51
TROA	6228.36	6228.28	6228.34	6228.45	6228.51	6228.69	6228.75	6229.00	6229.00	6229.00	6228.77	6228.50
Difference	-0.01	-0.02	0.00	0.01	0.02	0.04	0.00	0.00	0.00	0.00	-0.02	-0.01

Ken Adams (2003) compared the predicted water levels from the operations model to this shoreline angle elevation plus maximum wave runup. He considered three potential wave heights that he determined from the wave data he has analyzed: 1.45, 3.3 and 4.9 feet with periods ranging from 3 to 5 seconds. He also determined that 6227 feet would be the cutoff elevation below which no shoreline erosion would likely occur. He determined this by comparing the small, medium and large waves and the shoreline angle elevations. With the waves of 4.9 feet with a period of 5 seconds, approximately 4 of the 90 sites he identified were affected. Therefore, 6227.0 feet was considered as the cutoff elevation.

Adams (2003) also made some other assumptions to determine the effects of TROA. He assumed that the lake would never exceed the maximum water elevation, which is set at 6229.1 feet. Also, the natural rim of the lake is at elevation 6223 feet, so waves have only been acting on the shoreline elevation of 6229 feet for a portion of the last 120 years. Therefore, TROA or any other water management alternative would not affect the maximum water elevation of the lake, and, thus, should have no impact on the total long term erosion of the lake. In his analysis as well as the analysis that was used for the revised DEIS/EIR, comparisons were made between model runs as follows: current conditions vs. No Action,

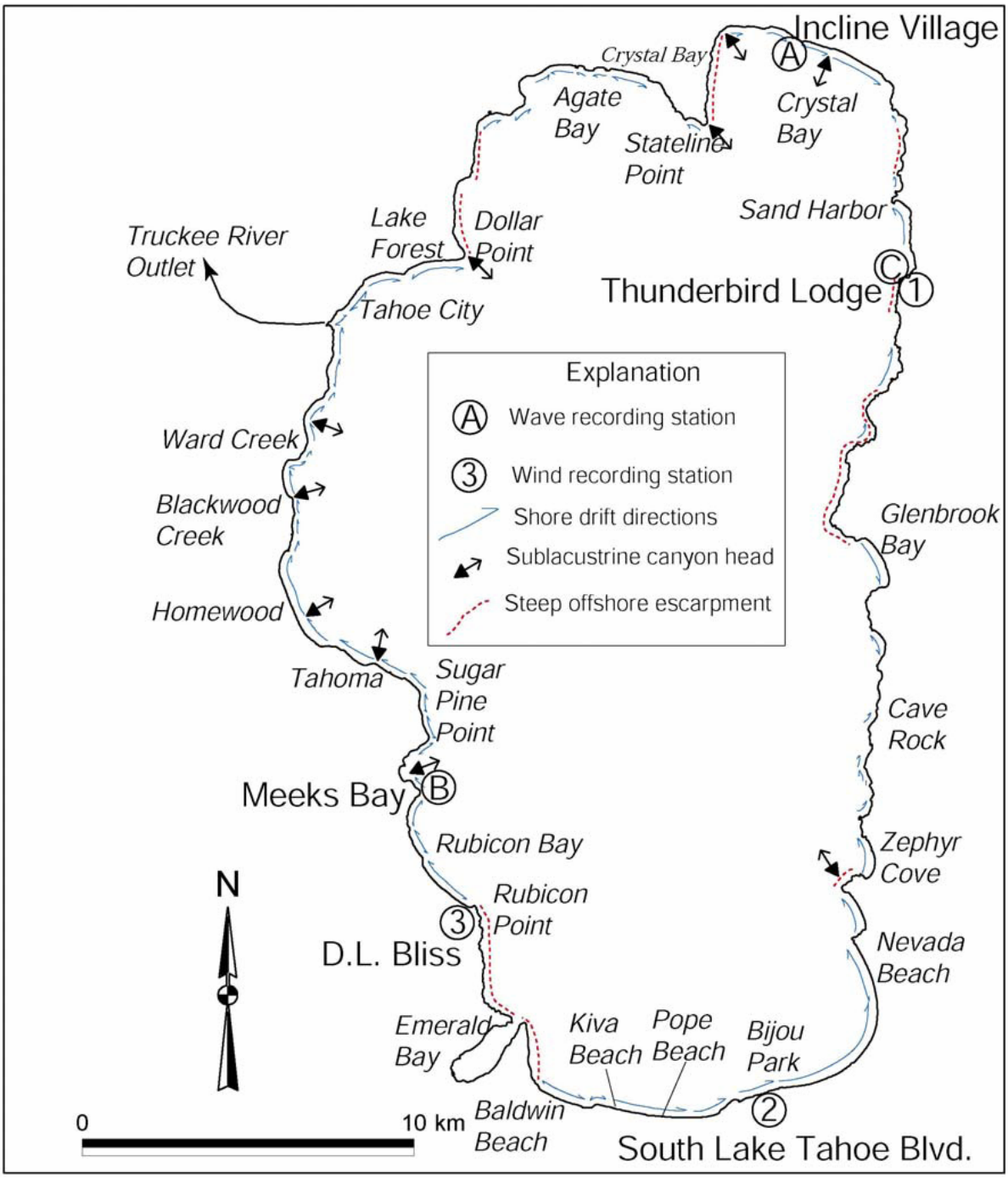
Incline Village
Crystal Bay
A
Agate Bay
Crystal Bay
Stateline Point
Sand Harbor
Truckee River Outlet
Lake Forest
Dollar Point
Thunderbird Lodge
C
1
Tahoe City
Explanation
Wave recording station
Wind recording station
Shore drift directions
Sublacustrine canyon head
Steep offshore escarpment
Ward Creek
Blackwood Creek
Glenbrook Bay
Homewood
Tahoma
Sugar Pine Point
Cave Rock
Meeks Bay
B
Rubicon Bay
Zephyr Cove
N
Rubicon Point
3
D.L. Bliss
Nevada Beach
Emerald Bay
Kiva Beach
Pope Beach
Bijou Park
0
10 km
Baldwin Beach
2
South Lake Tahoe Blvd.

Figure 1

current conditions vs. LWSA, current conditions vs. TROA, No Action vs. LWSA, and No Action vs. TROA. These comparisons were made for two frequencies: the 5 percent exceedence monthly elevations and the median or 50 percent exceedence monthly elevations.

In assessing the difference in monthly elevations between the alternatives, Ken Adams assessed the likelihood of TROA versus the other alternatives having a greater effect on shoreline erosion. In instances where the difference was negative or zero, there would be no difference in shore erosion. In comparing current conditions to No Action and current conditions to LWSA, and No Action to LWSA, either very little positive difference or no difference in water surface elevations was noted. This indicates no potential differences in erosion for either the median or very wet hydrologic conditions. However, in comparing current conditions to No Action in very wet hydrologic conditions, No Action was greater than current conditions for two different months for a range in elevations that were 0.04 to 0.09 foot. In comparing TROA to No Action and current conditions, the water surface elevations for TROA were greater in many months, and ranged from a low value of .02 foot to a maximum of .021 foot.

Adams (2003) evaluated whether or not the magnitude of lake-level change between TROA and the other alternatives would affect shorezone erosion by using the observed values of the elevations of the shoreline angles, the wave runup and a statistical method to check for significance. The basic stochastic model evaluated the probability of the shoreline angles being reached by different size waves, which included 90 shoreline locations (table SED-A.2). Given two different lake levels, for two different alternatives, an estimate would be completed of the difference in the number of shoreline angles that would be reached for the two different lake levels.

The basic procedure was to evaluate the probability of the shoreline angles being reached by runup from different sizes of waves under several lake-level scenarios. Given a lake level, Adams estimated the proportion of the 90 shoreline segments where the waves reach the shoreline angle. Further, given two lake levels from two different management options and wave parameters, Adams (2003) estimated the difference in the proportion of segments for which the waves reach the shoreline angle for each of the lake levels. Using stochastic techniques, Adams tests how many beach segments were affected by a given lake level plus an assumed wave height and then statistical techniques were used to determine if the results were significant.

The results of the stochastic analysis by Adams (2003) are as follows. For the 5 percent exceedence conditions or very wet hydrologic conditions, there were no significant differences in the proportions of (potentially) eroded shoreline segments for any lake levels and wave characteristics. For the 50 percent exceedence values or median hydrologic conditions with moderate –sized waves, (H=1.5 ft. and `5 sec.), one lake level comparison yielded a significant difference in the proportions of impacted shoreline angles under two lake level scenarios. Lake levels during the month of June under the No Action vs. TROA comparison would be increased from 6228.56 to 6228.59 feet, a difference of 0.03 foot. The sample proportion of not impacted shoreline angles under the No Action lake level (LL1) is 0.7444, but under TROA (LL2) the sample proportion is 0.7 (Adams, 2003). The observed difference of 0.0444 has a p-value of 0.03 and is therefore significant. For the largest waves

(H = 7 ft, t= 5 sec), three of the lake level comparisons yielded significant differences in the proportions of impacted shoreline angles under the two lake-level scenarios. These data are summarized in the following table (Adams, 2003).

Comparisons yielding significant differences in proportions of impacted shoreline angles under two lake levels (from Adams, 2003)

Comparison	Month	LL1	LL2	Lake-level difference	Proportion not impacted for LL1	Proportion not impacted for LL2	Difference	P-value
Current conditions vs. TROA	Oct.	6227.11	6227.23	0.012	0.9556	0.9111	0.0444	0.0455
No Action vs. TROA	Oct.	6227.07	6227.23	0.016	0.9556	0.9111	0.0444	0.0455
No Action vs. TROA	Feb.	6227.32	6227.47	0.015	0.9000	0.8444	0.0556	0.0253

For the 5 percent exceedence values (wet hydrologic conditions), there is no significant increase in erosion potential for any of the lake-level scenario comparisons (Adams, 2003). This means that when lake-levels are at their highest, implementing TROA would not affect shorezone erosion at Lake Tahoe.

For the 50 percent exceedence values (median hydrologic conditions), there are three discrete lake-level comparisons that produce significant differences in proportions of impacted shoreline angles under the two lake level scenarios (Adams, 2003). In each case, TROA levels would be higher by about 1.6 to 2 inches. Under TROA, approximately 84 to 91 percent of the measured shoreline angles and beach ridges would not be impacted in these comparisons. Under current conditions or No Action lake levels, from 90 to 96 percent of the sites would not be impacted. There is certainly a statistical difference in the number of sites impacted under the three comparisons. However, what effect it would have on shore zone erosion potential is not entirely clear, but is suspected to be minimal. Adams (2003), therefore, concludes that implementing TROA would have minor effects to the shorezone erosion at Lake Tahoe.

Effects on shoreline erosion at Lake Tahoe under No Action, LWSA, or TROA would cause no manmade degradation of its water quality. Effects would not meet the threshold of significance under any of the alternatives. No increased shoreline erosion is expected, and the maximum water surface elevation that the lake is currently operated at would not be exceeded.

III. STREAM CHANNEL EROSION AND SEDIMENT TRANSPORT

Comparisons are made between all of the alternatives for both median hydrologic conditions and very wet hydrologic conditions on a monthly basis. For stream channel erosion and

sediment transport, an effect was considered significant if it would cause widespread and measurable channel erosion or deposition. Based on professional judgment, widespread and measurable channel erosion is expected to occur when sediment transport capacity change is more than 10 percent greater than under current conditions on an annual basis, and the streambed is not already armored. Widespread and measurable channel deposition is expected when sediment transport capacity change is more than 10 percent less than under current conditions on an annual basis and there is a substantial upstream source of river or tributary sediment. For example, a channel downstream from a dam would not have an upstream source of sediment and the bed material sediments would be armored (not erodible). A decrease in sediment transport capacity change for a river downstream from a dam would not result in deposition without a large source of tributary sediment.

A. Erosion on Truckee River: Donner Creek to Little Truckee River Confluence

Monthly streamflows and changes in sediment transport capacity for the Truckee River downstream from Donner Creek to Little Truckee River confluence are summarized in Table SED-A.4. For current conditions vs. TROA, sediment transport capacity change is exceeded in the months of June-August in median hydrologic conditions. Also, for No Action vs. TROA, sediment transport capacity change exceeds the threshold change for the months of May-July. In very wet hydrologic conditions, sediment capacity change is exceeded for current conditions vs. No Action in October and for No Action vs. TROA in May. The estimated sediment capacity change does not meet the threshold of significance for any of the alternatives as compared to current conditions on an annual basis. Little change is sediment transport capacity on an annual basis is expected.

Table SED-A.4.—Monthly flows and change in sediment transport capacity on the Truckee River between Donner Creek and the Little Truckee River in **median** hydrologic conditions

Month	Current conditions (cfs)	No Action (cfs)	Range in sediment transport capacity change (percent)	
October	260	270	8	12
November	193	194	1	2
December	274	270	-3	-4
January	285	286	1	1
February	254	256	2	2
March	331	324	-4	-6
April	623	602	-7	-10
May	778	762	-4	-6
June	518	517	0	-1
July	173	174	1	2
August	110	112	4	6
September	223	226	3	4
Weighted average			-3	-5

Table SED-A.4.—Monthly flows and change in sediment transport capacity on the Truckee River between Donner Creek and the Little Truckee River in **median** hydrologic conditions (continued)

Month	Current conditions (cfs)	TROA (cfs)	Range in sediment transport capacity change (percent)	
October	260	202	-40	-53
November	193	165	-27	-38
December	274	220	-36	-48
January	285	236	-31	-43
February	254	240	-11	-16
March	331	307	-14	-20
April	623	621	-1	-1
May	778	805	7	11
June	518	551	13	20
July	173	218	59	100
August	110	116	11	17
September	223	137	-62	-77
Weighted average			-3	3

Month	Current conditions (cfs)	LWSA (cfs)	Range in sediment transport capacity change (percent)	
October	260	271	9	13
November	193	194	1	2
December	274	270	-3	-4
January	285	286	1	1
February	254	255	1	1
March	331	324	-4	-6
April	623	603	-6	-9
May	778	763	-4	-6
June	518	516	-1	-1
July	173	174	1	2
August	110	112	4	6
September	223	228	5	7
Weighted Average			-3	-5

Table SED-A.4.—Monthly flows and change in sediment transport capacity on the Truckee River between Donner Creek and the Little Truckee River in **median** hydrologic conditions (continued)

Month	No Action (cfs)	TROA (cfs)	Range in sediment transport capacity change (percent)	
October	270	202	-44	-58
November	194	165	-28	-38
December	270	220	-34	-46
January	286	236	-32	-44
February	256	240	-12	-18
March	324	307	-10	-15
April	602	621	6	10
May	762	805	12	18
June	517	551	14	21
July	174	218	57	97
August	112	116	7	11
September	226	137	-63	-78
Weighted average			0	9

Month	No Action (cfs)	LWSA (cfs)	Range in sediment transport capacity change (percent)	
October	270	271	1	1
November	194	194	0	0
December	270	270	0	0
January	286	286	0	0
February	256	255	-1	-1
March	324	324	0	0
April	602	603	0	0
May	762	763	0	0
June	517	516	0	-1
July	174	174	0	0
August	112	112	0	0
September	226	228	2	3
Weighted average			0	0

Table SED-A.4.—Monthly flows and change in sediment transport capacity on the Truckee River between Donner Creek and the Little Truckee River in **very wet** hydrologic conditions

Month	Current conditions (cfs)	No Action (cfs)	Range in sediment transport capacity change (percent)	
October	349	367	11	16
November	474	455	-8	-12
December	1087	1077	-2	-3
January	1342	1329	-2	-3
February	1723	1716	-1	-1
March	1779	1747	-4	-5
April	2193	2187	-1	-1
May	2148	2111	-3	-5
June	1572	1571	0	0
July	1122	1119	-1	-1
August	463	463	0	0
September	481	475	-2	-4
Weighted average			-2	-3

Month	Current conditions (cfs)	TROA (cfs)	Range in sediment transport capacity change (percent)	
October	349	325	-13	-19
November	474	434	-16	-23
December	1087	1091	1	1
January	1342	1373	5	7
February	1723	1723	0	0
March	1779	1800	2	4
April	2193	2188	0	-1
May	2148	2243	9	14
June	1572	1623	7	10
July	1122	1080	-7	-11
August	463	402	-25	-35
September	481	352	-46	-61
Weighted average			2	4

Table SED-A.4.—Monthly flows and change in sediment transport capacity on the Truckee River between Donner Creek and the Little Truckee River in **very wet** hydrologic conditions (continued)

Month	Current conditions (cfs)	LWSA (cfs)	Range in sediment transport capacity change (percent)	
October	349	367	11	16
November	474	455	-8	-12
December	1087	1077	-2	-3
January	1342	1328	-2	-3
February	1723	1716	-1	-1
March	1779	1739	-4	-7
April	2193	2188	0	-1
May	2148	2111	-3	-5
June	1572	1571	0	0
July	1122	1119	-1	-1
August	463	463	0	0
September	481	476	-2	-3
Weighted average			-2	-3

Month	No Action (cfs)	TROA (cfs)	Range in sediment transport capacity change (percent)	
October	367	325	-22	-31
November	455	434	-9	-13
December	1077	1091	3	4
January	1329	1373	7	10
February	1716	1723	1	1
March	1747	1800	6	9
April	2187	2188	0	0
May	2111	2243	13	20
June	1571	1623	7	10
July	1119	1080	-7	-10
August	463	402	-25	-35
September	475	352	-45	-59
Weighted average			4	7

Table SED-A.4.—Monthly flows and change in sediment transport capacity on the Truckee River between Donner Creek and the Little Truckee River in **very wet** hydrologic conditions (continued)

Month	No Action (cfs)	LWSA (cfs)	Range in sediment transport capacity change (percent)	
October	367	367	0	0
November	455	455	0	0
December	1077	1077	0	0
January	1328	1329	0	0
February	1716	1716	0	0
March	1739	1747	1	1
April	2188	2187	0	0
May	2111	2111	0	0
June	1571	1571	0	0
July	1119	1119	0	0
August	463	463	0	0
September	476	475	0	-1

B. Erosion on Little Truckee River: Stampede Dam to Boca Reservoir

Comparisons are made between all of the alternatives for both median hydrologic conditions and very wet hydrologic conditions on a monthly basis for the Little Truckee River: Stampede Dam to Boca Reservoir in table SED-A.5. For current conditions vs. No Action, sediment transport capacity change is greater than 10 percent in the months of December and May in median hydrologic conditions. Also for current conditions vs. TROA, sediment transport capacity change is greater than current conditions in October. For No Action vs. TROA, sediment transport capacity change is greater in August, September, and October. In very wet hydrologic conditions, sediment capacity change is greater for current conditions vs. No Action in October and December and for current conditions vs. TROA in October, December, August, and September. For No Action vs. TROA, sediment transport capacity change is greater in February, April, August, and September. Annual sediment capacity change is more than 10 percent greater under No Action and LWSA; thus, more erosion and sediment transport likely could occur in this reach, but because this reach is located downstream from a dam and the river is armored, very little change in sediment transport is expected. Annual sediment capacity change is only 11 percent greater under TROA than under current conditions in very wet hydrologic conditions, and annual sediment transport capacity change is much less in median hydrologic conditions; therefore, erosion and sediment transport in this reach under TROA would be about the same as under current conditions. This reach is downstream from Stampede Reservoir, and as such, is probably armored, and no significant erosion or sediment transport is expected.

Table SED-A.5.—Monthly flows and change in sediment transport capacity on the Little Truckee River between Stampede Dam and Boca Reservoir in **median** hydrologic conditions

Month	Current conditions (cfs)	No Action (cfs)	Range in sediment transport capacity change (percent)	
October	94	100	13	20
November	46	47	4	7
December	51	56	21	32
January	65	64	-3	-5
February	90	94	9	14
March	161	159	-2	-4
April	284	292	6	9
May	330	358	18	28
June	264	265	1	1
July	144	138	-8	-12
August	94	75	-36	-49
September	42	30	-49	-64
Weighted average			6	13

Month	Current conditions (cfs)	TROA (cfs)	Range in sediment transport capacity change (percent)	
October	94	177	255	568
November	46	45	-4	-6
December	51	46	-19	-27
January	65	46	-50	-65
February	90	72	-36	-49
March	161	142	-22	-31
April	284	233	-33	-45
May	330	314	-9	-14
June	264	225	-27	-38
July	144	122	-28	-39
August	94	85	-18	-26
September	42	57	84	150
Weighted average			-15	-24

Table SED-A.5.—Monthly flows and change in sediment transport capacity on the Little Truckee River between Stampede Dam and Boca Reservoir in **median** hydrologic conditions (continued)

Month	Current conditions (cfs)	LWSA (cfs)	Range in sediment transport capacity change (percent)	
October	94	100	13	20
November	46	48	9	14
December	51	56	21	32
January	65	64	-3	-5
February	90	94	9	14
March	161	159	-2	-4
April	284	293	6	10
May	330	359	18	29
June	264	265	1	1
July	144	138	-8	-12
August	94	74	-38	-51
September	42	30	-49	-64
Weighted average			6	14

Month	No Action (cfs)	TROA (cfs)	Range in sediment transport capacity change (percent)	
October	100	177	213	455
November	47	45	-8	-12
December	56	46	-33	-45
January	64	46	-48	-63
February	94	72	-41	-55
March	159	142	-20	-29
April	292	233	-36	-49
May	358	314	-23	-33
June	265	225	-28	-39
July	138	122	-22	-31
August	75	85	28	46
September	30	57	261	586
Weighted average			-20	-33

Table SED-A.5.—Monthly flows and change in sediment transport capacity on the Little Truckee River between Stampede Dam and Boca Reservoir in **median** hydrologic conditions (continued)

Month	Current conditions (cfs)	LWSA (cfs)	Range in sediment transport capacity change (percent)	
October	100	100	0	0
November	47	48	4	7
December	56	56	0	0
January	64	64	0	0
February	94	94	0	0
March	159	159	0	0
April	292	293	1	1
May	358	359	1	1
June	265	265	0	0
July	138	138	0	0
August	75	74	-3	-4
September	30	30	0	0
Weighted average			0	1

Table SED-A.5.—Monthly flows and change in sediment transport capacity on the Little Truckee River between Stampede Dam and Boca Reservoir in **very wet** hydrologic conditions

Month	Current conditions (cfs)	No Action (cfs)	Range in sediment transport capacity change (percent)	
October	328	373	29	47
November	151	151	0	0
December	173	182	11	16
January	201	201	0	0
February	212	212	0	0
March	413	428	7	11
April	669	689	6	9
May	1115	1109	-1	-2
June	643	644	0	0
July	304	286	-11	-17
August	187	172	-15	-22
September	107	89	-31	-42
Weighted average			2	1

Table SED-A.5.—Monthly flows and change in sediment transport capacity on the Little Truckee River between Stampede Dam and Boca Reservoir in **very wet** hydrologic conditions (continued)

Month	Current conditions (cfs)	TROA (cfs)	Range in sediment transport capacity change (percent)	
October	328	388	40	66
November	151	155	5	8
December	173	197	30	48
January	201	199	-2	-3
February	212	233	21	33
March	413	442	15	23
April	669	778	35	57
May	1115	1145	5	8
June	643	565	-23	-32
July	304	227	-44	-58
August	187	199	13	21
September	107	221	327	781
Weighted average			8	11

Month	Current conditions (cfs)	LWSA (cfs)	Range in sediment transport capacity change (percent)	
October	328	373	29	47
November	151	151	0	0
December	173	184	13	20
January	201	201	0	0
February	212	212	0	0
March	413	428	7	11
April	669	689	6	9
May	1115	1104	-2	-3
June	643	645	1	1
July	304	286	-11	-17
August	187	171	-16	-24
September	107	89	-31	-42
Weighted average			1	0

Table SED-A.5.—Monthly flows and change in sediment transport capacity on the Little Truckee River between Stampede Dam and Boca Reservoir in **very wet** hydrologic conditions (continued)

Month	No Action (cfs)	TROA (cfs)	Range in sediment transport capacity change (percent)	
October	373	388	8	13
November	151	155	5	8
December	182	197	17	27
January	201	199	-2	-3
February	212	233	21	33
March	428	442	7	10
April	689	778	28	44
May	1109	1145	7	10
June	644	565	-23	-32
July	286	227	-37	-50
August	172	199	34	55
September	89	221	517	1431
Weighted average			7	10

Month	No Action (cfs)	LWSA (cfs)	Range in sediment transport capacity change (percent)	
October	373	373	0	0
November	151	151	0	0
December	182	184	2	3
January	201	201	0	0
February	212	212	0	0
March	428	428	0	0
April	689	689	0	0
May	1109	1104	-1	-1
June	644	645	0	0
July	286	286	0	0
August	172	171	-1	-2
September	89	89	0	0
Weighted average			0	-1

C. Erosion on Truckee River Reno-Sparks to McCarran Blvd (Spice)

Comparisons are made between all of the alternatives for both median hydrologic conditions and very wet hydrologic conditions on a monthly basis for Truckee River from Reno-Sparks to McCarran Boulevard in table SED-A.6. For current conditions vs. No Action, sediment transport capacity change is greater than 10 percent in October in median hydrologic conditions. Also for current conditions vs. TROA, sediment transport capacity change does not exceed the threshold change in median hydrologic conditions. For No Action vs. TROA, sediment transport capacity change exceeds the threshold change in April, May, June, and August. In very wet hydrologic conditions, sediment capacity change is exceeded for current conditions vs. No Action in October, and for current conditions vs. TROA in October and September. For No Action vs. TROA sediment transport capacity exceeds the threshold change in February, April, August, and September. For the cases in which the sediment capacity change of TROA exceeds No Action or current conditions, the environmental effect may not be as great as predicted.

More sediment deposition could occur in this reach under No Action and LWSA than under current conditions, but because a source of sediment likely does not exist upstream, significant deposition also is not likely. Less erosion and sediment transport likely would occur in this reach under TROA than under current conditions in this reach.

Table SED-A.6.—Monthly flows and change in sediment transport capacity on the Truckee River from Reno-Sparks to McCarran Blvd Reno in **median** hydrologic conditions

Month	Current conditions (cfs)	No Action (cfs)	Range in sediment transport capacity change (percent)	
October	372	394	12	19
November	397	328	-32	-44
December	400	322	-35	-48
January	401	330	-32	-44
February	445	372	-30	-42
March	550	483	-23	-32
April	790	696	-22	-32
May	1062	980	-15	-21
June	774	726	-12	-17
July	347	325	-12	-18
August	304	282	-14	-20
September	275	280	4	6
Weighted average			-18	-25

Table SED-A.6.—Monthly flows and change in sediment transport capacity on the Truckee River from Reno-Sparks to McCarran Blvd Reno in **median** hydrologic conditions (continued)

Month	Current conditions (cfs)	TROA (cfs)	Range in sediment transport capacity change (percent)	
October	372	386	8	12
November	397	222	-69	-83
December	400	278	-52	-66
January	401	297	-45	-59
February	445	366	-32	-44
March	550	488	-21	-30
April	790	776	-4	-5
May	1062	1062	0	0
June	774	780	2	2
July	347	340	-4	-6
August	304	300	-3	-4
September	275	275	0	0
Weighted average			-11	-9

Month	Current conditions (cfs)	LWSA (cfs)	Range in sediment transport capacity change (percent)	
October	372	394	12	19
November	397	326	-33	-45
December	400	320	-36	-49
January	401	326	-34	-46
February	445	368	-32	-43
March	550	479	-24	-34
April	790	694	-23	-32
May	1062	979	-15	-22
June	774	724	-13	-18
July	347	325	-12	-18
August	304	281	-15	-21
September	275	280	4	6
Weighted average			-18	-25

Table SED-A.6.—Monthly flows and change in sediment transport capacity on the Truckee River from Reno-Sparks to McCarran Blvd Reno in **median** hydrologic conditions (continued)

Month	No Action (cfs)	TROA (cfs)	Range in sediment transport capacity change (percent)	
October	394	386	-4	-6
November	328	222	-54	-69
December	322	278	-25	-36
January	330	297	-19	-27
February	372	366	-3	-5
March	483	488	2	3
April	696	776	24	39
May	980	1062	17	27
June	726	780	15	24
July	325	340	9	14
August	282	300	13	20
September	280	275	-4	-5
Weighted average			9	21

Month	No Action (cfs)	LWSA (cfs)	Range in sediment transport capacity change (percent)	
October	394	394	0	0
November	328	326	-1	-2
December	322	320	-1	-2
January	330	326	-2	-4
February	372	368	-2	-3
March	483	479	-2	-2
April	696	694	-1	-1
May	980	979	0	0
June	726	724	-1	-1
July	325	325	0	0
August	282	281	-1	-1
September	280	280	0	0
Weighted Average			-1	-1

Table SED-A.6.—Monthly flows and change in sediment transport capacity on the Truckee River near Reno in **very wet** hydrologic conditions

Month	Current conditions (cfs)	No Action (cfs)	Range in sediment transport capacity change (percent)	
October	647	690	14	21
November	776	693	-20	-29
December	1550	1460	-11	-16
January	1895	1779	-12	-17
February	2198	2101	-9	-13
March	2522	2431	-7	-10
April	3273	3111	-10	-14
May	3914	3816	-5	-7
June	2398	2349	-4	-6
July	1475	1468	-1	-1
August	402	402	0	0
September	337	347	6	0
Weighted average			-7	-10

Month	Current conditions (cfs)	TROA (cfs)	Range in sediment transport capacity change (percent)	
October	647	699	17	26
November	776	712	-16	-23
December	1550	1514	-5	-7
January	1895	1849	-5	-7
February	2198	2111	-8	-11
March	2522	2505	-1	-2
April	3273	3326	3	5
May	3914	3956	2	3
June	2398	2470	6	9
July	1475	1476	0	0
August	402	407	3	4
September	337	361	15	23
Weighted average			1	2

Table SED-A.6.—Monthly flows and change in sediment transport capacity on the Truckee River near Reno in **very wet** hydrologic conditions (continued)

Month	Current conditions (cfs)	LWSA (cfs)	Range in sediment transport capacity change (percent)	
October	647	690	14	21
November	776	690	-21	-30
December	1550	1456	-12	-17
January	1895	1774	-12	-18
February	2198	2096	-9	-13
March	2522	2417	-8	-12
April	3273	3098	-10	-15
May	3914	3812	-5	-8
June	2398	2348	-4	-6
July	1475	1467	-1	-2
August	402	401	0	-1
September	337	347	6	9
Weighted average			-7	-11

Month	No Action (cfs)	TROA (cfs)	Range in sediment transport capacity change (percent)	
October	690	699	3	4
November	693	712	6	8
December	1460	1514	8	12
January	1779	1849	8	12
February	2101	2111	1	1
March	2431	2505	6	9
April	3111	3326	14	22
May	3816	3956	7	11
June	2349	2470	11	16
July	1468	1476	1	2
August	402	407	3	4
September	347	361	8	13
Weighted average			8	13

Table SED-A.6.—Monthly flows and change in sediment transport capacity on the Truckee River near Reno in **very wet** hydrologic conditions (continued)

Month	No Action (cfs)	LWSA (cfs)	Range in sediment transport capacity change (percent)	
October	690	690	0	0
November	693	690	-1	-1
December	1460	1456	-1	-1
January	1779	1774	-1	-1
February	2101	2096	0	-1
March	2431	2417	-1	-2
April	3111	3098	-1	-1
May	3816	3812	0	0
June	2349	2348	0	0
July	1468	1467	0	0
August	402	401	0	-1
September	347	347	0	0
Weighted average			0	-1

D. Erosion on Truckee River: McCarran Boulevard to Derby Diversion Dam (Lockwood)

Comparisons are made between all of the alternatives for both median hydrologic conditions and very wet hydrologic conditions on a monthly basis for the Truckee River: McCarran Boulevard to Derby Diversion Dam (Lockwood) in table SED-A.7. The minimum threshold set for an impact for sediment transport capacity is a positive change of 10 percent. For current conditions vs. No Action, sediment transport capacity change is greater than 10 percent in October in median hydrologic conditions. Also for current conditions vs. TROA, sediment transport capacity change does not exceed the threshold change in median hydrologic conditions. For No Action vs. TROA, sediment transport capacity change exceeds the threshold change for May, June, July, and September. In very wet hydrologic conditions, sediment capacity change is exceeded for current conditions vs. No Action in October, August, and September and for current conditions vs. TROA in October, June, July, and September. For No Action vs. TROA, sediment transport capacity is greater in April and June.

In median hydrologic conditions, monthly sediment capacity change is less in every month than under current conditions. Thus, much less sediment transport likely would occur in this reach under No Action or LWSA than under current conditions, and significant deposition is possible. Steamboat Creek is a potential source of sediment within this reach. More sediment transport could occur in this reach under TROA than under No Action, but because

sediment transport capacity under TROA is almost the same or less than under current conditions, no significant erosion or sediment transport is expected in this reach.

Table SED-A.7.—Monthly flows and change in sediment transport capacity on the Truckee River between McCarran Blvd to Derby Diversion Dam (Lockwood) under **median** hydrologic conditions

Month	Current conditions (cfs)	No Action (cfs)	Range in sediment transport capacity change (percent)	
October	434	460	12	19
November	508	476	-12	-18
December	509	476	-13	-18
January	539	516	-8	-12
February	620	596	-8	-11
March	716	688	-8	-11
April	884	823	-13	-19
May	1142	1054	-15	-21
June	835	784	-12	-17
July	405	374	-15	-21
August	370	338	-17	-24
September	339	337	-1	-2
Weighted average			-11	-17

Month	Current conditions (cfs)	TROA (cfs)	Range in sediment transport capacity change (percent)	
October	434	452	8	13
November	508	377	-45	-59
December	509	433	-28	-38
January	539	474	-23	-32
February	620	579	-13	-19
March	716	702	-4	-6
April	884	910	6	9
May	1142	1152	2	3
June	835	846	3	4
July	405	391	-7	-10
August	370	360	-5	-8
September	339	330	-5	-8
Weighted average			-5	-3

Table SED-A.7.—Monthly flows and change in sediment transport capacity on the Truckee River between McCarran Blvd to Derby Diversion Dam (Lockwood) under **median** hydrologic conditions (continued)

Month	Current Conditions (cfs)	LWSA (cfs)	Range in sediment transport capacity change (percent)	
October	434	460	12	19
November	508	478	-11	-17
December	509	478	-12	-17
January	539	519	-7	-11
February	620	598	-7	-10
March	716	691	-7	-10
April	884	825	-13	-19
May	1142	1054	-15	-21
June	835	785	-12	-17
July	405	374	-15	-21
August	370	339	-16	-23
September	339	338	-1	-1
Weighted average		614	-11	-17

Month	No Action (cfs)	TROA (cfs)	Range in sediment transport capacity change (percent)	
November	460	452	-3	-5
December	478	377	-38	-51
January	478	433	-18	-26
February	519	474	-17	-24
March	598	579	-6	-9
April	691	702	3	5
May	825	910	22	34
June	1054	1152	19	31
July	785	846	16	25
August	374	391	9	14
September	339	360	13	20
	338	330	-5	-7
Weighted average			7	17

Table SED-A.7.—Monthly flows and change in sediment transport capacity on the Truckee River between McCarran Blvd to Derby Diversion Dam (Lockwood) under **median** hydrologic conditions (continued)

Month	No Action (cfs)	LWSA (cfs)	Range in sediment transport capacity change (percent)	
November	460	460	0	0
December	478	476	-1	-1
January	478	476	-1	-1
February	519	516	-1	-2
March	598	596	-1	-1
April	691	688	-1	-1
May	825	823	0	-1
June	1054	1054	0	0
July	785	784	0	0
August	374	374	0	0
September	339	338	-1	-1
	338	337	-1	-1
Weighted average			0	-1

Table SED-A.7.—Monthly flows and change in sediment transport capacity on the Truckee River between McCarran Blvd. and Derby Diversion Dam in **very wet** hydrologic conditions

Month	Current conditions (cfs)	No Action (cfs)	Range in sediment transport capacity change (percent)	
October	745	775	8	13
November	930	902	-6	-9
December	1726	1717	-1	-2
January	2098	2054	-4	-6
February	2408	2394	-1	-2
March	2723	2697	-2	-3
April	3410	3308	-6	-9
May	3976	3891	-4	-6
June	2493	2448	-4	-5
July	1556	1547	-1	-2
August	461	454	-3	-4
September	402	408	3	5
Weighted average			-3	-6

Table SED-A.7.—Monthly flows and change in sediment transport capacity on the Truckee River between McCarran Blvd. and Derby Diversion Dam in **very wet** hydrologic conditions (continued)

Month	Current conditions (cfs)	TROA (cfs)	Range in sediment transport capacity change (percent)	
October	745	768	6	10
November	930	915	-3	-5
December	1726	1772	5	8
January	2098	2123	2	4
February	2408	2403	0	-1
March	2723	2770	3	5
April	3410	3478	4	6
May	3976	4032	3	4
June	2493	2550	5	7
July	1556	1548	-1	-2
August	461	457	-2	-3
September	402	416	7	11
Weighted average			3	5

Month	Current Conditions (cfs)	LWSA	Range in sediment transport capacity change (percent)	
October	745	775	8	13
November	930	899	-7	-10
December	1726	1714	-1	-2
January	2098	2051	-4	-7
February	2408	2391	-1	-2
March	2723	2685	-3	-4
April	3410	3298	-6	-10
May	3976	3888	-4	-6
June	2493	2447	-4	-5
July	1556	1545	-1	-2
August	461	454	-3	-4
September	402	408	3	5
Weighted average			-4	-6

Table SED-A.7.—Monthly flows and change in sediment transport capacity on the Truckee River between McCarran Blvd. and Derby Diversion Dam in **very wet** hydrologic conditions (continued)

Month	No Action (cfs)	TROA (cfs)	Range in sediment transport capacity change (percent)	
October	775	768	-2	-3
November	902	915	3	4
December	1717	1772	7	10
January	2054	2123	7	10
February	2394	2403	1	1
March	2697	2770	5	8
April	3308	3478	11	16
May	3891	4032	7	11
June	2448	2550	9	13
July	1547	1548	0	0
August	454	457	1	2
September	408	416	4	6
Weighted average			7	11

Month	No Action (cfs)	LWSA (cfs)	Range in sediment transport capacity change (percent)	
October	775	775	0	0
November	902	899	-1	-1
December	1717	1714	0	-1
January	2054	2051	0	0
February	2394	2391	0	0
March	2697	2685	-1	-1
April	3308	3298	-1	-1
May	3891	3888	0	0
June	2448	2447	0	0
July	1547	1545	0	0
August	454	454	0	0
September	408	408	0	0
Weighted average			0	-1

E. Erosion on the Lower Truckee River between Derby Diversion Dam and Pyramid Lake

Comparisons are made between all of the alternatives for both median hydrologic conditions and very wet hydrologic conditions on the Truckee River between Derby Diversion Dam and Pyramid Lake on a monthly basis in table SED-A.8. For current conditions vs. No Action, sediment transport capacity change is greater than 10 percent in October, August, and September in median hydrologic conditions. Also for current conditions vs. TROA, sediment transport capacity change is greater than 10 percent for October, June, July, and September. For No Action vs. TROA, sediment transport capacity change is greater for April and June. In very wet hydrologic conditions, sediment capacity change is greater for current conditions vs. No Action in September. For No Action vs. TROA, sediment transport capacity change is greater than 10 percent in April and June. The results suggest that almost the same sediment transport likely would occur in this reach under TROA and current conditions.

Table SED-A.8.—Monthly flows and change in sediment transport capacity on the Truckee River between Derby Diversion Dam and Pyramid Lake in **median** hydrologic conditions

Month	Current conditions (cfs)	No Action (cfs)	Range in sediment transport capacity change (percent)	
October	396	429	17	27
November	486	455	-12	-18
December	493	448	-17	-25
January	533	497	-13	-19
February	613	590	-7	-11
March	715	674	-11	-16
April	821	745	-18	-25
May	1012	1000	-2	-4
June	667	657	-3	-4
July	300	300	0	0
August	200	264	74	130
September	246	291	40	66
Weighted average			-6	-11

Table SED-A.8.—Monthly flows and change in sediment transport capacity on the Truckee River between Derby Diversion Dam and Pyramid Lake in **median** hydrologic conditions (continued)

Month	Current conditions (cfs)	TROA (cfs)	Range in sediment transport capacity change (percent)	
October	396	432	19	30
November	486	308	-60	-75
December	493	328	-56	-71
January	533	424	-37	-50
February	613	561	-16	-23
March	715	688	-7	-11
April	821	833	3	4
May	1012	1041	6	9
June	667	748	26	41
July	300	300	0	0
August	200	262	72	125
September	246	284	33	54
Weighted average			-5	-2

Month	Current conditions (cfs)	LWSA (cfs)	Range in sediment transport capacity change (percent)	
October	396	429	17	27
November	486	453	-13	-19
December	493	445	-19	-26
January	533	494	-14	-20
February	613	587	-8	-12
March	715	671	-12	-17
April	821	743	-18	-26
May	1012	1000	-2	-4
June	667	658	-3	-4
July	300	300	0	0
August	200	265	76	133
September	246	291	40	66
Weighted average			-7	-11

Table SED-A.8.—Monthly flows and change in sediment transport capacity on the Truckee River between Derby Diversion Dam and Pyramid Lake in **median** hydrologic conditions (continued)

	No Action (cfs)	TROA (cfs)	Range in sediment transport capacity change (percent)	
October	429	432	1	2
November	455	308	-54	-69
December	448	328	-46	-61
January	497	424	-27	-38
February	590	561	-10	-14
March	674	688	4	6
April	745	833	25	40
May	1000	1041	8	13
June	657	748	30	48
July	300	300	0	0
August	264	262	-2	-2
September	291	284	-5	-7
Weighted average			2	9

Month	No Action (cfs)	LWSA (cfs)	Range in sediment transport capacity change (percent)	
October	429	429	0	0
November	455	453	-1	-1
December	448	445	-1	-2
January	497	494	-1	-2
February	590	587	-1	-2
March	674	671	-1	-1
April	745	743	-1	-1
May	1000	1000	0	0
June	657	658	0	0
July	300	300	0	0
August	264	265	1	1
September	291	291	0	0
Weighted average			0	-1

Table SED-A.8.—Monthly flows and change in sediment transport capacity on the Truckee River between Derby Diversion Dam and Pyramid Lake in **very wet** hydrologic conditions

Month	Current conditions (cfs)	No Action (cfs)	Range in sediment transport capacity change (percent)	
October	732	752	6	8
November	911	867	-9	-14
December	1774	1748	-3	-4
January	2145	2086	-5	-8
February	2453	2438	-1	-2
March	2748	2708	-3	-4
April	3396	3302	-5	-8
May	3904	3850	-3	-4
June	2419	2389	-2	-4
July	1443	1464	3	4
August	300	300	0	0
September	300	342	30	48
Weighted average			-3	-5

Month	Current conditions (cfs)	TROA (cfs)	Range in sediment transport capacity change (percent)	
October	732	749	5	7
November	911	877	-7	-11
December	1774	1803	3	5
January	2145	2156	1	2
February	2453	2455	0	0
March	2748	2770	2	2
April	3396	3468	4	6
May	3904	3992	5	7
June	2419	2493	6	9
July	1443	1467	3	5
August	300	300	0	0
September	300	305	3	5
Weighted average			3	5

Table SED-A.8.—Monthly flows and change in sediment transport capacity on the Truckee River between Derby Diversion Dam and Pyramid Lake in **very wet** hydrologic conditions (continued)

Month	Current conditions (cfs)	LWSA (cfs)	Range in sediment transport capacity change (percent)	
October	732	752	6	8
November	911	864	-10	-15
December	1774	1745	-3	-5
January	2145	2083	-6	-8
February	2453	2435	-1	-2
March	2748	2696	-4	-6
April	3396	3296	-6	-9
May	3904	3847	-3	-4
June	2419	2389	-2	-4
July	1443	1463	3	4
August	300	300	0	0
September	300	342	30	48
Weighted average			-3	-5

Month	No Action (cfs)	TROA (cfs)	Range in sediment transport capacity change (percent)	
October	752	749	-1	-1
November	867	877	2	4
December	1748	1803	6	10
January	2086	2156	7	10
February	2438	2455	1	2
March	2708	2770	5	7
April	3302	3468	10	16
May	3850	3992	8	11
June	2389	2493	9	14
July	1464	1467	0	1
August	300	300	0	0
September	342	305	-20	-29
Weighted average			7	11

Table SED-A.8.—Monthly flows and change in sediment transport capacity on the Truckee River between Derby Diversion Dam and Pyramid Lake in **very wet** hydrologic conditions (continued)

Month	No Action (cfs)	LWSA (cfs)	Range in sediment transport capacity change (percent)	
October	752	752	0	0
November	867	864	-1	-1
December	1748	1745	0	-1
January	2086	2083	0	0
February	2438	2435	0	0
March	2708	2696	-1	-1
April	3302	3296	0	-1
May	3850	3847	0	0
June	2389	2389	0	0
July	1464	1463	0	0
August	300	300	0	0
September	342	342	0	0
Weighted average			0	0

IV. TRUCKEE RIVER DELTA FORMATION AT PYRAMID LAKE

Predicted model elevation change by alternative is shown in table SED-A.9 for Pyramid Lake. The threshold for consideration of an environmental impact at Pyramid Lake is no more than a 0.5 foot reduction in elevation by alternative on a monthly basis, when a comparison is made between the alternative and current conditions or No Action. A comparison of current conditions to No Action in median, very wet, and very dry hydrologic conditions indicates very little difference in elevation change between any of the modeling scenarios. A comparison of LWSA to current conditions shows no impact for any elevation change on a monthly basis for any modeling scenario. On a positive basis, LWSA shows a greater positive elevation change in the months of March through May. A comparison of TROA to current conditions in median, very wet, and very dry hydrologic conditions shows that none of the monthly elevation changes between TROA and current conditions decrease as much as 0.2 foot. Therefore, no impacts would be associated with TROA for the Truckee River delta. A comparison of No Action and LWSA shows very little difference in elevation changes by month for each modeling scenario. As a positive impact, LWSA shows more positive elevation change in the months of March through June. A comparison of No Action to TROA shows very little difference in elevation changes by month for each modeling scenario.

Sediment capacity changes by alternative for inflow to Pyramid Lake also can be identified with no environmental impacts. The change in annual sediment transport capacity under the all of the alternatives does not exceed the average threshold change of 10 percent when compared to either current conditions or No Action. Therefore, the potential for erosion for this reach is no greater than under either current conditions or No Action.

Table SED-A.9.—Water elevation differences at Pyramid Lake in very wet, median, and very dry hydrologic conditions

Month	Current			No Action			LWSA			TROA		
	Median	90%	10%	Median	90%	10%	Median	90%	10%	Median	90%	10%
Oct.	-0.16	-0.38	0.00	-0.16	-0.39	0	-0.165	-0.39	0.08	-0.2	-0.37	0
Nov.	-0.15	-.371	0.09	-0.15	-0.335	0.151	-0.15	-0.331	0.17	-0.16	-0.361	0.087
Dec.	-0.08	-.312	0.41	-0.08	-0.321	0.399	-0.08	-0.311	0.6355	-0.12	-0.32	0.495
Jan.	0.08	-0.16	0.77	0.08	-0.175	0.741	0.075	-0.175	1.045	0	-0.17	0.783
Feb.	0.16	-0.087	0.87	0.16	-0.15	0.801	0.16	-0.087	0.9615	0.15	-0.15	0.853
March	0.24	-0.08	0.90	0.225	-0.087	0.832	0.22	-0.08	1.1825	0.195	-0.087	0.93
April	0.23	-0.08	1.03	0.195	-0.08	0.945	0.17	-0.08	1.3125	0.23	-0.08	1.006
May	0.38	-0.071	1.35	0.38	-0.07	1.347	0.39	-0.07	1.9795	0.39	-0.07	1.361
June	0.08	-0.232	0.62	0.08	-0.221	0.566	0.08	-0.221	0.8925	0.08	-0.221	0.641
July	-0.31	-0.514	0.00	-0.31	-0.522	-0.072	-0.31	-0.524	0.247	-0.305	-0.514	0
Aug.	-0.43	-0.58	-0.29	-0.4	-0.56	-0.304	-0.41	-0.56	-0.2175	-0.4	-0.55	-0.259
Sept.	-0.39	-.551	-0.24	-0.38	-0.513	-0.23	-0.38	-0.52	-0.16	-0.38	-0.541	-0.54

REFERENCES

Adams, K.D., 2001. Shorezone Erosion at Lake Tahoe: Historical Aspects and Instrumental Monitoring, Desert Research Institute, University and Community College System of Nevada.

Adams, K.D., 2003. Shorezone Erosion at Lake Tahoe: Historical Aspects, Processes and Stochastic Modeling, Final Report Prepared for the Bureau of Reclamation.

Adams, K.D. and T.B. Minor, 2002. Historic Shoreline Change at Lake Tahoe from 1938 to 1998 and its Impact on Sediment and Nutrient Loading, Journal of Coastal Research, Vol, 18, No. 4, Fall, 2002.

Shorezone Erosion at Lake Tahoe: Historical Aspects, Processes, and Stochastic Modeling

FINAL REPORT FOR THE
U.S. BUREAU OF RECLAMATION
and
TAHOE REGIONAL PLANNING AGENCY

March 31, 2004

***Prepared by*:**

Dr. Kenneth D. Adams
Division of Earth and Ecosystem Sciences

with contributions by
Mr. Timothy B. Minor and Dr. Anna K. Panorska

DRI
Desert Research Institute

Table of Contents

Chapter 1
Introduction and Background

Introduction

This report summarizes results and interpretations of Lake Tahoe shorezone studies begun by the Desert Research Institute (DRI) in spring 2000. These studies were originally undertaken to quantify the amount of shorezone erosion since 1940 and to derive estimates of how much sediment and nutrients were introduced into the lake from this source. The studies gradually evolved to include monitoring and characterizing wave activity at the lake, quantifying particle size distributions of shorezone sediments eroded into the lake, and investigating processes of shorezone erosion. Most recently, we have developed stochastic models that predict where and how much shorezone erosion will occur given a set of controlling parameters and a separate modeling approach to assess the effects of different lake-level management schemes on shorezone erosion. In this report, the emphasis is on lateral changes to the shore position and not vertical changes to beach areas. The report is arranged into the following chapters:

- Chapter 1 provides background on previous Lake Tahoe studies that are relevant to shorezone erosion including the physical setting, climate, wave activity, water quality, and shorezone system.
- Chapter 2 includes information on development of the modern shorezone system at Lake Tahoe, the effects of shorezone protective structures on nearshore processes in general, and the possible effects of these types of structures at Lake Tahoe in particular.
- Chapter 3 discusses development of a technique to document the amount of historic shorezone erosion at Lake Tahoe since about 1940 when the earliest aerial photographs were made. This chapter also includes information about particle-size distributions of shorezone sediments. Chapter 3 was published in its present form, except for the particle-size data, in the *Journal of Coastal Research* (Adams and Minor, 2002).
- Chapter 4 presents instrumental wave monitoring procedures, data reduction techniques, and results documenting the wave climate at Lake Tahoe. Also discussed are relationships among wind, waves, and the amount of wave energy impacting a shore from different wave events.
- Chapter 5 presents results of an effort to develop a series of statistical models to predict where shorezone erosion will occur and how much material will be eroded, given a set of governing parameters. The approach uses data from Chapter 3 to develop statistical models but also incorporates field data and analytical modeling of wave run up processes.
- Chapter 6 presents results of a statistical analysis to assess the effects of different lake-level management scenarios on shorezone erosion. In particular, we address the question of whether or not the Truckee River Operating Agreement (TROA), if implemented, would significantly affect shorezone erosion.

Background

Physical Setting of Lake Tahoe

The geologic history of the Lake Tahoe basin provides an important context for studying the shorezone system of this high elevation lake. In particular, the Quaternary (0 to 2,000,000 years ago) history of the basin can be directly correlated to the material characteristics, processes, and rates of change found on different lengths of shoreline around the lake. Lake levels have naturally fluctuated at Lake Tahoe, depositing nearshore beach and other lacustrine deposits at higher levels than today. These deposits and their material properties need to be considered when studying shorezone change at Lake Tahoe. Therefore, this section includes a brief discussion of the early geologic development of the Lake Tahoe basin and focuses on the more recent history when glaciers repeatedly advanced and receded and lake levels rose and fell for reasons that are not as yet entirely understood. This section is based on existing literature and from observations made during the course of this study.

Lake Tahoe sits astride the crest of the Sierra Nevada in a large tectonic graben still bounded by active faults. This graben is the westernmost expression of Basin and Range extension at this latitude and is bounded on the east side by the Carson Range and on the west by the Sierra Nevada crest (Gardner et al., 2000). Although faults are more difficult to discern on land in the Tahoe basin, young fault scarps traversing the floor of the lake demonstrate that this basin is still tectonically active (Gardner et al., 1999; Kent et al., 2000). The majority of exposed bedrock in the basin consists of granitic rocks, but the north end is filled with a large pile of Tertiary and Pleistocene volcanic rocks. Scattered metamorphic rocks, particularly around Mt. Tallac, also exist in the basin (Burnett, 1971).

Figure 1-1 shows the distribution of rocks and sediments in the basin. This geologic map reveals a variety of different geologic units near lake level, each of which probably responds to wave action in different ways. Along the eastern shore of the lake, granitic bedrock dominates except for a few small pocket beaches including Sand Harbor, Glenbrook Bay, and Zephyr Cove. The southern shore is largely composed of glacial outwash deposits into which young lake deposits are inset (Fig. 1-1). At the shore, the outwash appears to be graded to levels higher than the current lake level of about 1899 m, which means that either there has been significant shorezone erosion since the outwash was deposited or that the outwash was deposited when lake levels were higher. The western shore of the lake is dominated by glacial moraines, outwash, and lake deposits, although granitic bedrock does crop out near Rubicon Point. The northern shore of the lake is largely comprised of Tertiary volcanic rocks with some granitics around Stateline Point and abundant areas of alluvial and lake deposits near the shore (Fig. 1-1).

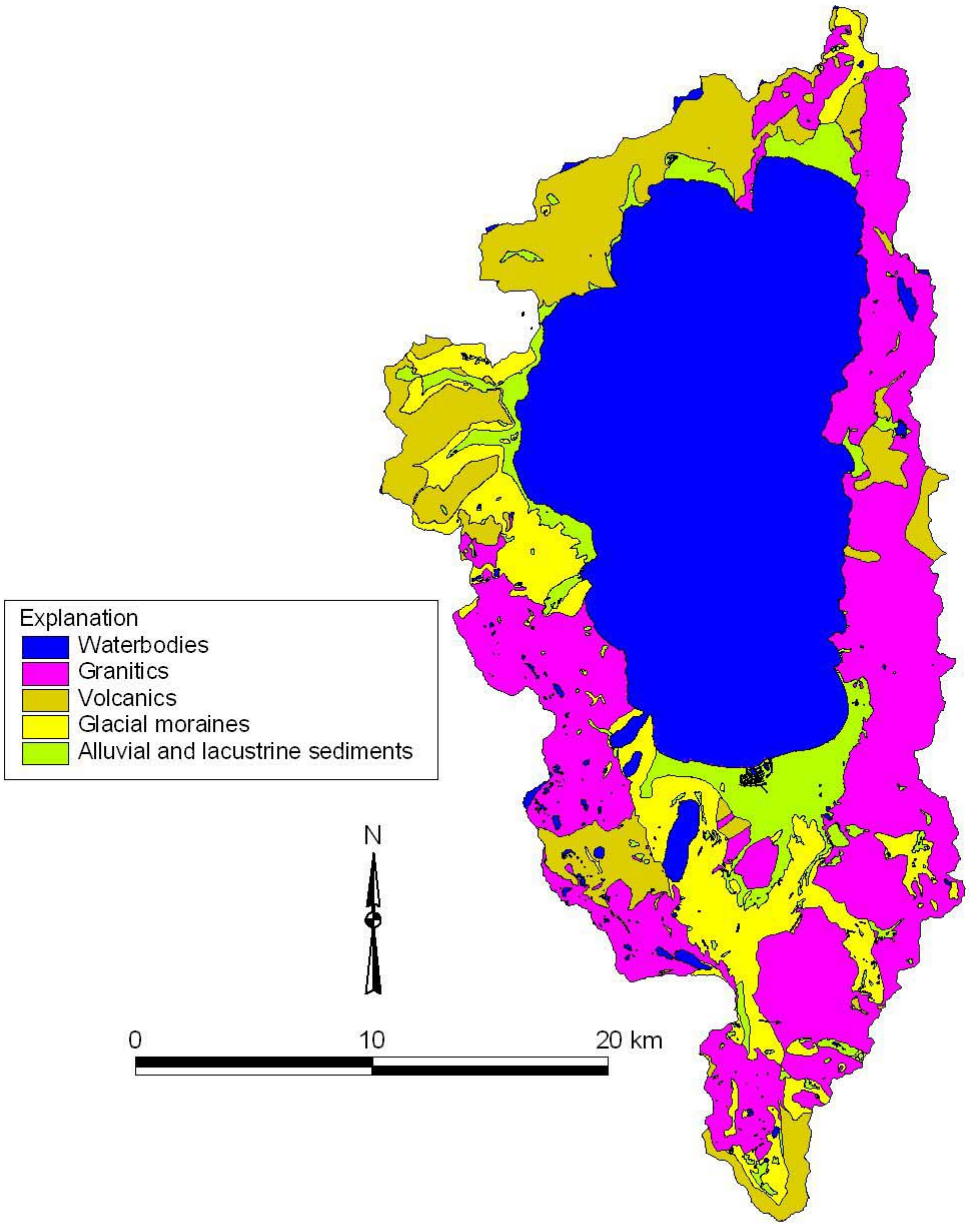

Figure 1-1. Simplified geologic map of the Lake Tahoe basin showing the distribution of rocks and sediment.

Glacial deposits adjacent to the lake generally date from one of three major glacial episodes that include—from oldest to youngest—the Donner Lake, Tahoe, and Tioga glaciations. The Donner Lake glaciation has been difficult to date but may be as old as 400,000 to 600,000 years (Birkeland, 1964). Till and moraines of Tahoe age have not

been directly dated in the basin but correlative deposits along the eastern side of the Sierra Nevada near Yosemite date from about 70,000 years ago, 140,000 years ago, or from both times (Bursik and Gillespie, 1993; Phillips et al., 1990). The Tioga glaciation was the last major glaciation and reached its maximum advance around 20,000 years ago, although large expanses of ice still may have been present as late as about 14,000 years ago (James et al., 2002).

The abundance of lake deposits cropping out near the shore of Lake Tahoe indicates that lake level, at times, has been much higher than the current level of 1899 m. Periodic ice dams just downstream from the lake outlet may have been one cause of these higher lake levels. Birkeland (1964) presents evidence that all three of the major glacial episodes may have dammed Lake Tahoe and caused higher than present lake levels. During Donner Lake time, most of the Truckee River Canyon was filled with ice flowing east from the Sierran crest. Lake deposits and benches found at elevations up to 2073 m may relate to this damming episode (Birkeland, 1964). In Tahoe time, ice from Squaw Creek blocked the Truckee River and caused Lake Tahoe to rise to about 1926 m before the dam broke. The sudden release of more than 14 cubic kilometers of water caused a catastrophic flood that coursed down the river and eventually ended up in Lake Lahontan, a large pluvial lake that at times occupied much of northwestern Nevada (Morrison, 1991). Birkeland (1964) thought that ice damming was negligible in Tioga time, even though his mapping clearly shows that Tioga ice blocked the Truckee River to an elevation of about 1902 m, or approximately 5 m above the natural outlet. The volume of water ponded by a dam at 1902 m equates to about 3 cubic kilometers, enough for a large flood event.

During the middle Holocene (4,000 to 7,000 years ago), lake level at Tahoe may have fallen below the natural rim for an extended period. Lindstrom (1990) presents evidence that rising waters between 4,000 and 5,000 years ago drowned currently submerged trees along the southern shore of Tahoe. The implication is that Tahoe did not spill for an extended period, allowing forests to colonize areas adjacent to the lower lake level. When climate became effectively wetter around 4000 years ago, Lake Tahoe again rose to its rim and drowned these trees. Davis et al. (1976) reviewed physical evidence for lower lake levels during this same time period. In particular, the major drainages of the upper Truckee River, Trout Creek, and Taylor Creek were graded to base levels much lower than present and deeply dissected into the glacial outwash plains along the south shore. When water level began to rise at the end of the middle Holocene, these drainages were backfilled and beach barriers developed at the lake-marsh interfaces. According to this model, much of the material filling the marshes around Lake Tahoe dates from the last few thousand years.

In the early part of the 20th century, lake levels commonly exceeded the now legally mandated maximum elevation of 1896.65 m (6229.1 ft) (Fig. 1-2). The highest historic level was in 1907 when the lake rose above 1899.29 m (6231.19 ft). Shoreline erosion undoubtedly occurred during these high water periods, but the aerial photography used in our study (Chapter 3) does not extend far enough back in time to capture the effects of these periods.

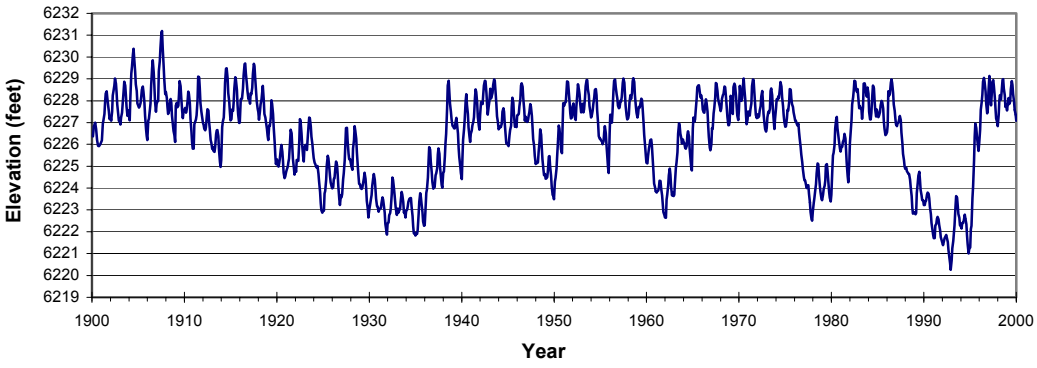

Figure 1-2. Lake levels at Lake Tahoe from 1900 to 2000.

Climate

The climate of Lake Tahoe is strongly influenced by topography and moist Pacific air masses traversing the area from the eastern Pacific Ocean (TRPA Staff, 1971). Elevations range from about 1898.65 m (maximum lake level) to more than 2750 m along both the Sierra crest to the west of the basin and the Carson Range bounding the east side of the lake. Even at the scale of the basin, a strong climatic gradient exists where average annual precipitation ranges up to 125 cm on the western side of the basin but only about 60 cm of precipitation falls along the east shore of the lake. Precipitation falls primarily in the winter months (November through March) as snow from Pacific frontal systems. Annual snowfall around the basin also reflects the climatic gradient. Tahoe City in the northwest part of the basin receives an average annual snowfall of 480 cm, whereas Glenbrook on the east shore and Stateline at the south shore only receive 243 and 161 cm of snowfall, respectively (data from Western Regional Climate Center, Desert Research Institute). Although abundant snow falls on the basin, winter temperatures are relatively mild with daytime high temperatures during January averaging between 2 and 4^{o} C at the lower elevations (TRPA Staff, 1971). Because of its large size and heat capacity, the lake actually has an ameliorating effect on winter temperatures—areas further from the lake are usually colder than areas along the lakeshore. Of course, elevation also plays an important role in controlling local temperature gradients. Summer temperatures around the lake are also mild, with highs commonly in the 21 to 27^{o} C range.

The climate of the Lake Tahoe basin has a strong controlling influence on its hydrology. Most of the annual precipitation is stored as a thick snowpack during the winter months and is released during spring snowmelt. This can be seen in the lake-level record (Fig. 1-2) that shows levels increasing each spring to an annual maximum in early summer, which then generally declines until the next snowmelt season. The timing of these high-water periods has important ramifications for shoreline erosion because it is likely that the most severe erosion occurs when strong winds blow across the lake when the water level is high.

Winds, Waves, Seiches, and Shoreline Erosion

Until recently, limited quantitative data was collected on concerning winds in the basin and how they affect wave generation, seiching, and shoreline erosion. The Western Regional Climate Center (WRCC) at DRI archived wind data from the South Lake Tahoe airport beginning in 1992, but this data is limited for wave growth studies because the site is far from the lakeshore and winds were only recorded during daylight hours. For the years prior to 1992, wind data is available for only sporadic periods. Wind velocity and direction were reported from the South Lake Tahoe airport from 1965 through 1967 (TRPA Staff, 1971), but again these statistics are for winds occurring only during daylight hours. Wind statistics also were reported by the U.S. Coast Guard Station at Tahoe City for the period January 1967 to September 1969 (TRPA Staff, 1971). Unfortunately, wind observations during this period were recorded just twice daily, once in the morning and once in the afternoon, so the duration of wind events is not known. Both Orme (1971) and Engstrom (1978) used wind statistics for Tahoe City to infer wave conditions, but both authors were hampered in their analyses by the lack of wind duration information which is critical for wave growth formulae.

More recently, Air Resource Specialists, Inc. (ARS) has been collecting wind data from at least three different sites near Lake Tahoe. These include D.L. Bliss State Park in the southwestern part of the basin, Thunderbird Lodge on the northeastern shore, and South Lake Tahoe Boulevard at South Shore. Data from these sites is discussed more thoroughly in Chapters 4 and 5.

Two other studies concerning wind conditions at Lake Tahoe are worthy of note. First, a study by Mulberg (1984) delineated seasonal wind patterns. The original report, however, has proved difficult to obtain. The only usable information is a series of figures reproduced in a guidebook article by Moory and Osborne (1984). These figures show winds in all seasons primarily from the south and southwest. From the regular wind flow patterns shown in the figures, however, it seems that local topographic effects were not considered in this study. In this same guidebook article (Moory and Osborne, 1984), a reference is made to wind data from eight locations along the shore of Lake Tahoe. Unfortunately, it is unclear whether this data was ever published; attempts to acquire the data have been fruitless.

Existing quantitative wave information for Lake Tahoe is also sparse. Orme (1971) reported that waves could reach up to 2 – 3 m in height, but waves of this magnitude were not observed. Instead, this range probably was derived from maximum fetch distances and theoretical considerations using the wave growth formulae suggested by the U.S. Army Corps of Engineers (CERC, 1984). Engstrom (1978) also used wave hindcasting procedures outlined in the Shore Protection Manual (CERC, 1984) combined with wind data reported by the Tahoe Regional Planning Agency (TRPA) for Tahoe City (TRPA Staff, 1971) to hindcast waves at Lake Tahoe. Again, because winds specified by both velocity and duration were lacking from the TRPA data set, Engstrom's (1978) analysis is considered preliminary.

Lake Tahoe, like virtually all inland water bodies, is subject to seiches, which are defined as periodic oscillations of a body of water the period of which is determined by resonant characteristics of the containing basin as controlled by its physical dimensions (McGarr and Vorhis, 1968). This means that each basin has a fundamental period of oscillation controlled by the size of the basin, regardless of the magnitude of the initial impulse. A seiche can be created in any number of ways including changes in atmospheric pressure over one part of the water body or by wind stress that causes the water surface to slope and pile-up at the downwind side of the lake (Carter, 1988). When the wind subsides, the water surface oscillates at a period determined by the dimensions of the basin. At a lake shore, occurrence of a seiche would appear as a sudden rise or fall in the water level. The importance of seiches to shorezone erosion is that they can temporarily raise water level along parts of a shore, allowing waves to penetrate further inland and cause accelerated erosion.

LeConte (1884) was the first to discuss the occurrence of seiches at Lake Tahoe, although they were not actually observed by him. Interviews with residents at the time suggested that sudden lake-level changes occasionally had occurred. LeConte (1884) estimated that the fundamental period of a seiche occurring at Lake Tahoe would be about 17 minutes in the north-south direction and about 10 minutes in the east-west direction. The maximum amplitude is currently unknown.

Budlong (1971) discusses the potential for seiches at Lake Tahoe and cites personal observations of seiches ranging in amplitude from 13 to 23 cm. Dramatic photographs documenting these relatively sudden changes in water level emphasize the potential importance of this phenomenon to shorezone erosion (Budlong, 1971). On a moderately sloping beach along the south shore, lateral distance in wave runup appeared to change by as much as several meters with a seiche of about 13 cm (Budlong, 1971).

Although there is substantial anecdotal evidence for shorezone erosion at Lake Tahoe, few detailed studies exist quantifying the rates of erosion and the conditions under which it occurred. A notable exception is the previously mentioned work of Budlong (1971) who studied processes and rates of shorezone erosion in the area of the then newly built Tahoe Keys development. In this work, he documented that rapid erosion occurred immediately west of the Keys East channel because of the interruption of longshore drift from the east by a pair of jetties "protecting" the entrance to the channel. During a single, ten-month period (6/01/69–3/31/70), the shoreline retreated up to 16 m over a distance of about 150 m. In this case, longshore drift was from the east, driven by easterly winds during the winter months. Budlong (1971) also surmised that willow-clearing activities along the shore by Tahoe Keys personnel substantially contributed to the magnitude of shore retreat by eliminating the root-binding effects of the vegetation.

Studies by Orme (1971, 1972) do not specifically quantify shorezone erosion, but they do provide useful information about the shorezone system of Lake Tahoe and factors affecting erosion. Orme (1971) presents an excellent discussion of the shorezone system at Lake Tahoe, the natural processes occurring along the shore, and how human activities

have altered the shorezone system and may continue to do so in the future. A significant contribution of Orme (1971) is the delineation of currents and littoral drift patterns at the lake. Although the map of shore drift directions is somewhat generalized, it provided a starting place for the refinements of Osborne et al. (1985) and observations made during the course of the present study (Fig. 1-3). A second significant contribution of this early report is that it served as the basis for constructing a shorezone plan for Lake Tahoe (Orme, 1972) that was officially adopted by TRPA in 1976 (TRPA Staff, 1999). Orme (1972) stated that eroding shorelines comprise 16.3% of the Lake Tahoe shoreline and wave-cut escarpments ranging in height from 0.5 to 18 m backed eroding shorelines.

Osborne et al. (1985) provide a comprehensive review of the lithologies, grain shapes and size distributions, sediment sources and sinks, and shore drift patterns of the littoral zone of Lake Tahoe. This study represents the synthesis of three master theses that include the studies of Waldron (1982), Edelman (1984), and Gaynor (1984). The major conclusions of Osborne et al. (1985), with respect to shorezone erosion, are that 1) the principal sediment source for the major sand beaches at Lake Tahoe is the backshore erosion of young lacustrine and fluvio-glacial outwash; 2) the major sediment source for the gravel and cobble beaches is also erosion of backshore areas and possibly nearshore erosion of older lakebed deposits, moraines, and volcanic rocks; 3) sand is primarily delivered to the smaller pocket beaches by weathering of local granodiorite bedrock and boulders; 4) the maximum depth of fair-weather sand transport is about 3 m and about 9 to 10 m under storm conditions; and 5) littoral sand transport is restricted to many small, well-defined drift cells separated by closely spaced topographic barriers (Fig. 1-3).

Reuter and Miller (2000) report the results of a preliminary study to determine the mass of sediment and nutrients introduced into the lake from shorezone erosion. In this study, the authors assumed that 55% of the Tahoe shore was eroding at a given rate and then applied nutrient (P and N) concentrations and a density factor to determine an order-of-magnitude estimate of the mass of sediment, nitrogen, and phosphorus introduced into the lake each year from shorezone erosion. The results indicate that approximately 450 to 900 MT (metric tons) of sediment, 0.3 to 0.6 MT of phosphorus, and 0.5 to 1.0 MT of nitrogen are introduced into the lake each year from this source (Reuter and Miller, 2000). These values will serve as a direct comparison to the estimates derived from the present study.

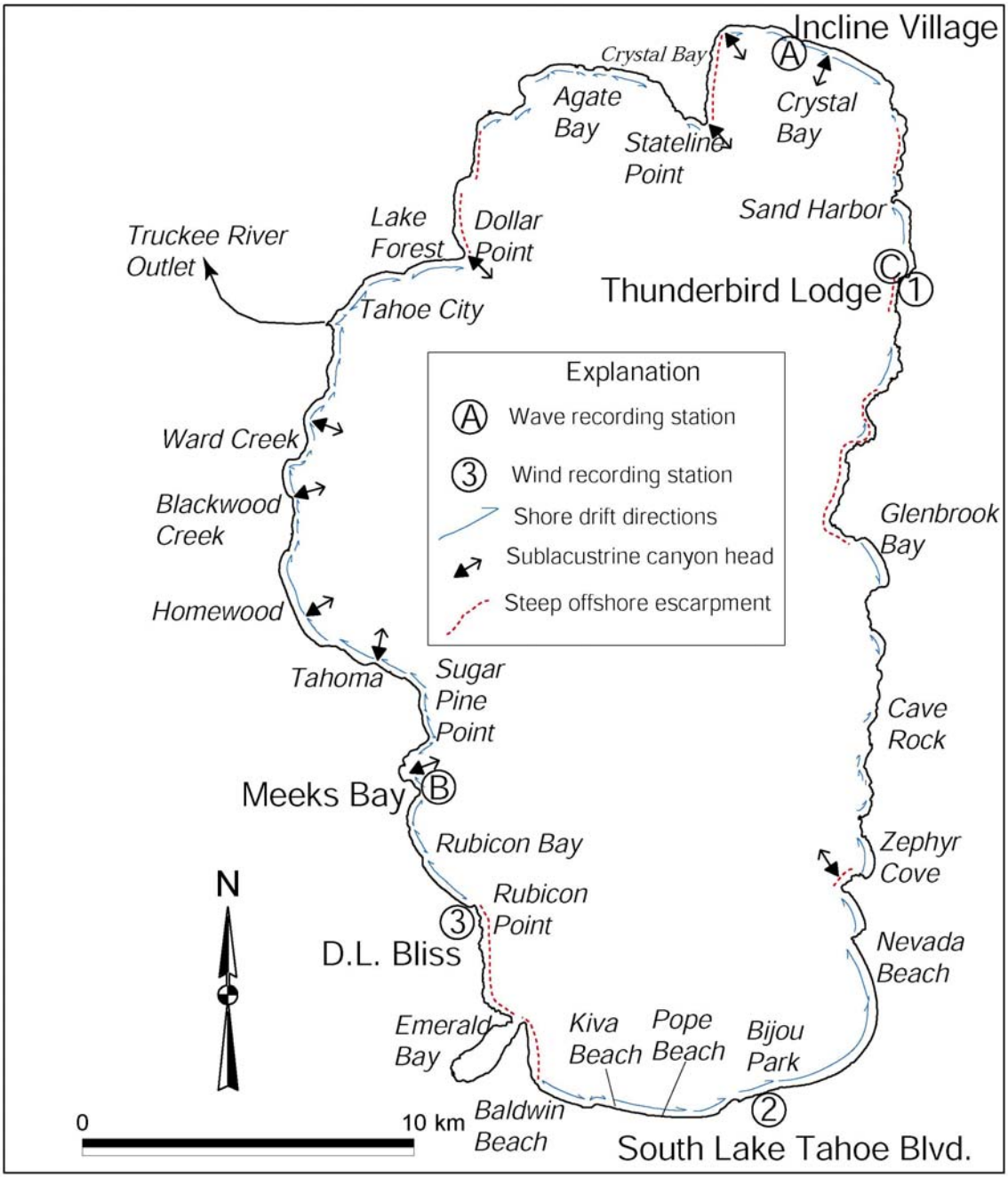

Figure 1-3. Map of Lake Tahoe showing dominant shore drift directions, locations of sublacustrine canyon heads, steep offshore escarpments, wave recording stations, wind recording stations, and locations mentioned in the report. Both the sublacustrine canyon heads and steep offshore escarpments are probably barriers to littoral drift. Data used to construct this figure are from Orme (1971), Osborne et al. (1985), and observations made during the course of this study.

Water Quality

Since the 1960s, hundreds of scientific papers and reports have been written about the Lake Tahoe watershed and its water quality. Up until recently, however, a comprehensive review and synthesis did not exist. The Lake Tahoe Watershed Assessment (Murphy and Knopp, 2000) fulfills this role by presenting the "state of the science" in what is known about environmental conditions, air quality, aquatic resources, water quality, limnology, biological integrity, and socioeconomic issues within the basin. In particular, one of the stated goals (Aquatic resources, water quality, and limnology of Lake Tahoe and its upland watershed; Reuter and Miller, 2000) is to provide "a comprehensive review of past studies with the focus of assessing both upland and lake water quality." The authors of this chapter succeed admirably at this task by reviewing and synthesizing approximately 450 reports, published papers, and other documents; a repeat of the information here would be redundant. Several publications were not included in the review, however, and warrant mention here.

Nolan and Hill (1991) derived suspended sediment budgets for four tributaries to Lake Tahoe during a four-year period (1984-87) and concluded that bed and bank erosion were the major sources of sediment during the period of study. They found that differences in climate, geology, basin physiography, and land use controlled the differences in sediment production from each of the study drainages. Two of the major implications from this study are that the hillslopes appear to be relatively disconnected from the fluvial systems and that land use changes within each of the drainages could lead to increased suspended sediment delivery to the lake.

Kilroy et al. (1997) provide an important synopsis of past United States Geological Survey (USGS) monitoring activities in the Tahoe basin and include tables and maps of all monitoring stations, their periods of record, and what constituents were analyzed. This document provides a valuable starting place for anyone implementing a water quality monitoring program in the Lake Tahoe basin.

Rowe and Allander (2000) studied the interactions between surface and groundwater for the Upper Truckee River and Trout Creek for the period July through December 1996. One of the major conclusions from this study is that in the upper sections of the watersheds, groundwater flow is generally toward the streams while in the lower reaches, groundwater flow generally parallels both the Upper Truckee and Trout Creek. Another important point is that during the latter part of their study period (November 1996), the groundwater level beneath the lower reaches of the drainages was at about the same elevation as the surface of Lake Tahoe implying that there was minimal groundwater flow directly into the lake. It is unknown how fluctuations in lake level affect groundwater levels.

Chapter 2
Lake Tahoe Shorezone

Development of the Modern Shorezone System

Shorezone erosion at Lake Tahoe is a direct consequence of wave energy acting upon the shore. Although most winds at the lake blow from the south, long-term shorezone erosion is not entirely dependent on the direction and magnitude of prevailing winds. Instead, shorezone erosion during the last 60 years appears to have been largely dependent on the type of geologic materials found along the shore (Fig. 1-1) (Adams and Minor, 2002). The areas that appear to be most susceptible to erosion generally are composed of unconsolidated alluvial and lacustrine sediments, but shores composed of Tertiary volcanics at the north end of the lake also display evidence of recent wave erosion. Not coincidently, shorezone areas composed of unconsolidated sediment are also where the highest concentration of shorezone protective structures is found. In particular, the south and west shores of Lake Tahoe appear to have the most of protective structures, although specific data on exactly how much of the shoreline is protected is not available. Orme (1972) estimated that approximately 16.3% of the shoreline was eroding while Reuter and Miller (2000) assumed that about 55% of the shoreline was eroding. Based on the geologic materials found along the shore and observations made during the course of this study, we conclude that about 67% of the natural Tahoe shoreline is capable of erosion or has eroded since lake level was raised in the late 1800s. This estimate does not account for the percentage of shorezone protected by revetments or other structures. The only type of shore that appears relatively immune from shorezone erosion is that composed of granitic rocks, which make up much of the east shore and the area between Emerald Bay and Rubicon Point (Fig. 1-1).

Another major factor that controls shorezone erosion is spatial-temporal relationships between water level and wave energy. At Lake Tahoe, the largest erosive events occur when strong winds blow and lake level is at or near its maximum level of 1898.65 m (6229.1 ft). Because of dam operations at Lake Tahoe, lake level typically fluctuates between about 1898 m (6227 ft) and 1898.65 m (6229.1 ft) (Fig. 1-2) but occasionally drops lower due to subnormal snowpack. High water or full pool is generally reached around May or June and remains there only a brief time before lake level steadily declines until a low water level of about 1898 m (6227 ft) is reached in late fall or early winter. The strongest winds commonly occur in late fall and winter when large frontal systems move across the area from the eastern Pacific and lake level is not at full pool. An exception occurred in January 1997 when strong easterly winds combined with an abnormally high lake level (~1898.79 m) produced widespread and severe erosion on the western shore of the lake. Interestingly, the severe erosion suffered in 1997 along many parts of the shore does not necessarily reflect long-term trends (Adams and Minor, 2002). This may be due to the relative rarity of strong easterly winds blowing across a higher than typical lake level.

Prior to installation of the first dam at Tahoe City in the late 1880s, the natural spill point of the lake was at about 1896.8 m (6223 ft). The shorezone system that formed around the lake at this elevation was probably in relative equilibrium because lake level likely was unable to rise much above the spill point. The spill point is not composed of bedrock but of light-colored, dense clay covered with patches of sand and gravel. Although this seems like an unstable condition for a lake's overflow point, the cohesive clay actually provides a relatively stable lip.

The shorezone presently forming at the 1898.65 m (6229 ft) level, however, is probably not in equilibrium around much of Lake Tahoe because the lake surface has not been at this elevation for much time since the first dam was installed. What this means is that shorezone erosion around the lake probably proceeded rapidly after the dam was first installed and has decreased through time as more and more waves have impacted the shorezone in the ensuing 120 years. Although we are only able to quantify shorezone erosion back to about 1938 (date of the earliest aerial photographs), it is likely that much erosion occurred between when the first dam was installed and 1938.

After the dam was installed, the lake rose several times to levels above 1898.65 m (6229.1 ft) in the early part of the 20th century (Fig. 1-2). On five separate occasions, lake level exceeded the current maximum for periods of up to several months at a time. In terms of shorezone erosion, the two most important high water periods probably occurred in 1904 and again in 1907 when lake level was above the current maximum beginning in March and lasting through the summer months. The effect of these early high lake periods is not exactly known, but it is likely that they caused widespread erosion around the lake. Evidence of these early high water periods may be found at Baldwin Beach (Fig. 2-1) and Nevada Beach (Fig. 2-2) where young beach features are found about 1 m above the modern shore.

Higher than natural lake levels since the upper limit was leally established in 1935 are causing the shorezone system of Lake Tahoe to seek a new equilibrium condition. Along much of the eastern shore and other rocky areas, bedrock and boulders are sufficiently resistant to change that the higher lake level has had limited impact (Fig. 2-3). Along many other parts of the shore, however, large wave-cut escarpments, overhanging banks, and other signs of active shore erosion are present (Figs. 2-4 to 2-6). This suggests that in many places the shorezone is not yet in equilibrium. Given current management of the Lake Tahoe dam, shorezone erosion will continue but may decrease through time as more areas along the shore reach equilibrium. Continuing erosion represents a direct threat to many properties and structures along the shore and will result in the introduction of sediment and nutrients into Lake Tahoe for the foreseeable future.

Figure 2-1. Vertical aerial photograph of Baldwin Beach (August 19, 1995) showing a series of beach ridges inland from the modern beach ridge. The older, slightly higher beach ridge crests are marked by red lines, and the extent of these older beach deposits are outlined in yellow. The modern ridge is marked by a blue line. The older beach ridges may have formed in the early 20th century when lake levels reached above 1899.23 m (6231 ft). See Fig. 1-2.

Figure 2-2. Aerial photograph of Nevada Beach (August 25, 1963) showing large beach platform that may have formed in early part of the 20th century when lake levels exceeded 1898.65 m (6229.1 ft). The yellow line marks marks the landward limit of this feature. Note the change in vegetation.

Figure 2-3. Armored shore along the east side of Lake Tahoe. This type of shorezone is relatively resistant to erosion from waves.

Figure 2-4. Fresh wave-cut escarpment in unconsolidated sediments. The shoreline angle is the abrupt break in slope at the top of the beach and at the base of the escarpment.

Figure 2-5. Two views of a wave-cut escarpment at Lake Forest on the northern shore of Lake Tahoe. In the photograph to the left, taken on May 17, 2000, lake level is near maximum and wave activity can directly impact the backshore area. In the photograph below, taken at the same place on August 28, 2003, lake level is much lower. The shore has undergone erosion here since May, 2000, as evidenced by the blocks of sediment at the base of the small escarpment. This erosion probably occurred from undercutting by wave activity when water level was high.

Figure 2-6. Photograph of actively eroding shoreline at Sugar Pine Point on the western shore of Lake Tahoe. Note how the trees are being undercut, causing them to lean and eventually fall into the lake.

Shorezone Protective Structures and Their Effects on Coastal Processes

Shorezone protective structures are almost invariably designed and built to do one thing, protect the backshore area directly behind the structure from further erosion. They are not designed to protect the beach in front of the structure, nor are they designed to protect areas of the shore on either side of the structure. We make a distinction between static, vertical, impermeable structures and sloping, dynamic structures. Vertical seawalls and sheet pile structures are examples of the former and permeable structures composed of boulders, cobbles, and gravel are examples of the latter. In addition to the references cited within the text below, the following discussion is also based on the works of McDougal et al. (1987), Weggel (1988), Bruun (1988), Wood (1988), Kraus (1988), Komar and McDougal (1988), Griggs and Fulton-Bennett (1988), Griggs and Tait (1988), Plant and Griggs (1992), Lorang (1992), and Kraus and McDougal (1996).

The debate over whether or not seawalls or other types of “hard” engineering solutions negatively affect beaches has been vigorous during the last 20 years. At this time, there does not appear to be a clear consensus on how structures affect beach processes, probably because of the wide range of parameters that control how a particular beach system responds to changes in one or more of these parameters. However, much of the

controversy about the harmful effects of sea walls on beaches could be due to practitioners failing to distinguish between "passive" and "active" erosion. Pilkey and Wright (1988) referred to passive erosion as being "…due to tendencies which existed before the wall was in place," and active erosion as being "…due to the interaction of the wall with local coastal processes." In other words, active erosion is when the wall or other type of revetment directly increases erosion in front of, or to either side of, the structure.

Seawalls and other types of static revetments can negatively interact with coastal processes in several ways, including reducing sediment supply, inhibiting storm response and recovery, shoreface steepening, and narrowing of the surf zone (Pilkey and Wright, 1988). Constructing seawalls at the base of eroding bluffs immediately cuts off this source of beach sand. Considering that Osborne et al. (1985) documented that much of the beach sand at Lake Tahoe is derived from eroding backshore areas, elimination of this source of sediment likely has had negative effects on many of the lake's beaches. It must be borne in mind, however, that this effect will occur regardless of the type of structure.

When steep storm waves impact a shore, they commonly move sand offshore causing a narrowing and steepening of the beach (Komar, 1998). Along the western coast of the U.S., this process commonly occurs during the winter months. During subsequent summer months, long-period swell arriving from far distant parts of the Pacific Ocean gradually move the sand back toward shore causing a widening and flattening of the beach, thus completing the yearly cycle (Komar, 1998). Because swell does not exist at Lake Tahoe, relatively steep storm waves are the most geomorphically effective waves that impact the Lake Tahoe shoreline. Sand transport during these periods is dominantly directed either alongshore or offshore. Once sand is moved offshore, it may be lost to the shore system. Without continued renewal from eroding bluffs or alongshore sources, protective beaches are reduced. During calmer periods, the presence of ripples oriented parallel to the shore may be evidence that, at times, there is a net shoreward movement of sand-sized sediment. At present, however, the relative magnitude of onshore versus offshore sand transport is not known.

Another way that shorezone protective structures may impact the beach is by reflecting wave energy back toward the lake which causes scour in front of the structure (Pilkey and Wright, 1988). The degree to which this occurs may be dependent on where the structure is placed relative to water level and the wave run up zone. If a structure is placed above the wave run up zone, then its presence is likely to have little influence on beach dynamics. If the structure is placed within the active swash zone, however, it can cause wave reflection and net offshore sediment transport. Because sloping dynamic revetments absorb some of the wave energy through kinetic motions of individual particles, there may not be as much wave energy reflectance and consequent beach scour (Komar, 1998). The permeable nature of dynamic revetments also tends to reduce the amount of backwash that may reduce scour in front of the structure.

Shorezone Protective Structures at Lake Tahoe

To examine the specific effects of protective structures on shorezone processes at Lake Tahoe, we compared detailed topographic-bathymetric maps of individual parcels that had shorezone protective structures installed to detailed basin-wide bathymetry. Basin-wide bathymetry was obtained with a LIDAR-equipped airplane in July 2000. For this phase of the study, TRPA supplied twelve project files, each with topographic-bathymetric maps with one or two foot contours. Three of these were deemed unsuitable for our objectives because they were pier replacement or pier modification projects. Of the remaining project files, most structures were classified as sloping, dynamic revetments and only one was considered to be a vertical, static revetment.

Project topographic maps were scanned in order to begin a rectification process using ENVI image processing software. Once the image was digitized, an attempt was made to rectify the project maps to 1992 and 1998 digital orthophoto quadrangles (DOQs). The rectification technique used was similar to that applied in an earlier phase of this study to rectify aerial photographs around the perimeter of Lake Tahoe (see Chapter 3 and Adams and Minor, 2002). Whereas an aerial photograph might cover several square miles and have many roads, buildings, and natural features to select as common ground control points[1], topographic maps of the revetment projects were much smaller. A typical project map shows one or two small buildings, often within a dense canopy of trees, immediately inland from a short stretch of shore. Consequently, rectification posed a significant challenge because common ground control points were exceedingly difficult to identify. In effect, virtually all of the project maps did not have enough common ground control points to accurately rectify them to the DOQs. An exception is the Fleur de Lac topographic map that possessed enough common ground control points to be rectified and imported into ArcView geographic information system (GIS) software where contour lines were traced as a separate theme.

Although LIDAR shallow-water bathymetry data were collected on July 16 and 17, 2000, DRI did not receive the first dataset (10 x 10 x 0.15 m) until January 20, 2001 and the second, more detailed (4 x 4 x 0.15 m) dataset until May 31, 2001. Resolution of the original bathymetric data was 4 x 4 x 0.15 m, which means that each pixel was 4 m on a side and had a vertical resolution of 15 cm. The original data was resampled to 10 x 10 x 0.15 m (herein referred to as coarse bathymetric data) and then released to DRI. In the resampling process, the heights of all objects in a given pixel are averaged and recorded to the nearest 15 cm. Although the vertical resolution is still 15 cm after resampling, this is an average height for the pixel and much information is lost.

The coarse bathymetric data was merged with deep-water bathymetry (Gardner et al., 1999) to yield an impressive view of the bed of Lake Tahoe. Many features can be seen in the shallow areas around the lake that were never seen before (e.g., submerged shorelines, abrasion platforms, and large scale bed forms). Contour lines derived from the

[1] Common ground control points are features that can be identified on both the base DOQ and the image or map that is being rectified.

coarse bathymetric data delineate large-scale features along the shore but are not sufficiently detailed to look at near-shore changes at the parcel level.

The fine bathymetric data (4 x 4 x 0.15 cm) represents a six-fold increase in resolution over the coarse data because of the much smaller 4 x 4 m cell size. Elevation averaging still occurred within the 16 m^2 cells of the fine data, however. The high quality and resolution of the LIDAR bathymetric data must be emphasized because this represents a significant advance over all other readily available topographic or bathymetric sources of data. Limitations discussed below are more a function of the proposed application than of the data itself.

To evaluate these limitations, a comparison was made between a project contour map from Fleur De Lac Estates at Tahoe Pines (1 foot contours; September, 1997) and contours derived from the fine bathymetric data (Figs. 2-7 and 2-8). This part of the shore consists of two breakwaters that nearly enclose a marina or lagoon and have been in place since at least 1939. From site drawings and other information gleaned from the project file and various aerial photographs, vertical shorezone protective structures are also located to the north and south of the breakwaters. Contours derived from the LIDAR 4 x 4 x 0.15 m bathymetry data are shown in Fig. 2-7. Although the higher-resolution data offers a significant improvement over the lower-resolution data, the high-resolution data still does not appear to be appropriate for comparison to project contour maps. Note how resolution of the data affects the creation of the contour lines and the mismatch between the "0" contour line and the shore (Fig. 2-7) Data gaps are also clearly evident where the data grid does not coincide with the shoreline.

As can be seen from Fig. 2-8, project-file and LIDAR contours are not at all coincident. In places, the two sets of contour lines are nearly orthogonal to one another. This situation can mean one of two things. Either there has been a large amount of change in near-shore bathymetry or one or the other data sets is inaccurate or too coarse to make the comparison. Because the project contours appear sufficiently detailed and fit the shore geometry very well, we conclude that this data is reasonably accurate. In contrast, contour lines generated from the LIDAR data do not perfectly follow the shoreline and many are not continuous. The discontinuous nature of many of the contour lines appears largely due to edge effects, where the contours are inadvertently controlled by the edge of the grid. Edge effects are particularly prominent around some of the piers where contours close around data gaps (Figs. 2-7 and 2-8). The LIDAR data is accurate, but does not appear to be able to provide high enough resolution to make these types of comparisons at the parcel level.

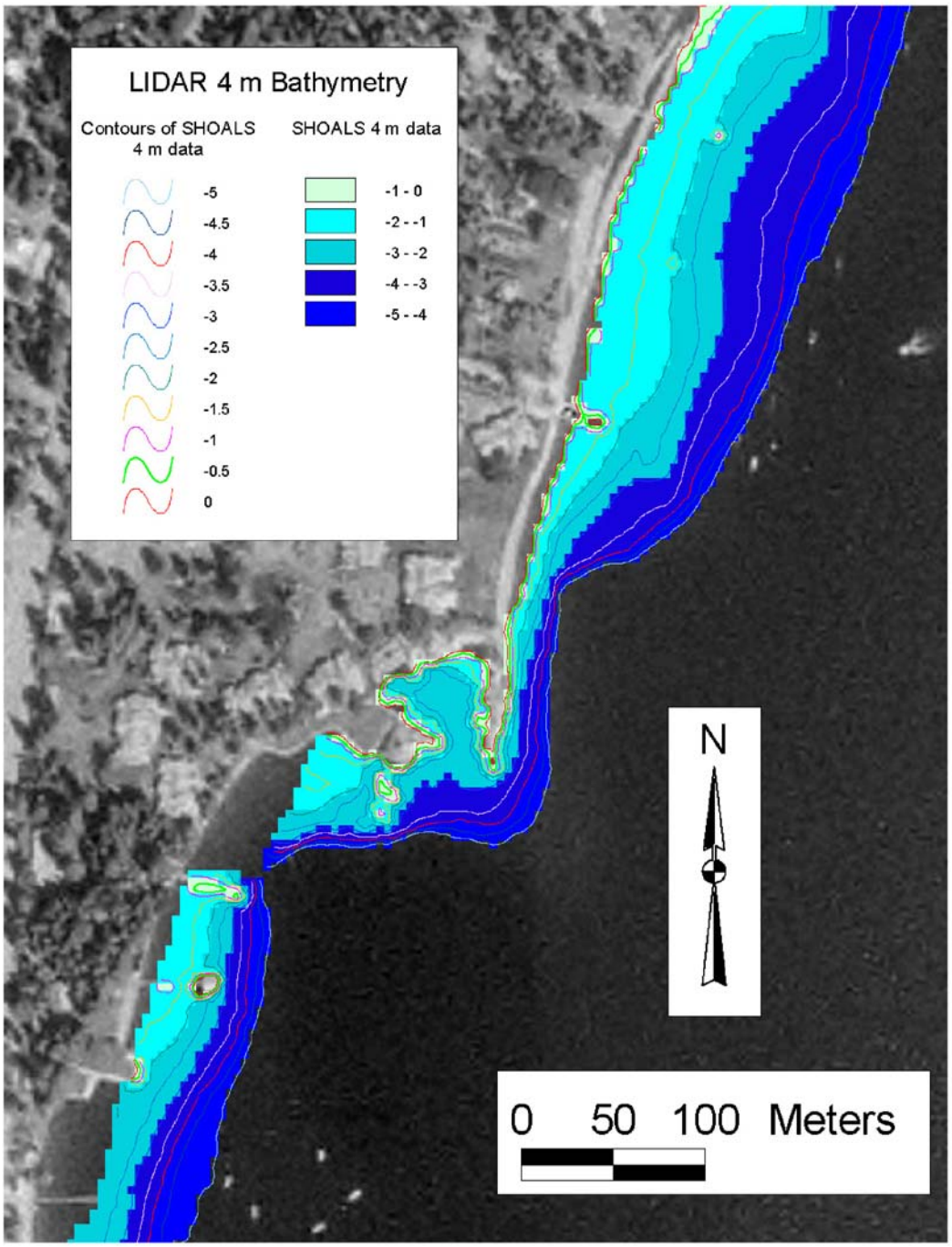

Figure 2-7. Map of the Fleur de Lac site with shallow-water bathymetry and 0.5 m contours superimposed on the 1998 DOQ.

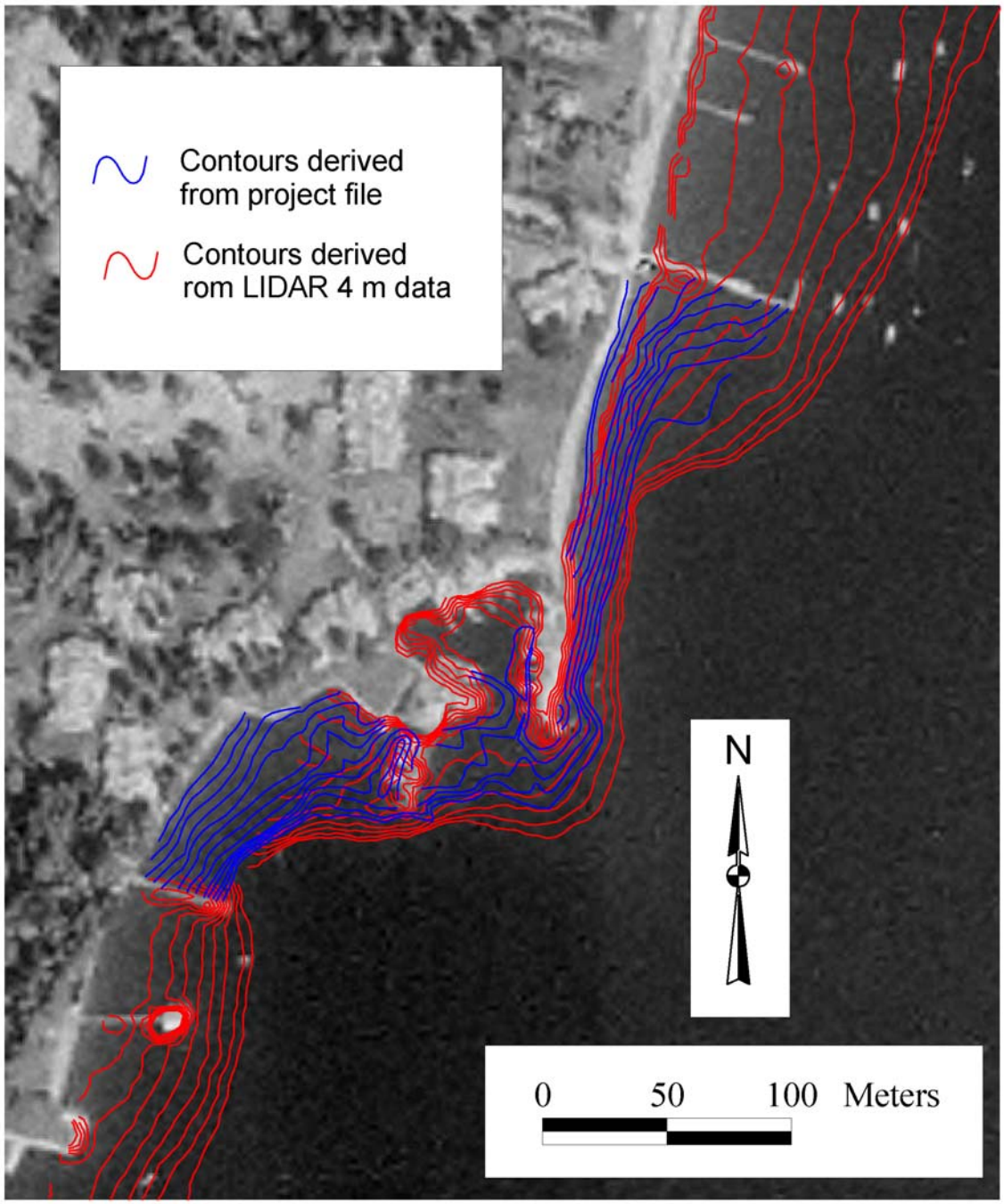

Figure 2-8. Map of the Fleur de Lac area showing a comparison between contours derived from project files and contours derived from LIDAR data. Note how in some places the contour lines are nearly orthogonal.

From this exercise, we conclude that assessing bathymetric change by comparing project contour maps to high precision LIDAR bathymetry is not feasible. The hypotheses proposed in the DRI/TRPA Shorezone Erosion Study Phase II proposal dated November 1, 2000 are, therefore, not testable by this means. These hypotheses stated that vertical,

impermeable, static revetments cause significantly elevated rates of erosion in the foreshore and that dynamic, permeable, sloping revetments slow shorezone erosion and have insignificant impacts on foreshore bathymetry.

Although the above hypotheses could not be tested, general recommendations concerning shorezone protective structures can be made based on a literature survey and observations made during the course of this study. The main concern with vertical, static revetments is that they may reflect wave energy back toward the lake, thus causing accelerated erosion in front of the structure. Whether or not this occurs depends on several factors including the position of the vertical revetment relative to wave run-up and the particle size distribution of sediments in front of the structure. A vertical wall placed outside of the maximum run-up zone clearly will have no effect on beach processes, whereas a wall placed well within the surf zone will reflect some of the wave energy and may adversely affect beach processes (Weggel, 1988). The degree to which beach processes are affected depends on the wave climate at the site and the particle size distribution of the foreshore in front of the wall. If the foreshore is armored with gravel, cobbles, or boulders, probably little change will be induced by wave reflection. If the foreshore is composed of sand, however, then wave reflection may cause significant scour.

Sloping, dynamic revetments absorb some wave energy through movement of particles within the revetment (Komar, 1998). Because of the sloping design, additional energy is expended as waves break and run-up the structure. Both of these processes absorb wave energy and decrease reflected wave energy. Scour due to backwash is also reduced because some of the run-up percolates into the structure, thereby decreasing the amount of water in the backwash. All of these features mimic natural processes on a coarse gravel beach, which makes them less likely to adversely affect beach processes in the vicinity.

We recommend against rigid implementation of a blanket policy uniformly applied to all lake front properties. A more reasonable approach would be to treat each project individually, taking into consideration site-specific factors including foreshore particle size distributions, height of total swash elevation relative to the location of the revetment, composition of the backshore, beach gradient, and the local wave climate. Generally, sloping dynamic revetments are less likely to have adverse affects on shorezone processes than do seawalls, but they may not be appropriate for every situation. Because total swash elevation is so important to shorezone erosion and wave interactions with revetments, the manner in which it is calculated should conform to the most recent and defensible research of this process (Komar, 1998). Examples using this procedure to calculate the height of wave run-up are presented in Chapter 4.

Chapter 3
Historic Shorezone Erosion and its Impact on Sediment and Nutrient Loading

Kenneth D. Adams
Timothy B. Minor

This chapter reports the results of a detailed study that incorporates georectified air photographs into a GIS database to track shoreline changes over a 60-year period. These results were then combined with field observations and nutrient sampling to determine the amount and processes of sediment, phosphorus, and nitrogen input into Lake Tahoe from shorezone sources. We compared mass estimates derived from this study to other sources to determine the relative magnitude of nutrient and sediment input from the shorezone. In addition, we used particle-size data for sediment samples from around the lake to estimate total masses of sand, silt, and clay introduced into the lake from shorezone sources from 1938 to 1998. Most of this chapter was published independently, except for the particle-size data, in the *Journal of Coastal Research* in 2002 (Adams and Minor, 2002).

Methods

Aerial Photograph Acquisition

Historical aerial photographs and mosaicked DOQs spanning 60 years were acquired from the U.S. Geological Survey (USGS), U.S. Forest Service (USFS), and Tahoe Regional Planning Agency (TRPA). Table 3-1 indicates the dates the photographs were taken, the geographic location, photographic scale, and responsible agency. Photographic scales ranged from 1:8,000 to 1:20,000. A scale of 1:20,000 is considered the smallest usable for shoreline mapping (Moore, 2000). The color and black and white photographic prints were scanned and digitized using a flat bed scanner. Resolution varied between 300 dots per inch (dpi) and 600 dpi, depending on the scale and quality of the photographic prints. Using the resolution, print dimensions, and digital image dimensions (in picture elements or pixels), the nominal ground resolutions of the aerial photographs were calculated. For the 1:20,000 scale prints, the ground resolution was 2 m; for the 1:8,000 scale photographs from 1995, the ground resolution was 1 m; ground resolution for the two DOQs was also one meter.

Image Processing Methods

The multi-date, multi-scale aerial photographs of the Lake Tahoe basin were rectified to the 1 m DOQs in a standard, polynomial-based, image-to-map rectification process using ENVI image processing software. Initial attempts to orthorectify the historical photographs proved unsuccessful, as the camera parameters required to build interior orientation were not available for the older photographs. Fiducial marks and focal length are required to establish the relationship between the camera model, the aerial photographs, ground control points (GCPs), and a digital elevation model (DEM) (Thieler and Danforth, 1994). We also attempted to rectify the aerial photographs using a Delaunay

Table 3-1. Information about aerial photographs used in this study.

Year and Photo	Scale	Agency	Location	Water Surface Elevation
1938				
BPB14-69	1:20,000	USFS	Glenbrook Bay	1898.18 m
BPB14-75	1:20,000	USFS	Zephyr Cove	1898.18 m
1939				1898.18 m
CDJ14-51	1:20,000	USFS	Sunnyside/Tahoe City	1898.18 m
CDJ14-53	1:20,000	USFS	Sunnyside/Ward Creek	1898.18 m
CDJ14-55	1:20,000	USFS	Idlewild/Blackwood Creek	1898.18 m
CDJ14-70	1:20,000	USFS	Meeks Bay/Rubicon Bay	1898.18 m
CDJ14-72	1:20,000	USFS	Sugar Pine Point	1898.18 m
CDJ14-72revised	1:20,000	USFS	Sugar Pine Point	1898.18 m
CDJ14-74	1:20,000	USFS	Homewood/Sugar Pine Point	1898.18 m
CDJ14-79	1:20,000	USFS	Tahoe City	1898.18 m
CDJ15-52	1:20,000	USFS	Dollar Point	1898.18 m
CDJ15-54	1:20,000	USFS	Carnelian Bay	1898.18 m
CDJ15-56	1:20,000	USFS	Carnelian Bay/Agate Bay	1898.18 m
CDJ16-44	1:20,000	USFS	Agate Bay/Stateline Point	1898.18 m
CDJ16-48	1:20,000	USFS	Stateline Point/Crystal Bay	1898.18 m
CDJ16-112	1:20,000	USFS	Crystal Bay/Incline Village	1898.18 m
CDJ17-15	1:20,000	USFS	Sand Harbor	1898.18 m
1940				
CNL23-2	1:20,000	USFS	Rubicon Bay	1898.36 m
CNL23-3	1:20,000	USFS	Rubicon Point	1898.36 m
CNL23-4	1:20,000	USFS	Emerald Bay	1898.36 m
CNL23-5	1:20,000	USFS	Emerald Bay	1898.36 m
CNL23-68	1:20,000	USFS	Baldwin Beach	1898.36 m
CNL23-74	1:20,000	USFS	Camp Richardson/Truckee Marsh	1898.36 m
CNL23-137	1:20,000	USFS	Truckee Marsh/South Lake Tahoe	1898.36 m
CNL23-140	1:20,000	USFS	Nevada Beach/Marla Bay	1898.36 m
CNL23-141	1:20,000	USFS	Nevada Beach	1898.36 m
1952				
ABM3k-63	1:20,000	USFS	Carnelian Bay/Agate Bay	1898.52 m
ABM3k-103	1:20,000	USFS	Agate Bay/Stateline Point	1898.52 m
DSC6k-121	1:20,000	USFS	Sugar Pine Point	1898.55 m
DSC6k-177	1:20,000	USFS	South Lake Tahoe	1898.55 m
DSC6k-178	1:20,000	USFS	South Lake Tahoe/Nevada Beach	1898.55 m
1963				
EME-8-69	1:20,000	DRI	Bijou Park	1897.86 m
EME-8-70	1:20,000	DRI	Bijou Park/Edgewood	1897.86 m
EME-8-71	1:20,000	DRI	Edgewood/Nevada Beach	1897.86 m
1992				
DOQ	1:12,000	USGS	Entire basin	1896.25 m
1995				
TAH-12N-170	1:8,000	TRPA	Dollar Point	1897.95 m
TAH-11N-139	1:8,000	TRPA	Lake Forest	1897.95 m
TAH-10N-138	1:8,000	TRPA	Lake Forest	1897.95 m
TAH-9N-109	1:8,000	TRPA	Tahoe City	1897.95 m
TAH-8N-220	1:8,000	TRPA	Tahoe City/Tahoe Tavern	1897.95 m
TAH-8N-219	1:8,000	TRPA	Sunnyside	1897.95 m
TAH-8N-218	1:8,000	TRPA	Sunnyside	1897.95 m

Table 3-1 **(c**ont.)

TAH-8N-217	1:8,000	TRPA	Sunnyside/Ward Creek	1897.95 m
TAH-8N-215	1:8,000	TRPA	Ward Creek/Kaspian	1897.95 m
TAH-8N-213	1:8,000	TRPA	Kaspian/Blackwood Creek	1897.95 m
TAH-8N-211	1:8,000	TRPA	Tahoe Pines/Homewood	1897.95 m
TAH-8N-209	1:8,000	TRPA	Homewood	1897.95 m
TAH-9S-125	1:8,000	TRPA	Chambers Lodge/Tahoma	1897.95 m
TAH-10S-122	1:8,000	TRPA	Tahoma/Sugar Pine Point	1897.95 m
TAH-11S-54	1:8,000	TRPA	Sugar Pine Point	1897.95 m
TAH-11S-56	1:8,000	TRPA	Meeks Bay	1897.95 m
TAH-11S-58	1:8,000	TRPA	Rubicon Bay	1897.95 m
TAH-11S-60	1:8,000	TRPA	Rubicon Bay	1897.95 m
TAH-12s-47	1:8,000	TRPA	Emerald Bay	1897.95 m
TAH-12s-49	1:8,000	TRPA	Emerald Point	1897.95 m
TAH-12s-50	1:8,000	TRPA	D.L. Bliss State Park	1897.95 m
TAH-13s-2	1:8,000	TRPA	Emerald Point/Eagle Point	1897.95 m
TAH-13s-4	1:8,000	TRPA	Baldwin Beach-west side	1897.95 m
TAH-14s-209	1:8,000	TRPA	Baldwin Beach	1897.96 m
TAH-15s-154	1:8,000	TRPA	Baldwin Beach/Kiva Beach	1897.96 m
TAH-16s-153	1:8,000	TRPA	Pope Beach	1897.96 m
TAH-17s-72	1:8,000	TRPA	Pope Beach/Tahoe Keys	1897.96 m
TAH-18s-71	1:8,000	TRPA	Tahoe Keys/Upper Truckee River	1897.96 m
TAH-19s-207	1:8,000	TRPA	Truckee Marsh/South Lake Tahoe	1897.96 m
TAH-20s-205	1:8,000	TRPA	S. Lake Tahoe	1897.96 m
TAH-21s-144	1:8,000	TRPA	Nevada Beach	1897.96 m
TAH-21s-146	1:8,000	TRPA	Stateline/Edgewood Golf Course	1897.96 m
TAH-21s-148	1:8,000	TRPA	South Lake Tahoe	1897.96 m
1998				
DOQ	1:12,000	USGS	Entire basin	1898.50 m

triangulation warping method, which fits triangles to irregularly spaced GCPs and interpolates new values. This method was unsuccessful, however, because it required control points on all sides of the feature of interest—in this case the shoreline—and selecting control points in the lake was not possible.

The image-to-map rectification process that proved to be successful involved selection of ground control points common to both the scanned aerial photography and the USGS DOQs. Several rule bases were developed for the point selection process in order to minimize potential errors that can accumulate and contribute to inaccurate shoreline interpretation results. Favorable control points selected included anthropogenic and natural features that were distinct and common to both data sets (road intersections, buildings, trees, and near-shore boulders). Care was taken to be cognizant of shadowing effects in the photographs and DOQs when selecting GCPs, as these sometimes distorted the precise location of a feature. To avoid introduction of spatial errors due to lens distortion and camera tilt, control points were preferentially selected in the center of each unrectified photograph. Along steep shores, control points were only selected near the shore zone to avoid errors related to topographic relief displacement. Selecting control points at elevations significantly higher than lake level introduces significant errors into the rectification process. This was evident when selecting control points on photographs

taken over the Emerald Bay region; greater errors were observed for points selected at higher elevations along Highway 89 than those located near the shore.

A minimum of ten GCPs was selected for each scanned photograph. Older photographs presented greater challenges in the process, as there were often few common features found between the historical aerial images and the more recent DOQs. Root mean square error (RMSE), the average error that describes the difference between the predicted and observed control point locations in an input image relative to the DOQs, was between 2.0 to 2.25 image picture elements (pixels or cells) for each of the rectified photographs. That is, for each of the photographic images rectified, the RMSE for all control points in that image was approximately 2.1 pixels. In ground distance, a RMSE of 1.0 for the 1:20,000 scale photographs was 2m. For the 1:8,000 scale 1995 photographs, the RMSE ground distance was 1m per image pixel. Several iterations were required in many of the GCP selection processes to arrive at a satisfactory RMS level for all the photographs. Once the GCPs were selected, a first-degree polynomial-warping algorithm was implemented, with a nearest-neighbor resampling method. The uncorrected images were warped and resampled to the DOQs and cast into a Universal Transverse Mercator (UTM) coordinate system (Zone 10) based on the 1927 North American Datum (NAD27).

Based on the calculated RMSE observed in the rectification process, the observed spatial error in ground distance over an entire photograph was +/- 4.0 m (RMSE of 2.1). In actuality, however, that error term is much less for the feature of interest, the shorezone, where the error is closer to +/- 2 m for the 1:20,000 scale photography, and even less (+/- 1 m) for the 1995 imagery (RMSE of 1.0 in both cases). This estimate is based on an examination of the errors for individual control points along the immediate shorezone, where the RMSE was sometimes found to be below 1.0. This occurred because most of the control points in each image were selected near the shorezone, ensuring a better polynomial fit of the rectification model in that portion of the image. The control points selected further away from the shorezone were located on slopes, where the change in elevation contributed to the distortion found in the image, and thus increased overall RMSE for the entire image. These tolerances all exceed the National Mapping Accuracy Standards defined by the USGS in 1941 (10.2 m for 1:20,000 scale data; 8.0 m for 1:8,000 scale).

Delineating the Shoreline

The first challenge in mapping the former position of a shoreline is to define a consistent and obvious shoreline feature, one that can be recognized on multiple generations of aerial photographs of varying quality. The line between wet sediment and dry sediment is the most commonly used proxy for shoreline position because it approximates the mean high water line (Dolan et al., 1980; Moore, 2000). Most studies using this proxy have been conducted on open marine coasts, however, where the lateral position of the high water line varies considerably depending on tidal range, beach slope, wave energy, and other parameters (Dolan et al., 1980). Fortunately, Lake Tahoe does not have tides and is not affected by large waves that would affect the shoreline position shown in an aerial photograph. Therefore, we selected the linear interface between the water and shore to

represent the shoreline position in this study. Other markers (e.g., debris lines, crests of barriers, and bases of wave-cut scarps) may be visible in the field but are often difficult to discern in aerial photographs and may have different relationships to still-water level. In contrast, the shore-water interface is readily discernible in all photographs used in this study but presents other challenges (described below).

The lateral position of the shore-water interface through time is affected by a number of parameters including wave runup, wave setup, seiches, human activities, variations in lake level, and shoreline erosion and accretion. Lateral changes in the position of the shoreline due to wave runup, wave setup, and seiches are not significant in this study because none of the images appear to have been acquired when strong winds were affecting the lake. Human activities, such as infilling portions of the lakeshore or constructing seawalls or other revetments, are commonly discernable from aerial photographs and represent permanent alterations.

After georectifying the aerial photographs and importing them into a GIS database (ESRI ArcView 3.2), the shore-water interface was mapped at a scale of 1:3,000 as a separate theme for each year. At this scale, 1 mm equals 3 m on the ground, which is close to the resolution of the georectification process. Where adjacent photographs of the same age and water level overlapped, the image that most closely matched the two orthophotoquad bases (1992 and 1998) was used to map the shoreline. "Goodness of fit" was determined by how closely common ground features (e.g., roads, buildings, boulders, and other features) matched the base images for each of the rectified photographs. Almost the entire shoreline was mapped from 1938, 1939, and 1940 images (Table 3-1). Additional areas of the shoreline also were mapped from 1952, 1963, and 1995 images as well as 1992 and 1998 DOQs.

During the last 60 years, lake-level fluctuations were the most significant factor affecting the lateral position of the shore-water interface. These fluctuations cause the lateral position to migrate tens of meters with relatively minor changes. This effect, of course, depends on the slope of the shore, which is particularly pronounced on gently sloping offshore areas at the south end of the lake and near the outlet. In areas where the shore is relatively steep, this effect is relatively minor. During the last 100 years, the surface of Lake Tahoe has fluctuated from a historic high of 1899.29 m in July 1907 to a historic low of 1895.96 m on November 30, 1992 (Fig. 1-2). These fluctuations have been largely controlled by the rate of inflow into the basin relative to the volume of water released by the dam, which only controls the upper 2 m or so of lake level, and the volume of water evaporated from the surface of the lake. Since 1935, when the Truckee River Agreement went into effect, the upper legal limit of Lake Tahoe has been defined as 1898.65 m (6229.1 ft). Table 3-1 presents water surface elevations for the particular days that aerial photographs were taken from 1938 to 1998. These elevations range from a low of 1896.25 m on August 26, 1992 to a high of 1898.55 m on August 14, 1952, a difference of 2.3 m. During the last 15 years, Lake Tahoe has undergone the most dramatic lake-level changes in recorded history, fluctuating between its historic lowstand (1895.96 m)

in late 1992 to a level about 9 cm above the legal limit in early January, 1997. The net result of lake-level fluctuations is an apparent migration of the shoreline.

Superimposed on yearly lake-level fluctuations are real accretion and erosion changes to the Lake Tahoe shoreline. The challenge is to devise a methodology using multiple generations of aerial photographs taken on days with different lake levels to discern changes in the high shoreline position. Although most shoreline change likely happens when the lake is at or near its legal limit, the photographs were taken over a range of lake levels. We developed the following technique to estimate the position of the shore through time by correcting for different water levels.

This technique is based on the assumption that on a stable, sloping shore, the shore-water interface will migrate laterally in a predictable way depending on water level. This is essentially a process of inundation but may not apply perfectly to shores composed of unconsolidated sediment where subsequent wave action can regrade the shoreline causing a shift in the shoreline planform. At Lake Tahoe, this assumption is reasonably valid but may not apply to other bodies of water. Fig. 3-1 portrays the relationship between different lake levels impinging on a stable shoreline. In this image, all of the projected shorelines are parallel, and the distance between them is proportional to the difference in lake levels and the slope of the shore. The addition or subtraction of sediment along the shore is reflected in an apparent change in the shoreline position for a given water level with respect to the other projected shorelines.

We encountered four different situations were encountered when mapping the shoreline from 1938 to the present. The most common situation is represented by figure 3-1 where there has been no change and the shorelines plot primarily in a regular and parallel manner. The three other situations involve erosion, accretion, or oscillation and are represented by Figs. 3-2, 3-3, and 3-4, respectively. For each of these situations, we used the nearshore slope and simple trigonometry to estimate the amount of shoreline change that occurred. In this study, we assumed that the shape of the nearshore profile remained relatively constant through time although it may have shifted in space (Hands, 1983).

Based on water level, shoreline positions observed in the 1940 and 1952 photographs should plot in nearly identical positions to the 1998 shoreline (Table 3-1). If the 1940 or 1952 shorelines plot lakeward of the 1998 shoreline, then erosion must have occurred. If the 1940 or 1952 shorelines plot landward of the 1998 shoreline, then that particular location along the shore must have accreted. This also holds true for the lower-water-level 1938 and 1939 shorelines. If they plot landward of the 1998 shoreline, then shoreline accretion must have taken place (Fig. 3-3). If the 1938 and 1939 shorelines plot lakeward of the 1998 shoreline, change may still have occurred but is more difficult to document.

The first step in documenting change using the 1938 and 1939 photos is to calculate the nearshore slope at a particular location. Because we have no historical profile data we used the average slope at a location as a proxy for the profile. The average slope is

measured by using the 1992 and 1998 images combined with simple trigonometry (Fig. 3-5a). Assuming a constant slope through time, the 1938 or 1939 shorelines can be projected to reflect a lake level equal to that of 1998 (Fig. 3-5b). In other words, 0.5 m of water is added to the 1939 lake level to estimate where that shoreline would plot if the water level were the same as in 1998. If the 1998 shoreline plots significantly landward of the projected 1939 shoreline, then erosion must have occurred. When calculating volumes of eroded sediment, we only considered the volume of eroded subaerial bluff or beach material.

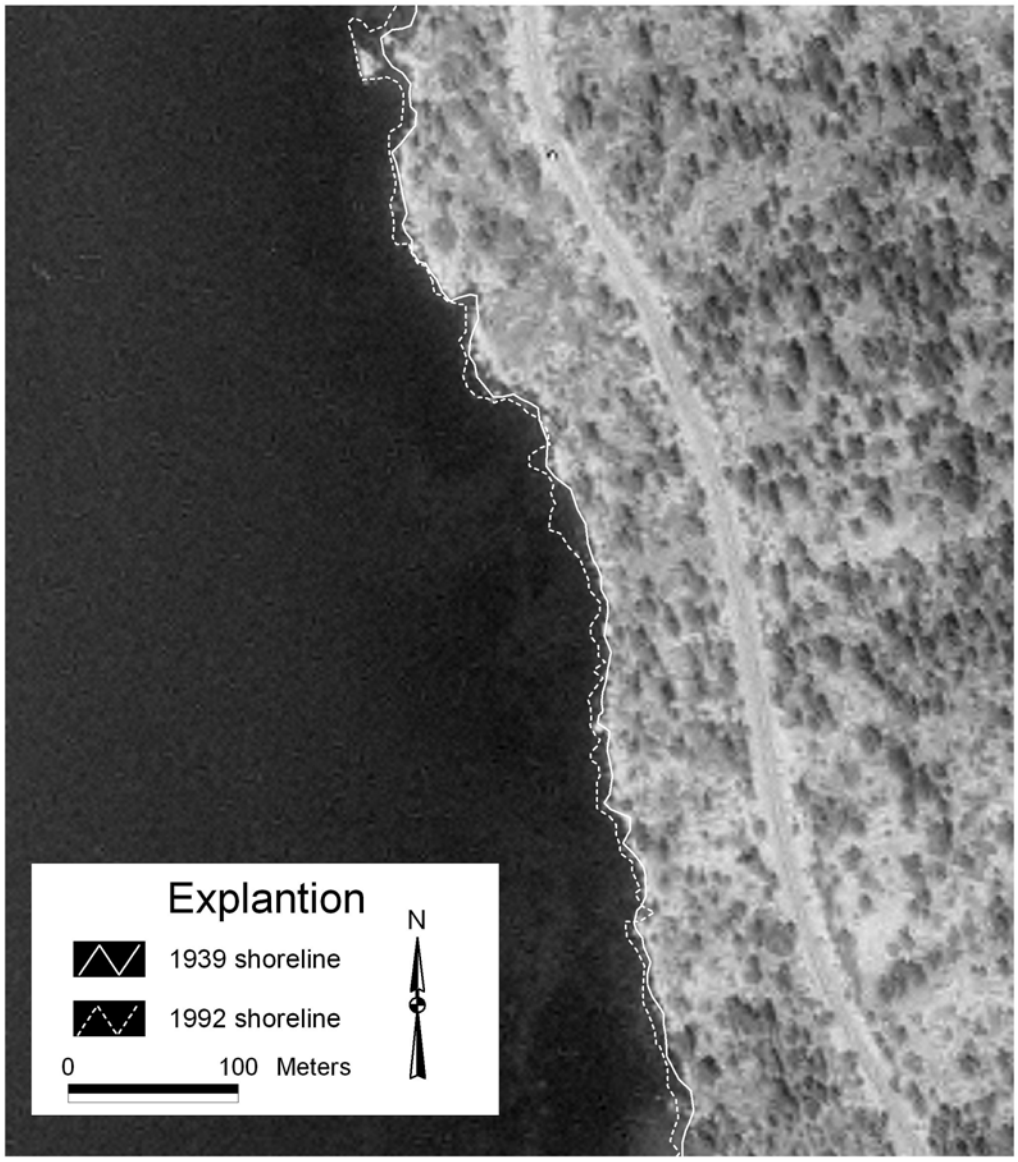

Figure 3-1. Shorelines from 1939 and 1992 superimposed on a 1998 image of the eastern shore of Lake Tahoe north of Sand Harbor. This section of shore apparently has been stable during the last 60 years. In 1998, lake level was at 1898.5 m; in 1939, at 1898.0 m; and in 1992, at 1896.25 m. Note how the superimposed shorelines form contour lines on this stable bedrock shore, with their spacing dependent on local slope.

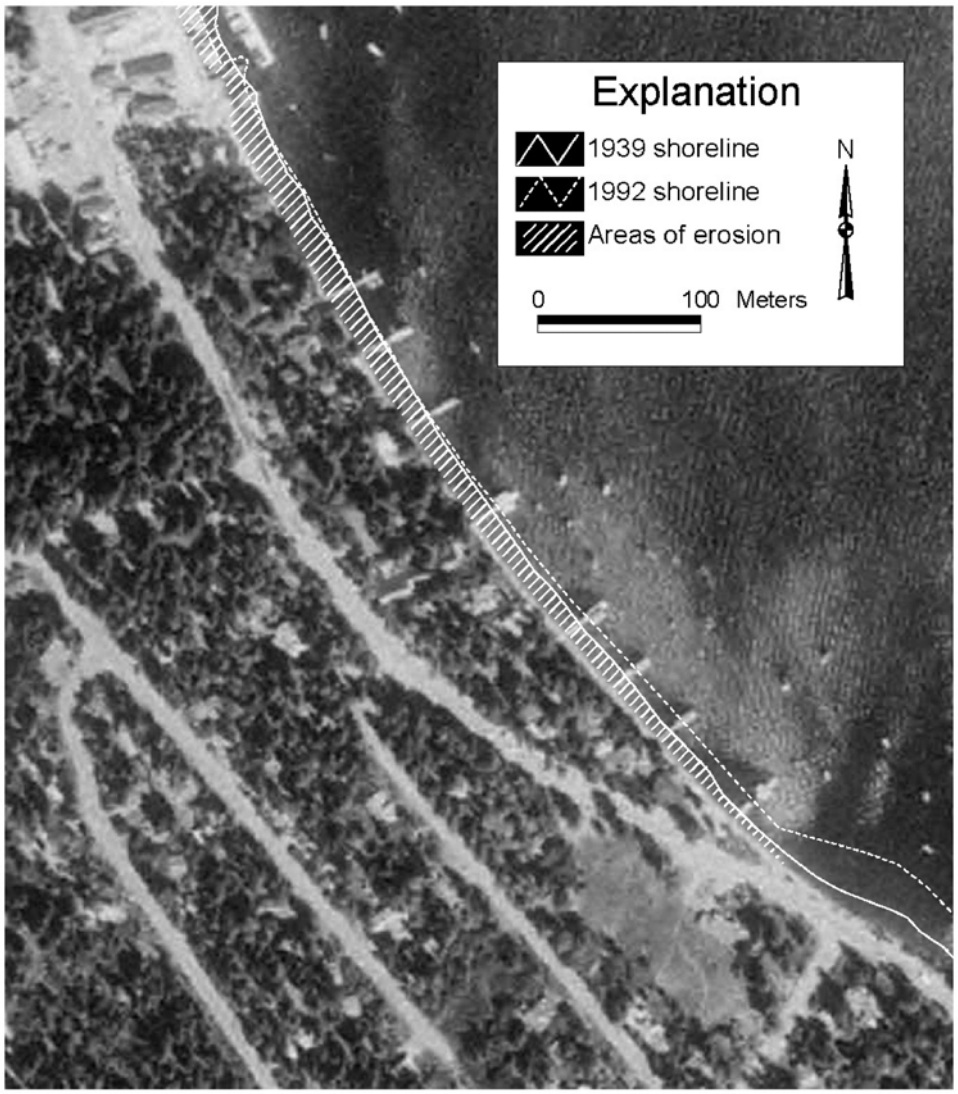

Figure 3-2. Shorelines from 1939 and 1992 superimposed on a 1998 image of the Homewood area. In this case, erosion is indicated because the 1939 shoreline (1898.0 m) is coincident with the 1992 shoreline (1896.25 m) along part of its length.

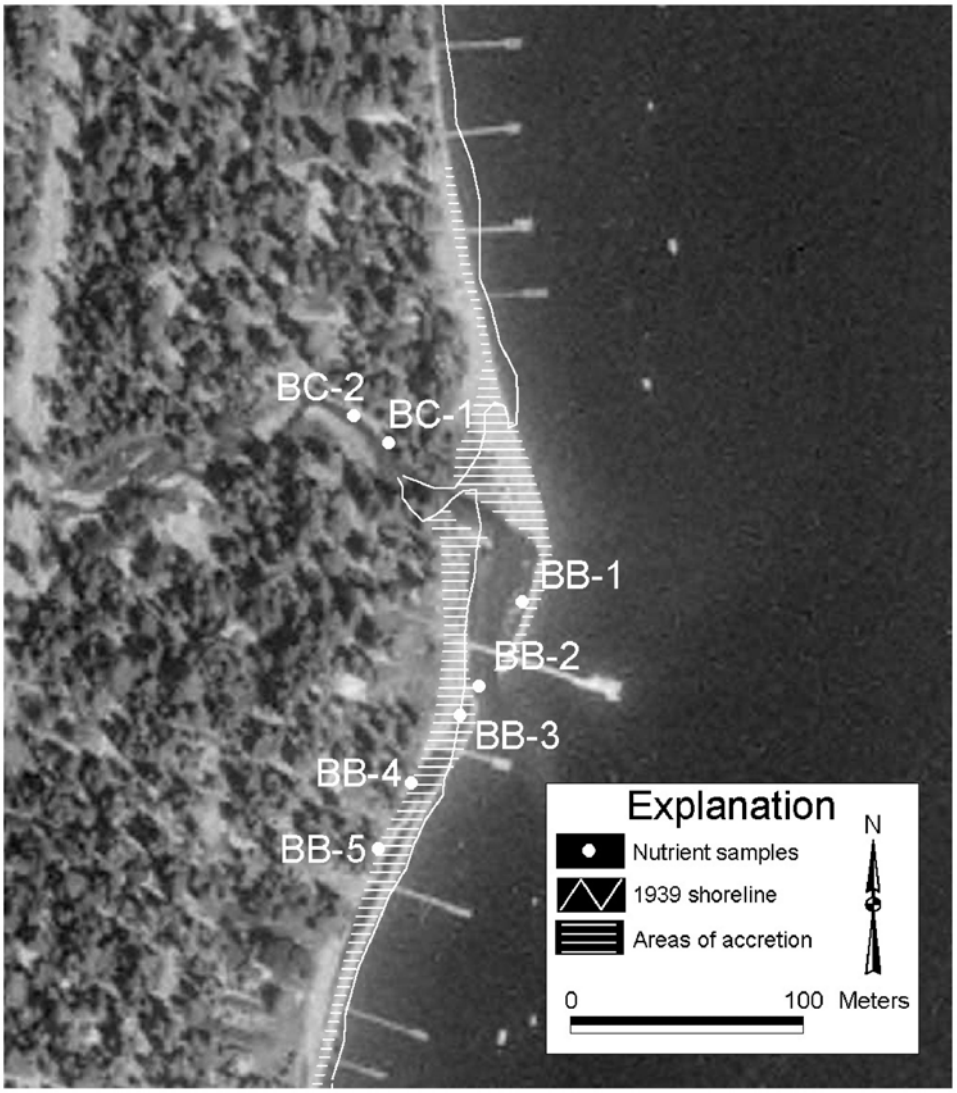

Figure 3-3. The shoreline from 1939 (1898.0 m) superimposed on a 1998 image (lake level = 1898.5 m) of the mouth of Blackwood Creek. Note that the shore has built lakeward even though lake level in 1939 was about one half meter below that in 1998.

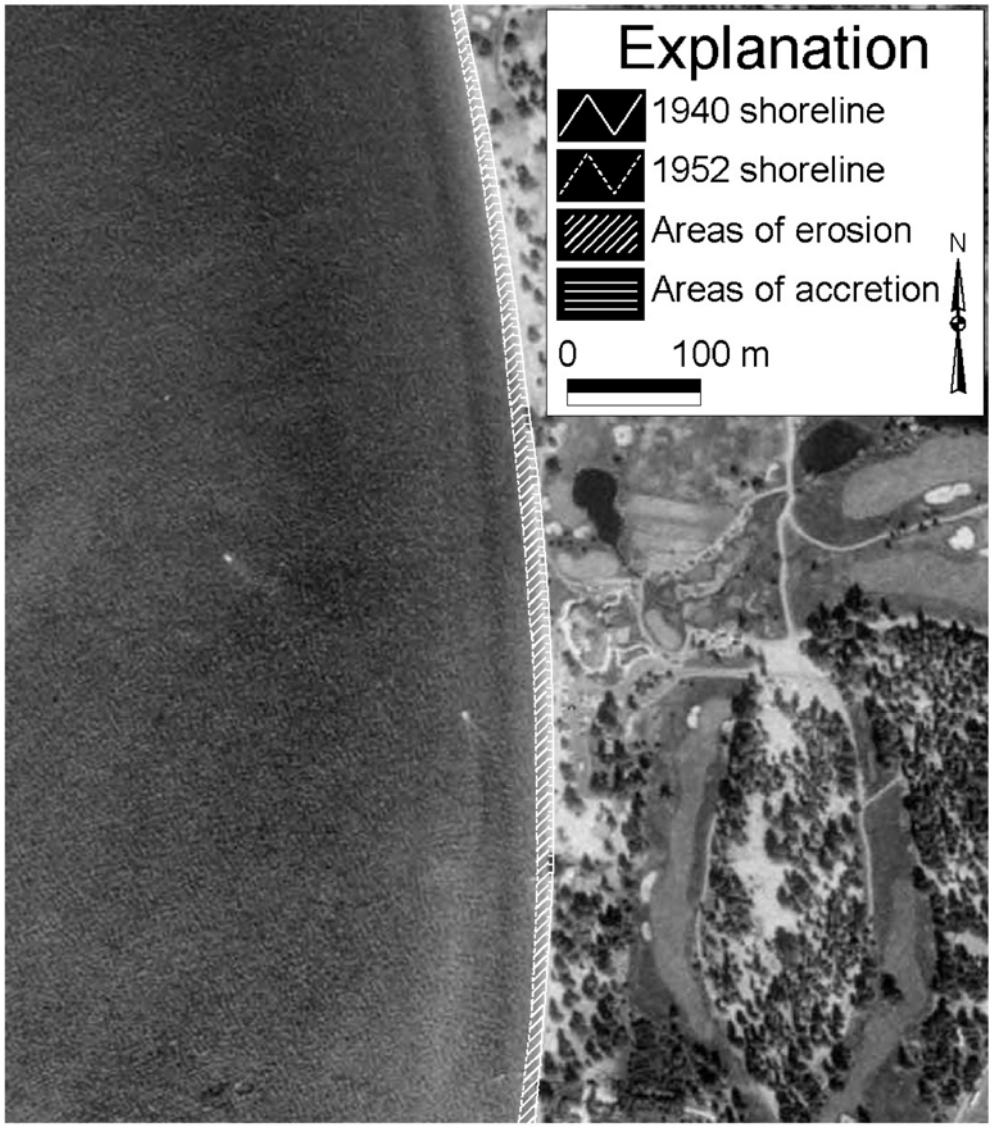

Figure 3-4. Shorelines from 1940 (1898.36 m) and 1952 (1896.25 m) superimposed on a 1998 image (lake level = 1898.5 m) from Edgewood Golf Course along the southeastern shore of Lake Tahoe. In this case, there was accretion from 1940 to 1952 followed by erosion from 1952 to 1998.

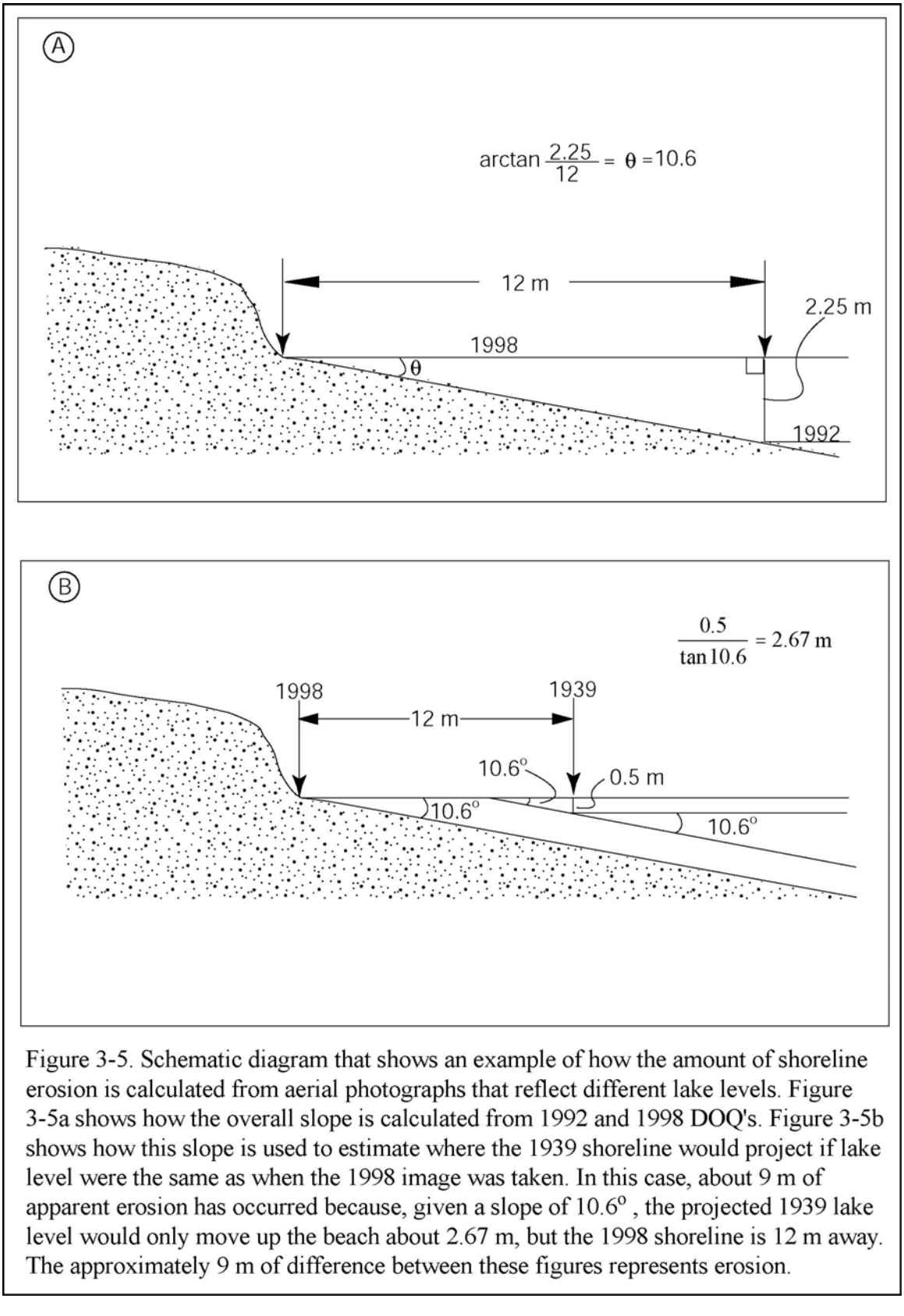

Figure 3-5. Schematic diagram that shows an example of how the amount of shoreline erosion is calculated from aerial photographs that reflect different lake levels. Figure 3-5a shows how the overall slope is calculated from 1992 and 1998 DOQ's. Figure 3-5b shows how this slope is used to estimate where the 1939 shoreline would project if lake level were the same as when the 1998 image was taken. In this case, about 9 m of apparent erosion has occurred because, given a slope of 10.6^{o} , the projected 1939 lake level would only move up the beach about 2.67 m, but the 1998 shoreline is 12 m away. The approximately 9 m of difference between these figures represents erosion.

In this case, comparing the 1940 shoreline position to that of 1998 indicates that accretion has taken place. Comparing the 1952 shoreline position with 1998, however, indicates that the shore has eroded. We interpreted these changing shoreline positions through time to represent a dynamic situation where from 1940 to 1952 the shoreline was accreting, but from 1952 to 1998 the shoreline eroded back to near the 1940 position. Therefore, although both erosion and accretion have taken place along this shore during the last 60 years, shorezone processes have resulted in net erosion.

Nutrient Sampling and Analysis

Grab samples of shorezone sediments were taken at multiple locations around the lake to analyze nutrient content (Table 3-2). Grain size was characterized in the field and compared to analyses performed by Osborne et al., (1985). Typically, samples for this study were taken from beaches, wave-cut scarps, and backshore areas. Grab samples were collected at a depth of about 10 cm on beaches and backshore areas and at depths of up to 3 m in wave-cut scarps.

Samples were analyzed for total phosphorus and total Kjeldahl nitrogen by DRI's Division of Hydrological Sciences analytical chemistry laboratory. Total phosphorus and total kjeldahl nitrogen analytical procedures were used as a conservative measure of nutrient content because it is unlikely that additional nutrients could be extracted from the samples by lake water. Therefore, the nutrient content of the samples should be considered a maximum estimate and directly comparable to nutrient flux rates reported by Reuter and Miller (2000). Additionally, several analyses were performed on 1:1 soil-water extracts.

Particle Size Distributions of Shorezone Sediment

A total of 43 samples were collected from various types of sedimentary units around the lake and analyzed for their sand, silt, and clay content (Table 3-3). Not all of the areas that have eroded were sampled, primarily due to limited access. The collected samples, however, represent the range of sedimentary types encountered around the Tahoe shorezone and serve for estimating the amount of sand, silt, and clay eroded into the lake.

Results

Both erosion and accretion have occurred along the Lake Tahoe shore during the last 60 years. Figure 3-6 presents a map delineating the areas where change has occurred. Twenty-two areas along the shore have undergone erosion. The largest of these encompasses an area of about 32,000 m^2 (Table 3-4). The total surface area of the eroded shorezone equates to about 190,600 m^2. By contrast, 20 areas have undergone accretion, comprising a total area of about 56,500 m^2.

Table 3-2. Nutrient sample data. Samples were analyzed for total phosphate (TPO_4) and total Kjeldahl nitrogen (TKN). All location data is referenced to UTM Zone 10, NAD 27.

Sample Name	Sample Date	Easting	Northing	TPO_4 (mgP/kg)	TKN (mgN/kg)
SB-1	17-May-00	763682	4347495	212	18
SB-2	17-May-00	763681	4347521	316	229
SB-3	17-May-00	763637	4347520	192	22
SB-4	17-May-00	763610	4347540	264	25
SB-5	17-May-00	763580	4347562	656	31
SB-6	17-May-00	763575	4347559	224	18
SB-7	17-May-00	763598	4347635	452	338
SB-8	17-May-00	763619	4347653	444	108
SB-9	17-May-00	763544	4347581	172	22
SB-10	17-May-00	763499	4347606	740	37
SB-11	17-May-00	763474	4347624	756	97
SB-12	17-May-00	763449	4347637	1800	16
SB-13	17-May-00	763396	4347657	960	37
SB-14	17-May-00	763409	4347669	572	171
SB-15	17-May-00	763450	4347671	408	216
KB-1	17-May-00	757082	4346895	4	33
KB-2	17-May-00	757021	4346930	92	76
KB-3	17-May-00	756940	4346962	55	35
KB-4	17-May-00	756920	4346986	40	67
KB-5	17-May-00	756882	4346986	47	32
KB-6	17-May-00	756832	4347008	54	39
KB-7	17-May-00	756788	4347005	100	18
KB-8	17-May-00	756763	4347011	58	15
KB-9	17-May-00	756751	4347038	16	67
KB-10	17-May-00	756687	4347046	55	39
SPP-1	18-May-00	749888	4326641	320	20
SPP-2	18-May-00	749927	4326294	168	20
SPP-3	18-May-00	749947	4326252	148	274
SPP-4	18-May-00	749955	4326256	328	218
SPP-5	18-May-00	749955	4326256	272	32
SPP-6	18-May-00	749998	4326140	784	926
SPP-7	18-May-00	750030	4326073	79	4330
SPP-8	18-May-00	750026	4326079	584	628
SPP-9A	4-Aug-00	749805	4326977	299	297
SPP-9B	4-Aug-00	749805	4326977	205	219
SPP-9C	4-Aug-00	749805	4326977	172	83
SPP-9D	4-Aug-00	749805	4326977	477	50
SPP-10A	4-Aug-00	749809	4327071	484	167
SPP-10B	4-Aug-00	749809	4327071	445	62
SPP-10C	4-Aug-00	749809	4327071	171	203
BB-1	18-May-00	745806	4332280	648	58
BB-2	18-May-00	745784	4332237	576	41
BB-3	18-May-00	745774	4332222	740	56

Table 3-2. (cont.)

BB-4	18-May-00	745749	4332187	624	51
BB-5	18-May-00	745732	4332153	636	67
LF-1	17-May-00	749414	4340749	729	1320
LF-2	17-May-00	749342	4340675	328	61
LF-3	17-May-00	749291	4340628	1410	1950
LF-4	17-May-00	749197	4340634	388	1360
LF-5	17-May-00	749197	4340634	542	1520
LF-6	17-May-00	749197	4340634	254	1360
NV-1	3-May-00	763884	4318954	80	18
NV-2	3-May-00	763904	4318962	88	112
NV-3	3-May-00	763930	4318969	168	136
NV-4	3-May-00	763962	4318989	172	321
NV-5	3-May-00	763995	4318992	164	363
NV-6	3-May-00	764034	4319003	128	265
CL-1	18-May-00	747392	4328651	380	42
CL-2	18-May-00	747427	4328625	416	43
CL-3	18-May-00	747454	4328595	324	145
TV-1	17-May-00	754976	4347261	72	50
TV-2	17-May-00	754925	4347267	64	486
UT-1	17-May-00	759883	4314321	132	41
UT-2	17-May-00	759900	4314321	192	31
UT-3	17-May-00	759910	4314321	130	35
BC-1	18-May-00	745737	4332362	467	185
BC-2	18-May-00	745719	4332376	506	139
ZC-1	6-Jun-00	764212	4322331	84	24
ZC-2	6-Jun-00	764224	4322331	552	315
ZC-3	6-Jun-00	764250	4322254	122	11
ZC-4	6-Jun-00	764268	4322250	285	258
ZC-5	6-Jun-00	764281	4322180	90	12
ZC-6	6-Jun-00	764293	4322169	330	199
ZC-7	6-Jun-00	764298	4322118	62	11
ZC-8	6-Jun-00	764308	4322120	114	240
GB-1	6-Jun-00	764768	4330898	196	36
GB-2	6-Jun-00	764749	4331014	132	21
GB-3	6-Jun-00	764744	4331079	189	32
GB-4	6-Jun-00	764726	4331157	266	25
GB-5	6-Jun-00	764722	4331197	690	1270
GB-6	6-Jun-00	764713	4331225	502	814
UT-3 Soil ext.	17-May-00	759910	4314321	0.06	1.2
LF-6 Soil ext.	17-May-00	749197	4340634	0.23	4.2
SB-11 Soil ext.	17-May-00	763474	4347624	0.44	1.6
KB-3 Soil ext.	17-May-00	756940	4346962	0.02	0.6
NV-4 Soil ext.	17-May-00	749197	4340634	0.13	1.9

Table 3-3**.** Particle-size information for samples collected from the Lake Tahoe shorezone.

Location	Field ID	UTM Zone	Easting	Northing	Total Sand (% wt.)	Total Silt (% wt.)	Clay (% wt.)
Sugar Pine point	SPP-1	10	749888	4326641	100.0	0.0	NA
Sugar Pine point	SPP-2	10	749927	4326294	100.0	0.0	NA
Sugar Pine point	SPP-3	10	749947	4326252	96.0	4.0	NA
Sugar Pine point	SPP-4	10	749955	4326256	99.5	0.5	NA
Sugar Pine point	SPP-5	10	749955	4326256	100.0	0.0	NA
Sugar Pine point	SPP-6	10	749998	4326140	93.5	6.5	NA
Sugar Pine point	*SPP-6D*	10	749998	4326140	*93.1*	*6.9*	*NA*
Sugar Pine point	SPP-8	10	750026	4326079	72.3	19.6	8.1
Sugar Pine point	SPP-9a	10	749805	4326977	93.8	6.2	NA
Sugar Pine point	SPP-9b	10	749805	4326977	92.9	7.1	NA
Sugar Pine point	SPP-9c	10	749805	4326977	96.8	3.2	NA
Sugar Pine point	SPP-9d	10	749805	4326977	60.3	34.8	4.9
Sugar Pine point	SPP-10a	10	749809	4327071	74.9	18.7	6.5
Sugar Pine point	*SPP-10aD*	10	749809	4327071	*74.8*	*19.0*	*6.1*
Sugar Pine point	SPP-10b	10	749809	4327071	99.3	0.7	NA
Sugar Pine point	*SPP-10bD*	10	749809	4327071	*99.4*	*0.6*	*NA*
Sugar Pine point	SPP-10c	10	749809	4327071	6.3	65.5	28.3
Upper Truckee Riv.	UT-2	10	7598900	4314321	99.9	0.1	NA
Upper Truckee Riv.	UT-3	10	759910	4314321	100.0	0.0	NA
Kings Beach	Kings Beach 5	10	756882	4346986	99.9	0.1	NA
Kings Beach	Kings Beach 6	10	756832	4347008	99.5	0.5	NA
Kings Beach	Kings Beach 7	10	756788	4347005	100.0	0.0	NA
Lake Forest	LF-1	10	749414	4340749	69.5	17.4	13.0
Lake Forest	LF-2	10	749342	4340675	99.6	0.4	NA
Lake Forest	*LF-2D*	10	749342	4340675	*99.7*	*0.3*	*NA*
Lake Forest	LF-3	10	749291	4340628	80.7	10.9	8.3
Lake Forest	LF-4	10	749197	4340634	45.0	29.2	25.8
Lake Forest	*LF-4D*	10	749197	4340634	*45.7*	*27.7*	*26.6*
Lake Forest	LF-5	10	749197	4340634	32.0	34.6	33.4
Lake Forest	LF-6	10	749197	4340634	28.5	36.1	35.5
Nevada Beach	NB-1	10	763975	4318772	100.0	0.0	NA
Nevada Beach	NB-2	10	764040	4318641	100.0	0.0	NA
Nevada Beach	NB-3	10	764115	4318478	100.0	0.0	NA
Nevada Beach	NB-4	10	764212	4318220	100.0	0.0	NA
Nevada Beach	NB-5	10	764285	4317977	100.0	0.0	NA
Kiva Beach	KB-1	10	755805	4314116	51.0	44.1	4.9
Kiva Beach	KB-2	10	755749	4314134	40.4	52.3	7.3
Kiva Beach	KB-3	10	755686	4314146	57.0	37.5	5.5
Kiva Beach	KB-4	10	755652	4314158	75.7	16.4	7.9
Pope Beach	PB-1	10	757159	4313851	100.0	0.0	NA
Pope Beach	PB-2	10	757270	4313842	100.0	0.0	NA

Table 3-3 (cont.)

Pope Beach	PB-3	10	757397	4313826	100.0	0.0	NA
Pope Beach	PB-4	10	757633	4313801	100.0	0.0	NA
Pope Beach	PB-5	10	757922	4313784	100.0	0.0	NA
Bijou Park	BP-1	10	763548	4315479	99.9	0.1	NA
Bijou Park	BP-2	10	763408	4315373	99.9	0.1	NA
El Dorado Beach	EDB-1	10	762205	4314836	40.7	43.4	15.9
El Dorado Beach	EDB-2	10	762205	4314836	98.7	1.3	NA
El Dorado Beach	*EDB-2D*	10	762205	4314836	*98.7*	*1.3*	*NA*

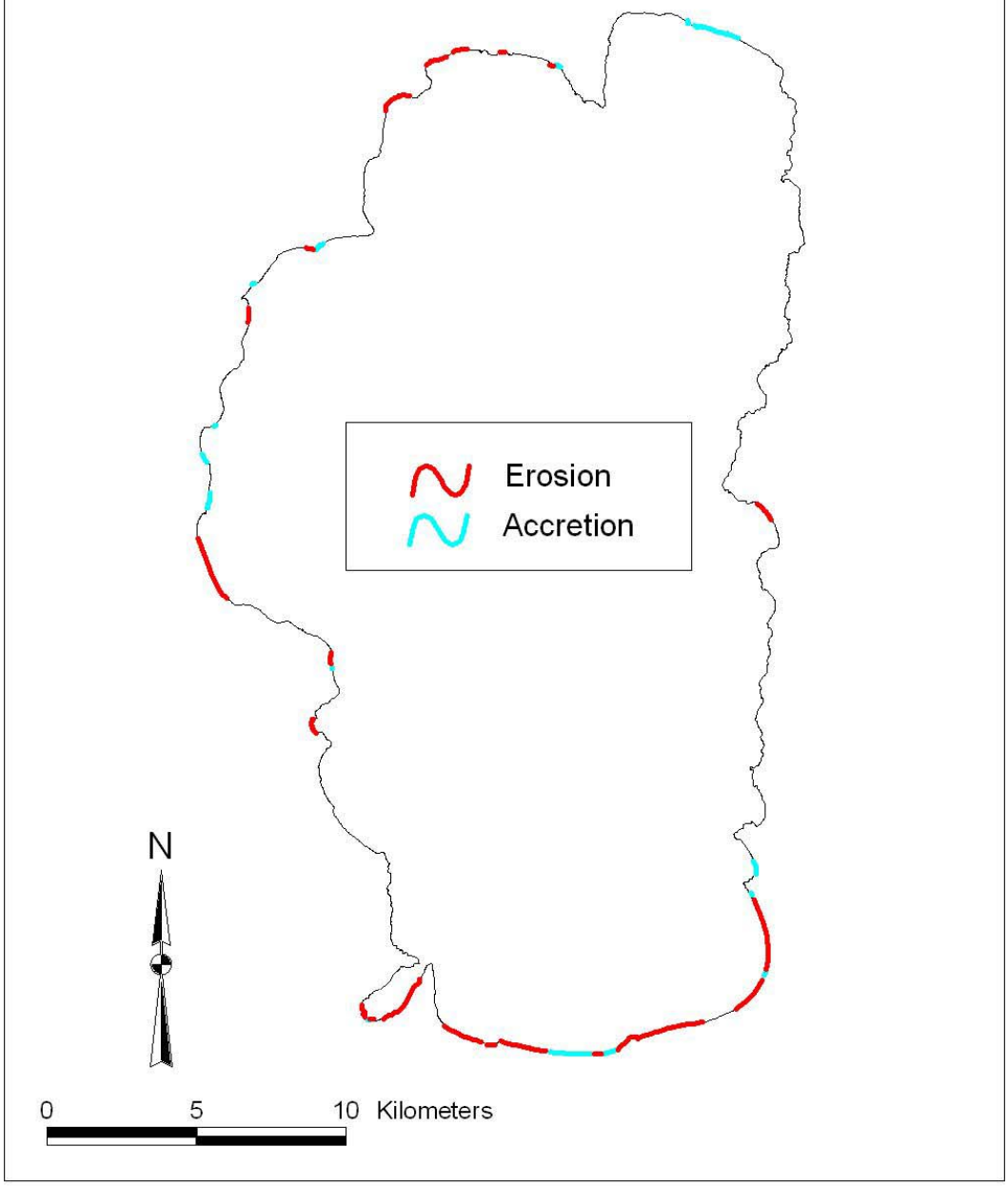

Figure 3-6. Map of Lake Tahoe that shows areas that have undergone erosion and accretion since 1938. Most of the areas undergoing erosion are located in embayments backed by unconsolidated lacustrine deposits, alluvial deposits, or both. See Fig. 1-1 for comparison.

Table 3-4. Sediment and nutrient calculations for areas with eroded shorezones.

Location	Material type	Area (m^2)	Thickness (m)	Volume (m^3)	Mass (kg)	P (mg/kg)	N (mg/kg)	Tot P (MT)	Tot N (MT)
Nevada Beach-Stateline	old granitic beach sand	21,898	1	21,898	32,847,000	280	330	9.20	10.84
Stateline	old granitic beach sand	361	1	361	541,500	280	330	0.15	0.18
Bijou Park	old granitic beach sand	11,644	1	11,644	17,466,000	280	330	4.89	5.76
Al Tahoe-Regan Beach	old granitic beach sand	11,275	6	67,650	101,475,000	280	330	28.41	33.49
Upper Truckee River	granitic beach sand	31,643	1	31,643	47,464,500	150	35	7.12	1.66
Tahoe Keys	old granitic beach sand	1234	1	1234	1,851,000	280	330	0.52	0.61
Kiva Beach-Camp Richardson	old granitic beach sand	10,272	2	20,544	30,816,000	280	330	8.63	10.17
Baldwin Beach	old granitic beach sand	13,600	1	13,600	20,400,000	280	330	5.71	6.73
SE shore of Emerald Bay	glacial till	15,544	2	31,088	46,632,000	315	120	14.69	5.60
Emerald Bay-Vikingsholm	glacial till	8304	1	8304	12,456,000	315	120	3.92	1.49
Meeks Bay	old granitic beach sand	6996	1	6996	10,494,000	280	330	2.94	3.46
Sugar Pine Point	old granitic beach sand	4008	3	12,024	18,036,000	280	330	5.05	5.95
Homewood	volcanic beach sand	18,813	1	18,813	28,219,500	320	230	9.03	6.49
Tahoe Tavern	volcanic beach sand	9545	1	9545	14,317,500	320	230	4.58	3.29
Lake Forest	gravelly silt	1962	1	1962	2,943,000	395	1415	1.16	4.16
Carnelian Bay	volcanic beach sand	8160	1	8160	12,240,000	320	230	3.92	2.82
Agate Bay	volcanic beach sand	4562	2	9124	13,686,000	320	230	4.38	3.15
Tahoe Vista	volcanic beach sand	3449	1	3449	5,173,500	68	270	0.35	1.40
Brockway	old granitic beach sand	1190	1	1190	1,785,000	280	330	0.50	0.59
Kings Beach-west side	volcanic beach sand	728	1	728	1,092,000	50	40	0.05	0.04
Kings Beach-east side	volcanic beach sand	903	2	1806	2,709,000	50	40	0.14	0.11
Glenbrook	old granitic beach sand	4471	1	4471	6,706,500	280	330	1.88	2.21
								P	**N**
	TOTALS =	190562		28,6234	429,351,000		**TOTALS (MT)=**	117	110

In order to calculate the volume of sediment and nutrients introduced into the lake by erosion, the thickness of each area had to be estimated. Large-scale (1:2400) U.S. Bureau of Reclamation topographic maps with one and five foot contours dating from 1918 and 1919 were used to calculate the thickness of discrete sediment packages. These packages typically were 1-2 m thick but ranged up to 6 m thick along parts of the south shore. Total volume of the eroded shorezone material equates to about 286,000 m^3 (Table 3-4). To convert this volume of sediment into a mass, a density of 1.5 g/cm^3 was assumed because this value represents typical soil densities found in the Lake Tahoe basin (Rodgers, 1974). From Table 3-4, the total mass of sediment eroded into Lake Tahoe from the shorezone since 1938 amounts to approximately 429,000 metric tons (MT). If averaged over the 60 year study period, about 7,150 MT of sediment have been washed into the lake each year from shorezone erosion. The areas that have undergone accretion are not included as sediment sinks in this budget.

Results from particle-size analyses (Table 3-3) were used to derive estimates of how much sand, silt, and clay have been introduced into the lake since 1938. As stated above, the total mass of sediment introduced into the lake from shorezone sources equates to about 429,000 MT. Of this mass, approximately 396,350 MT (~92%) is composed of sand-size sediment, with the remaining composed of approximately 26,500 MT (~6%) and 6,500 MT (~1.5%) of silt and clay, respectively (Table 3-5). These values equate to about 6,600, 440, and 110 MT/yr of sand, silt, and clay, respectively.

Phosphorus and nitrogen contents of the sampled sediment have wide ranges, but generally the sediment around the lake is higher in phosphorus than nitrogen (Table 3-2). A notable exception is at Lake Forest (samples LF-1 through LF-6; Table 3-2) where nitrogen is unusually high. Samples LF-3 through LF-6 were collected from a single vertical exposure through a gravelly silt or clay loam. Samples GB-5 and GB-6 from Glenbrook are also relatively high in nitrogen, but these came from a seep emanating from a wave-cut scarp below a large grassy area. Several stream samples were collected adjacent to their respective beaches, including samples from Third Creek at Incline Village (SB-7 and SB-8) and from Blackwood Creek (BC-1 and BC-2) along the west shore. Both of these drainages supply sediment that is apparently much higher in nitrogen than the beaches upon which they divulge.

All sediment samples were analyzed for total phosphorus and nitrogen by digestion procedures, although several duplicate samples were analyzed with a 1:1 soil-water extract procedure to check for consistency. These samples include UT-3 Soil ext., LF-6 Soil ext., SB-11 Soil ext., KB-3 Soil ext., and NV-4 Soil ext. (Table 3-2). All of the samples analyzed by the soil-water extract procedure show similar nutrients values but yield nutrient concentrations at least an order of magnitude less than their duplicates where the sediment was first digested and then analyzed.

Table 3-5. Particle size distributions and total mass calculations for sand, silt, and clay for eroded shorezone areas from 1938 to 1998.

			Size Distribution (% wt.)			Total Mass (kg)		
Location	**Material type**	**Mass (kg)**	**Sand**	**Silt**	**Clay**	**Sand**	**Silt**	**Clay**
Nevada Beach-Stateline	old granitic beach sand	32,847,000	100.0	0.0	0.0	32,847,000	0	0
Stateline	old granitic beach sand	541,500	100.0	0.0	0.0	541,500	0	0
Bijou Park	old granitic beach sand	17,466,000	100.0	0.0	0.0	17,466,000	0	0
Al Tahoe-Regan Beach	old granitic beach sand	81,180,000	98.7	1.3	0.0	80,124,660	1,055,340	0
Al Tahoe-Regan Beach	silty interbeds (~20%)	20,295,000	40.7	43.4	15.9	8,260,065	8,808,030	3,226,905
Upper Truckee River	granitic beach sand	47,464,500	100.0	0.0	0.0	47,464,500	0	0
Tahoe Keys	old granitic beach sand	1,851,000	100.0	0.0	0.0	1,851,000	0	0
Kiva Beach-Camp Richardson	Mixed sediments	30,816,000	56.0	37.6	6.4	17,265,072	11,576,493	1,974,435
Baldwin Beach	old granitic beach sand	20,400,000	100.0	0.0	0.0	20,400,000	0	0
SE shore of Emerald Bay	glacial till	46,632,000	96.8	3.2	0.0	45,122,078	1,509,922	0
Emerald Bay-Vikingsholm	glacial till	12,456,000	96.8	3.2	0.0	12,052,681	403,319	0
Meeks Bay	old granitic beach sand	10,494,000	100.0	0.0	0.0	10,494,000	0	0
Sugar Pine Point	Mixed sediments	18,036,000	81.5	14.3	4.1	14,704,267	2,584,218	747,515
Homewood	volcanic beach sand	28,219,500	100.0	0.0	0.0	28,219,500	0	0
Tahoe Tavern	volcanic beach sand	14,317,500	100.0	0.0	0.0	14,317,500	0	0
Lake Forest	gravelly silt	2,943,000	62.6	19.6	17.8	1,841,989	576,528	524,483
Carnelian Bay	volcanic beach sand	12,240,000	100.0	0.0	0.0	12,240,000	0	0
Agate Bay	volcanic beach sand	13,686,000	100.0	0.0	0.0	13,686,000	0	0
Tahoe Vista	volcanic beach sand	5,173,500	100.0	0.0	0.0	5,173,500	0	0
Brockway	old granitic beach sand	1,785,000	100.0	0.0	0.0	1,785,000	0	0
Kings Beach-west side	volcanic beach sand	1,092,000	100.0	0.0	0.0	1,092,000	0	0
Kings Beach-east side	volcanic beach sand	2,709,000	100.0	0.0	0.0	2,709,000	0	0
Glenbrook	old granitic beach sand	6,706,500	100.0	0.0	0.0	6,706,500	0	0
TOTALS (kg) =		429,351,000				396,363,812	26,513,850	6,473,338

Because all tasks in this part of the study proceeded concurrently, not all locations that experienced erosion were sampled for nutrient content. Where sample locations coincided with areas of erosion, average nutrient concentrations were used to calculate the mass of phosphorus and nitrogen contained within a particular package of sediment. Along eroded reaches of shore where no sample data exists, average nutrient concentrations of similar geologic materials were used.

A total of about 117 MT of phosphorus and 110 MT of nitrogen have been introduced into the lake during the period 1938 to 1998 from shoreline erosion (Table 3-4). If averaged over the 60 years, these volumes equate to about 2 MT per year of phosphorus and about 1.8 MT per year of nitrogen.

Sources of Error

Several sources of error could affect estimates of the mass of sediment and nutrients delivered into Lake Tahoe from shorezone erosion. These include errors introduced by data sources, measurement methods, analytical uncertainty, and natural variability in the concentration of nutrients in shorezone sediments. Each of these sources will be discussed in turn to quantify the overall precision of the estimates.

The first source of error is associated with the area and volumetric calculations of the amount of shorezone erosion. Precision of the aerial photograph rectification procedure is about $\pm$ 2.0 m. Using this error, the total eroded shorezone area could be as low as 112,000 m^2 or as high as 272,600 m^2, a difference of about $\pm$ 43% from the observed value of 190,600 m^2. Converting this area to a volume required interpretation of contour intervals. We assumed that thickness values were within 25% of the true value.

The value used for density of eroded sediment was 1.5 g/cm^3 which is near the average density for soils exposed near the shoreline of Lake Tahoe (Rodgers, 1974). The standard deviation for the density of the soils analyzed by Rodgers (1974) is about $\pm$ 13%.

Error associated with nutrient concentrations may stem from analytical error as well as natural variability. Because most of the shorezone sediment eroded at Lake Tahoe is composed of alluvial and lacustrine deposits (Fig. 1-1), we use the standard deviation of phosphorus and nitrogen concentrations associated with these deposits (68% and 95%, respectively).

To arrive at total error from all sources for these calculations, we summed the fractional errors from each of the sources (Taylor, 1997). If we were to compute the error just for the mass of sediment introduced into the lake from shorezone erosion, it would be about $\pm$ 80%. By adding in the fractional uncertainties associated with the nutrient measurements, the overall uncertainties increase to about $\pm$ 150% for phosphorus and about $\pm$ 176% for nitrogen loading.

Discussion

Shorezone change around Lake Tahoe is discontinuous in space and appears to be well correlated with the type of geologic materials found along the shore (Figs. 1-1 and 3-6). Virtually no significant change was found in shorezones primarily composed of bedrock, either granitic or volcanic. Instead, the areas where both erosion and deposition have occurred are almost all composed of alluvium or older lacustrine deposits. An exception is along the southeastern shore of Emerald Bay where there appears to be significant shorezone erosion in glacial till. This assessment is largely in agreement with the studies of Orme (1971; 1972) and the evaluation of disturbance potential outlined in the Lake Tahoe Shore Zone Ordinance Amendments (TRPA Staff, 1999). Contrary to the studies of Engstrom (1978), shoreline stability apparently has more to do with composition of shorezone materials than with prevailing winds and the amount of fetch, although these parameters are certainly important.

Observations made during the course of this study also confirm the conclusions of Osborne et al. (1985) who demonstrated that most of the material found along the beaches of Lake Tahoe is locally derived from erosion of backshore areas and that littoral transport tends to occur in relatively small, isolated cells. Evidence for littoral drift also was seen in our study where areas of erosion were adjacent to small areas of accretion, suggesting a redistribution of material along the shore.

Quantitative results of this study document net shoreline change during the last 60 years, but additional observations suggest similar longer-term trends. Almost all of the areas of significant shoreline erosion occur within bays or reentrants along the shore backed by relatively erodible sediment. The shapes of these bays suggest that during the long term (hundreds to thousands of years) net erosion has taken place, causing the bays to enlarge relative to more stable portions of the shore (Fig. 3-6). On much shorter time scales, obvious erosional features (e.g., shoreline scarps, fallen trees, etc.) observed in the field do not always reflect longer term (decadal) conditions because, overall, many of these areas have changed relatively little during the last 60 years. In places like Kiva Beach and Sugar Pine Point (see Fig. 1-3), fresh evidence of erosion is matched by a noticeable change during the last 60 years. Along many lower elevation parts of the shore—including Baldwin Beach (Fig. 2-1), parts of Sugar Pine Point, and Nevada Beach (Fig. 2-2)—relatively young beach barriers are located inland from the shore and rise only a small vertical distance (1–2 m) above current maximum lake level. It is unknown if these features date from the early part of the 20th century when lake levels regularly exceeded the legal limit of 1898.65 m. If so, the development and positions of these barriers provide insight into the effects of higher lake levels on Lake Tahoe.

Field observations also confirmed that seawalls and other types of revetments now protect some of the areas with documented erosion. Therefore, these areas are no longer able to contribute sediment and nutrients to the lake, provided these structures remain in functional working order. The effect of shore protective structures on offshore and alongshore erosion is relatively unknown, however, and should be investigated (see Chapter 2). In terms of stability analyses, the data collected and utilized for this study

have been for a basin-wide assessment of shoreline change. Results are not intended to be used for local studies of shoreline stability but may form a valuable framework within which to conduct more detailed stability studies on a variety of scales.

Conclusions

Results of this study indicate that a total of 429,000 MT of sediment, 117 MT of phosphorus, and 110 MT of nitrogen have been introduced into Lake Tahoe from shorezone erosion during the last 60 years. These values indicate that, on average, about 7150 MT per year of sediment, 2 MT per year of phosphorus, and 1.8 MT per year of nitrogen are being introduced into Lake Tahoe by shorezone erosion. These values represent long-term averages and probably have decreased through time. Additionally, these values likely vary considerably from year to year depending on lake level, frequency and intensity of storms, and other factors. Based on total error from all sources, we consider these estimates accurate to within a factor of two.

Not all sediment sizes affect the water quality of Lake Tahoe in the same way. Sand and coarser sediment have rapid settling velocities that cause these coarse particles to quickly fall to the bottom when introduced into the lake by stream flow or shorezone erosion. Silt and clay, however, have slower settling velocities so that they spend a much longer period of time in the water column and can, in certain circumstances, be easily resuspended by wave action or other types of bottom agitation. Silt and clay-sized particles also can act as transport agents when nutrients adhere to their surfaces (Murphy and Knopp, 2000). The majority of sediment introduced into the lake from shorezone sources appears to be in the sand-sized range (Tables 3-3 and 3-5). It is difficult to compare the mass of silt and clay from shorezone sources to the mass of silt and clay introduced into the lake from inflowing streams because total suspended sediment measurements are not commonly broken down into different sized fractions. The mass of fine sediment introduced into the lake from shorezone erosion is significant, however, and should not be ignored when assessing impacts to lake water quality.

The Lake Tahoe Watershed Assessment (Murphy and Knopp, 2000) identified five sources of phosphorus and nitrogen for Lake Tahoe including atmospheric deposition, stream loading, direct runoff, groundwater, and shorezone erosion. Based on the previous assessment, shorezone erosion was thought to account for about 0.45 and 0.75 MT of phosphorus and nitrogen per year, respectively. Results of this study, however, indicate that loading due to shorezone erosion is appreciably higher for phosphorus (~ 4%) but still relatively low (<1%) for nitrogen (Table 3-6). It must be emphasized, however, that these percentages are normalized so that if estimates for any of the other sources are scaled back, the relative importance of shorezone erosion to nutrient loading becomes greater and needs to be reconsidered.

Table 3-6. Yearly sources for nitrogen and phosphorous for Lake Tahoe in MT.

Nutrient Inputs	Total N (MT)	Total P (MT)
Atmospheric deposition*	233.9 (56%)	12.4 (26%)
Stream loading*	81.6 (20%)	13.3 (28%)
Direct runoff*	41.8 (10%)	15.5 (33%)
Groundwater*	60 (14%)	4 (9%)
Shorezone erosion[#,**]	1.8 (<1%)	2 (4%)

Source comparison:

*Lake Tahoe Watershed Assessment (Murphy and Knopp, 2000).

[#]Estimates from the Watershed Assessment for yearly contributions of nitrogen and phosphorous are 0.75 and 0.45 metric tons, respectively.

**From this study.

Although the amount of phosphorus and nitrogen loading from shorezone erosion ranks last with respect to the other four nutrient sources, sediment loading from shorezone erosion probably ranks second. All of the other sources, except groundwater, contribute fine sediment to the lake. Annual sediment input from stream loading is estimated to be a minimum of about 11,300 MT/yr (Reuter and Miller, 2000). Firm estimates of the mass of sediment introduced from atmospheric deposition (dust) and direct runoff are lacking, but the average input from shorezone erosion (~7150 MT/yr) may greatly exceed these other two sources. Thus, shorezone erosion is an important component of the sediment and, to a lesser extent, nutrient budget of Lake Tahoe.

Chapter 4
Waves at Lake Tahoe

Kenneth D. Adams
Anna K. Panorska

Introduction

Waves are generated as winds blow across a body of water and some of the wind energy is transferred to the water due to frictional drag (Komar, 1998). This energy transfer, which increases the size of the waves, continues until the wind stops, changes direction, or the edge of the body of water is reached. The velocity at which the wave groups travel across the water is dependent on the wave period, with longer period waves traveling at progressively faster rates. On Lake Tahoe, wave periods for the largest waves probably reach about 6.5 seconds, indicating that these waves travel at approximately 10 m/s (22 mph). Shorter period waves travel at lower velocities. As waves approach the shore and enter shallower water, they begin to interact with the bottom, causing the waves to undergo a series of transformations. As they shoal, wave velocity and length progressively decrease, wave height increases, and the wave period remains constant (Komar, 1998). Waves finally break when the crests become oversteepened, unstable, and tumble forward on themselves. This expenditure of energy on the shore is the main driving force in sediment erosion, transport, and deposition.

Waves are periodic oscillations of the water surface that are typically measured in terms of their height, wavelength, period, and velocity (celerity) (Fig. 4-1). In nature, a wind-whipped water surface is usually composed of a combination of different wave groups, each with its own height, period, and velocity. When observed from the shores of Lake Tahoe during a windstorm, waves pounding the shore appear as a confused mix of smaller waves superimposed on larger waves, but definite patterns present themselves. Typically, larger waves dominate the surface and arrive every several seconds or so. When instruments are used to record these waves, all of this variation is present and must be processed in order to characterize wave heights and periods (Fig. 4-2).

The two most common measurements derived from raw wave data are significant wave height and peak spectral period (Earle et al., 1995). Significant wave height is defined as the average of the highest one-third of the waves. This measurement is approximately the average wave height reported by observers watching waves on a shore (Komar, 1998). Peak spectral period is derived through spectral analysis of raw wave data (Fig. 4-3), which presents the energy density per unit frequency interval for each frequency or period. In other words, the energy of different waves is separated into different "energy peaks" (Fig. 4-3). From significant wave height and peak spectral period estimates, many other wave characteristics—including maximum wave height, wavelength, velocity, shoaling transformations, breaking wave height, and run-up height—can be calculated (Komar, 1998). Water waves are predictable because they obey simple physical laws that are common to many different types of waves including sound and seismic waves.

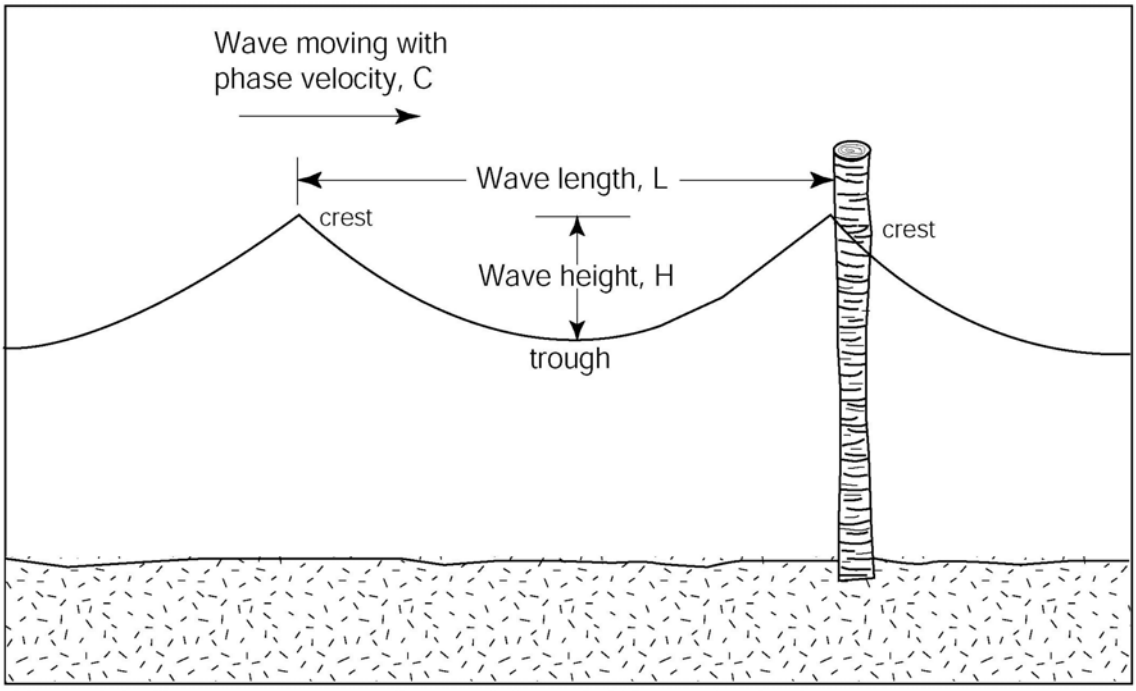

Figure 4-1. Wave parameters that, along with the period *T*, describe simple wave motions (after Komar,1998).

An simple approach for making wave predictions, known as wave hindcasting, is outlined in the Shore Protection Manual (CERC, 1984) and discussed in Komar (1998). This wave spectrum approach predicts the significant wave height and peak spectral period if the wind velocity and duration as well as the fetch are known. When waves cannot reach their maximum potential, they are restricted by either a duration-limited or a fetch-limited condition. When wave growth is duration-limited, winds do not blow long enough from a particular direction for the waves to reach their maximum height for a given wind strength. For example, when a 9 m/s (20 mph) wind blows for only a single hour across the surface of Lake Tahoe, waves grow to approximately 0.35 m high with 2.2 second periods. If this same wind were to blow for a longer period of time, say two hours, wave height would increase to about 0.55 m and the wave period would increase to about 3.0 seconds. Because the longest fetch (the distance of open water over which the winds blow) at Lake Tahoe is limited to about 33 km (measured north to south), waves could only reach a maximum height of 0.95 m with about 4.25 second periods, given a 9 m/s wind. This is the fetch-limited condition where, no matter how long the wind blew at 9 m/s, waves would be limited to this maximum height.

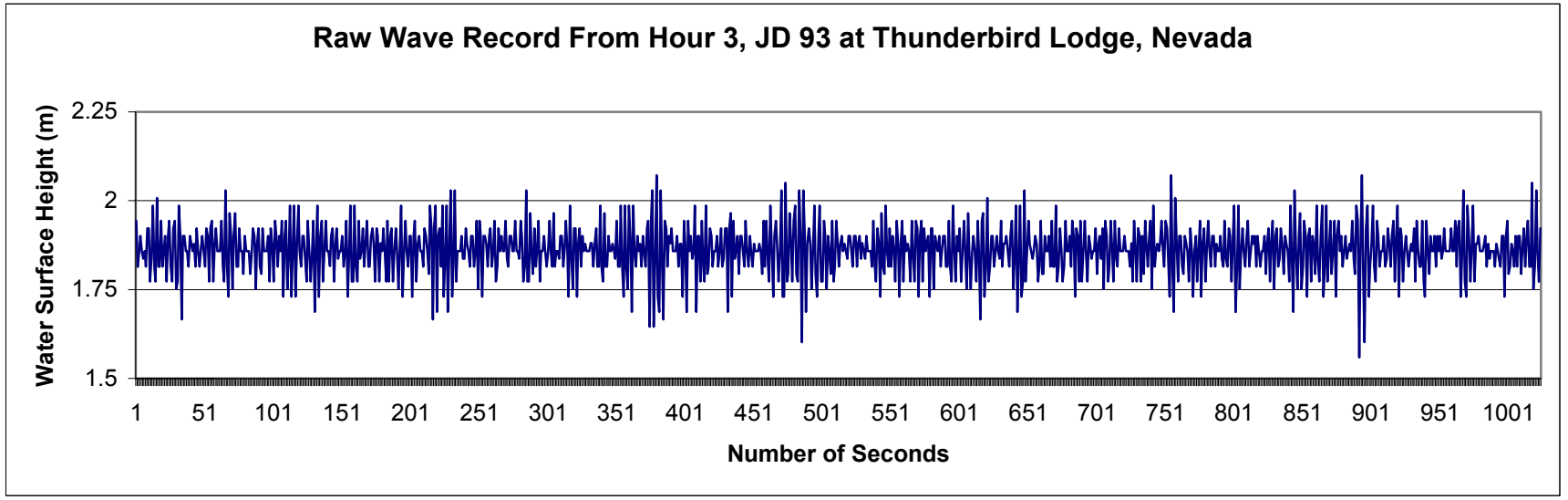

Figure 4-2. Thunderbird Lodge site wave record consisting of 1024 water-level measurements at a frequency of one measurement per second for a duration of approximately 17 minutes.

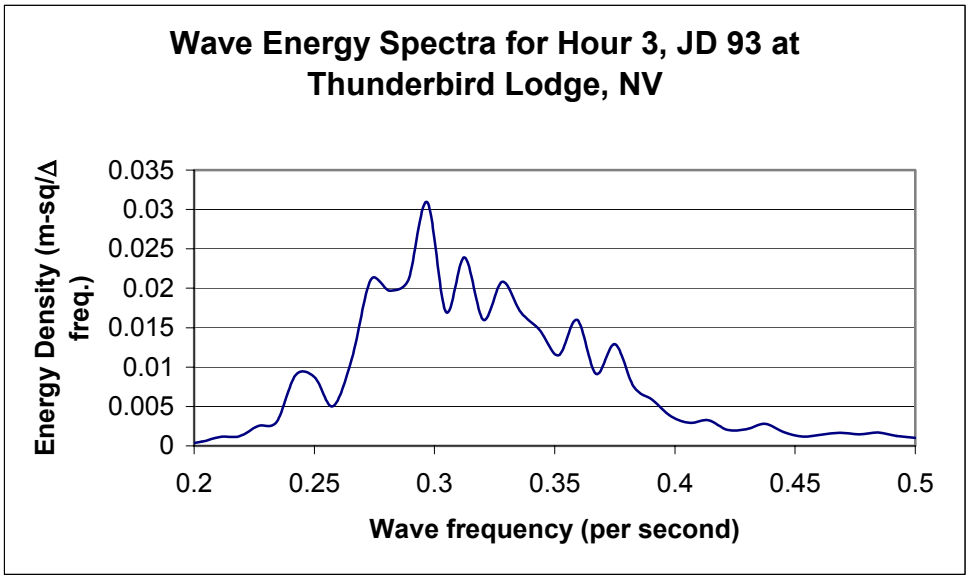

Figure 4-3. Wave energy spectra plot processed from the raw wave record shown in Fig. 4-2. The greatest amount of energy is contained in waves with a frequency of 0.3 seconds, which corresponds to a period of about 3.3 seconds.

Wave Monitoring Procedures and Data Reduction

As part of the effort to quantify shorezone erosion and its effects on water quality at Lake Tahoe, three wave-recording stations were deployed—one each at Incline Village, Meeks Bay, and the Thunderbird Lodge (Fig. 4-4). These stations ran for a period of over one year. Data was recorded and processed according to the "Wave Data Analysis Standard" published by the U.S. Army Corps of Engineers (Earle et al., 1995). Each station consisted of a submerged pressure transducer that registered water surface elevation changes at 1-second intervals for a period of 1024 seconds (approximately 17 minutes) at the top of each hour and transmitted this information to a data logger (Fig. 4-2). The stations recorded wave data each hour, 24 hours per day. Each station also was equipped with a cellular phone that was called once or twice per day to download the stored data to a computer at DRI.

The first site was on a pier at Incline Village that looks down the entire length of the lake (Fig. 4-5), a fetch of about 33 km. The pressure transducer was strapped to a concrete piling facing to the south. When installed on January 19, 2001 (JD 19), lake level was at 1897.84 m (6226.42 ft), water depth at the site was about 2 m, and the pressure transducer was submerged at a depth of 1.04 m. The lake bottom beneath the pier (and presumably extending offshore) consists of coarse gravel, cobbles, and boulders.

The Meeks Bay site is relatively sheltered from the prevailing south to southwest winds but has a significant fetch (21.5 km) to the northeast (Fig. 4-4). Water depth on the day we installed the station (January 24, 2001; JD 24) was about 2 m, lake level was at 1897.82 m (6226.38 ft), and the transducer, mounted on a pier piling, was submerged to a

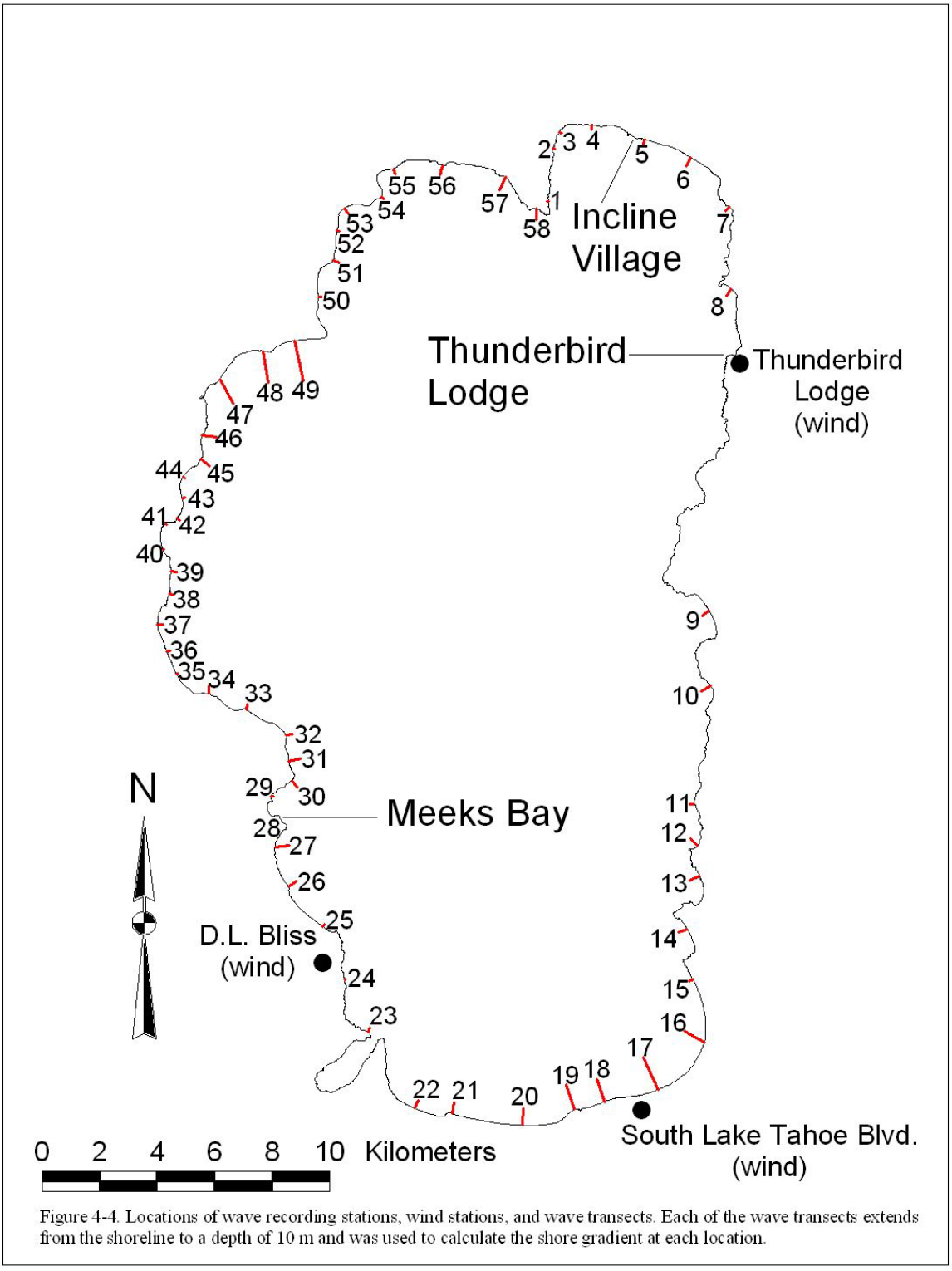

Figure 4-4. Locations of wave recording stations, wind stations, and wave transects. Each of the wave transects extends from the shoreline to a depth of 10 m and was used to calculate the shore gradient at each location.

Figure 4-5. Photograph looking south from the Incline Village wave monitoring site. The fetch here is approximately 33 km.

depth of 1.82 m. Lake bottom in the vicinity of the pier consists of large boulders to >2 m with scattered sand and gravel patches between the large boulders.

The Thunderbird Lodge site was located along the northeast shore of Lake Tahoe and has a long fetch to the west and southwest (Fig. 4-4). Installation was more challenging at this site because there is no pier and the shore is extremely rocky and bouldery, as along much of the eastern shore. Large granitic boulders litter the nearshore area with small, scattered sand patches found among them. On a calm, early February morning (February 1, 2001; JD 32), we installed our pressure transducer about 15 m from shore on a small sand patch in approximately 1.9 m of water. The pressure transducer was mounted on a small metal stand weighted down with small boulders found in the area. The cable was strung back to shore where the data logger enclosure was located. This site was also completely autonomous, with a solar panel that charged a battery that ran the electronics.

Although there were a few data gaps during the time periods that each of the stations was operating, overall the stations performed admirably. The data was processed to determine significant wave height, peak spectral period, and zero-crossing period according to the

specifications outlined in Earle et al. (1995). Steps involved in the wave data analysis were 1) initial data quality assurance tests to reject poor quality data, 2) data segmenting to reduce statistical uncertainties of spectra, 3) mean removal, 4) trend removal, 5) use of windows to reduce spectral leakage, 6) corrections for window use, 6) fast Fourier transforms (FFTs), and 7) cross-spectral analysis, including segment averaging. Because the instruments did not record wave direction, directional statistics were not produced. A statistical software program (S-Plus 2000) was used to process the wave data and produce estimates.

Wave Monitoring Results

Hourly wave observations were collected for more than one year, providing quantitative data on the Lake Tahoe wave climate. As expected, wave energy was episodic and varied from place to place. Figures 4-6, 4-7, and 4-8 show hourly plots of significant wave heights at Incline, Meeks Bay, and Thunderbird Lodge, respectively, for Julian Day[1] (JD) 60 to JD 430 (March 1, 2001 through March 6, 2002). In these plots, all waves less than 5 cm are shown as calm. During the period of record, it was calm (waves <5 cm) about 64% of the time at Incline Village, 85% of the time at Meeks Bay, and 65% of the time at Thunderbird Lodge. Significant wave heights reached as high as 60 cm at Thunderbird Lodge, 40 cm at Incline, and only about 30 cm at Meeks Bay. It is not surprising that the wave records of Incline and Thunderbird appear very similar (Figs. 4-6 and 4-8); they are both located in the northeastern part of the lake basin with large fetches to the south and southwest (Fig. 4-4). In contrast, the wave record from Meeks Bay contains less frequent wave events of generally lower magnitude occurring at different times than wave events at Incline and Thunderbird. This difference likely can be explained by the fact that the Meeks Bay site is largely sheltered from wind and waves from the south-southwest but is exposed to waves from the northeast that are less frequent. Hence, the differences in the wave records of Incline and Thunderbird compared to Meeks probably reflect distinct wave events from different directions recorded at the respective stations.

Discussion

Relationships Between Wind and Waves

Wave growth at Lake Tahoe is directly driven by local winds, so there should be a good correlation between wind and waves. We compared wind data from three meteorological stations, maintained by Air Resource Specialists, Inc. (ARS), to wave data. These stations are located at the Thunderbird Lodge, South Lake Tahoe Blvd., and D.L. Bliss State Park (Fig. 4-4). Although there are many similarities between the wind data from each of these stations, there are also some distinct differences.

Figure 4-9 compares wind records from each of the three meteorological sites located around the lake. Although peak wind velocities were similar, there were distinct

[1] The Julian Day (JD) system counts the days of the year beginning at JD 1 on January 1 and ending with JD 365 on December 31. In this study, sequential numbering of Julian Days past 365 is used for a simplified way of keeping track of the date in computer programming.

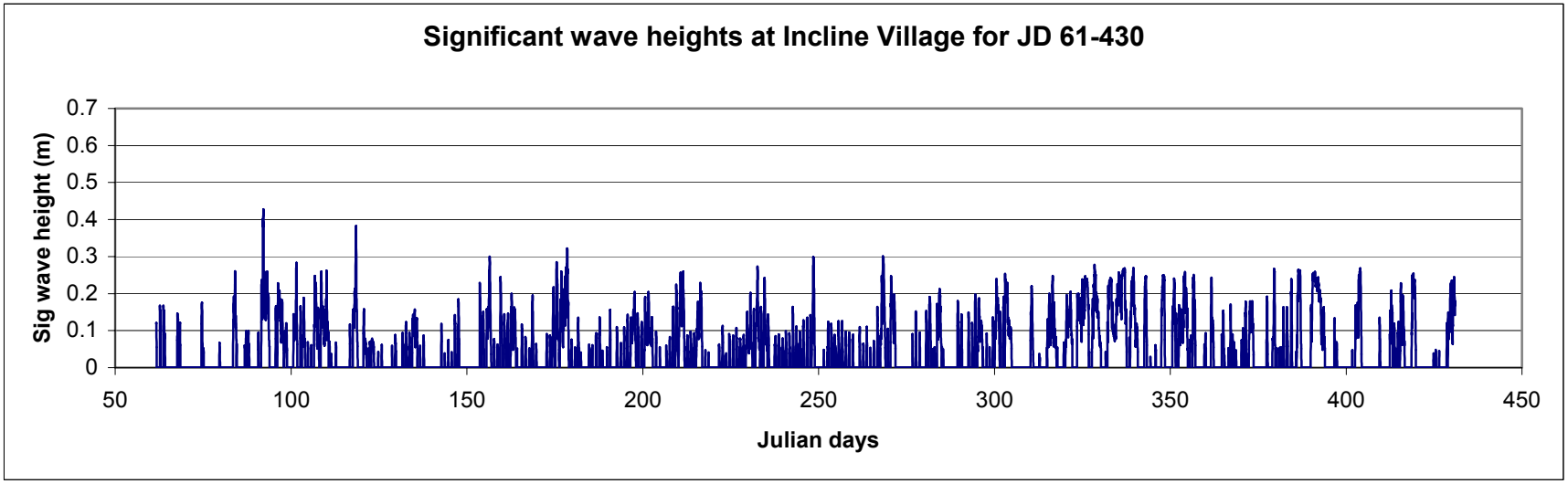

Figure 4-6. Plot of significant wave heights at the Incline Village site for Julian Days 61-430.

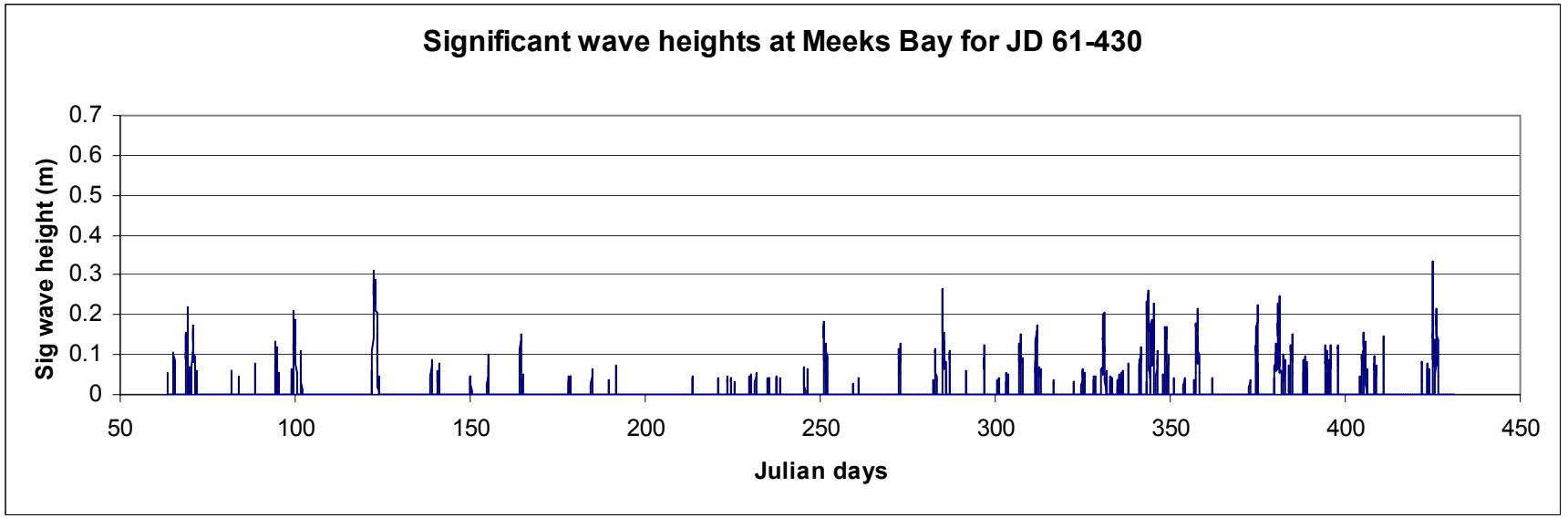

Figure 4-7. Plot of significant wave heights at the Meeks Bay site for Julian Days 61-430.

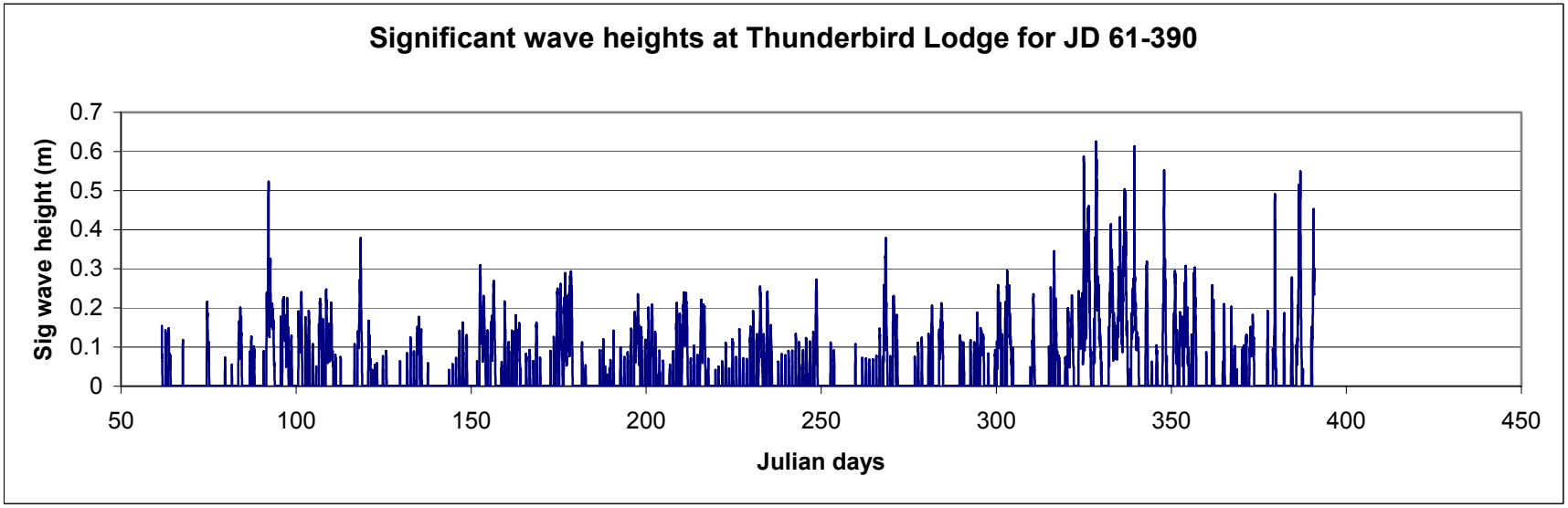

Figure 4-8. Plot of significant wave heights at the Thunderbird Lodge site for Julian Days 61-390.

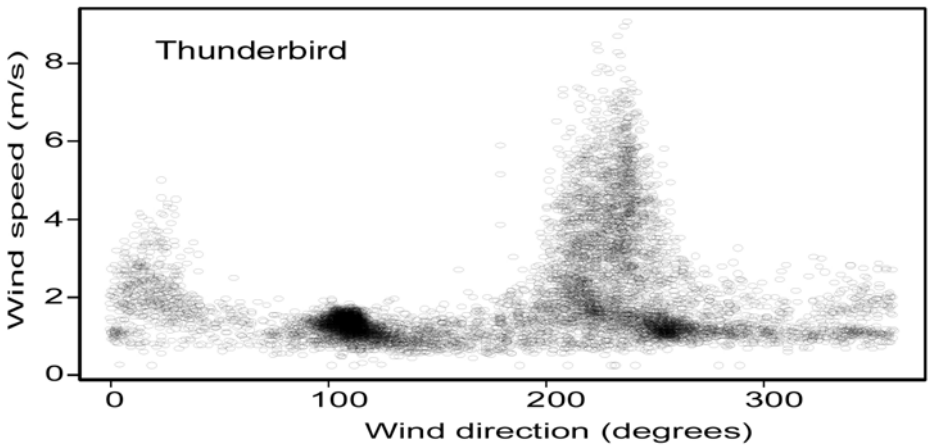

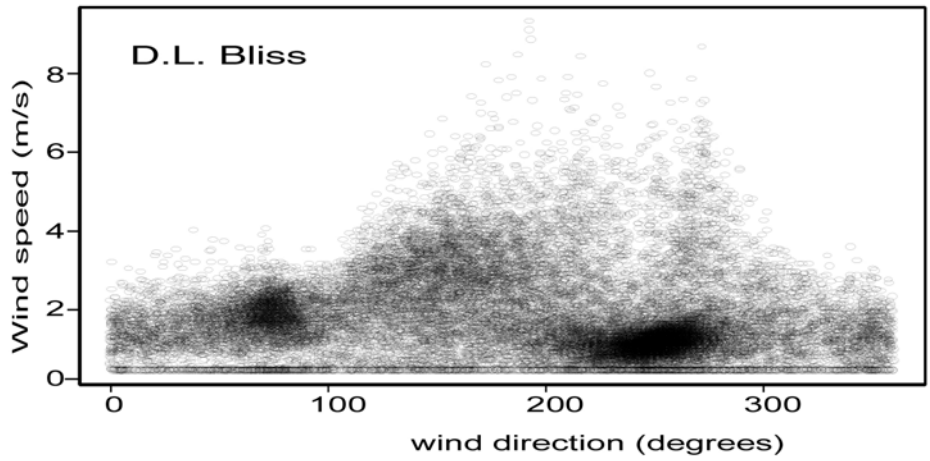

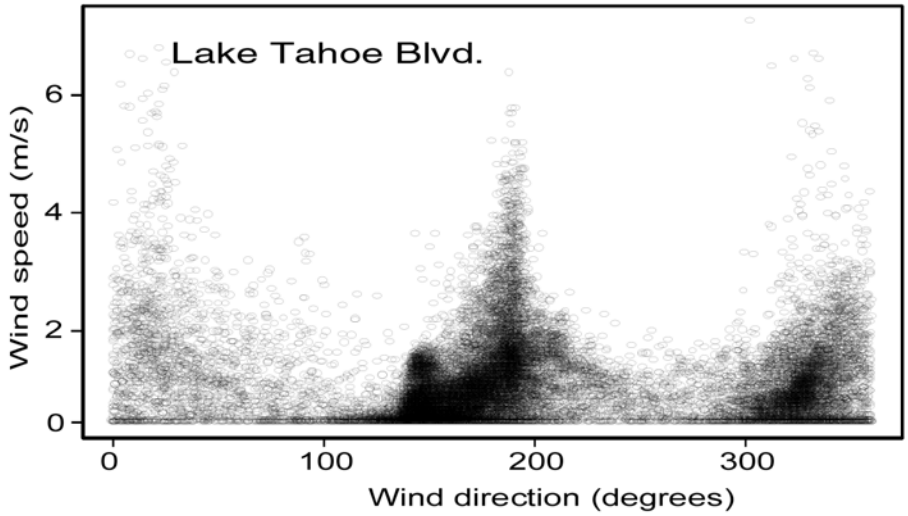

Figure 4-9. Plots of wind speed vs. direction for the Thunderbird Lodge, D.L. Bliss, and Lake Tahoe Blvd. meteorological stations. See Fig 4-4 for locations.

differences in directional components. Both the Thunderbird Lodge and Lake Tahoe Blvd. records show a high frequency of winds from the south-southwest with secondary peaks from the north. The D.L. Bliss record, however, shows a less peaked distribution ranging from east through west. The exact causes of these differences in direction are not known but probably relate to local factors such as topography and wind shielding.

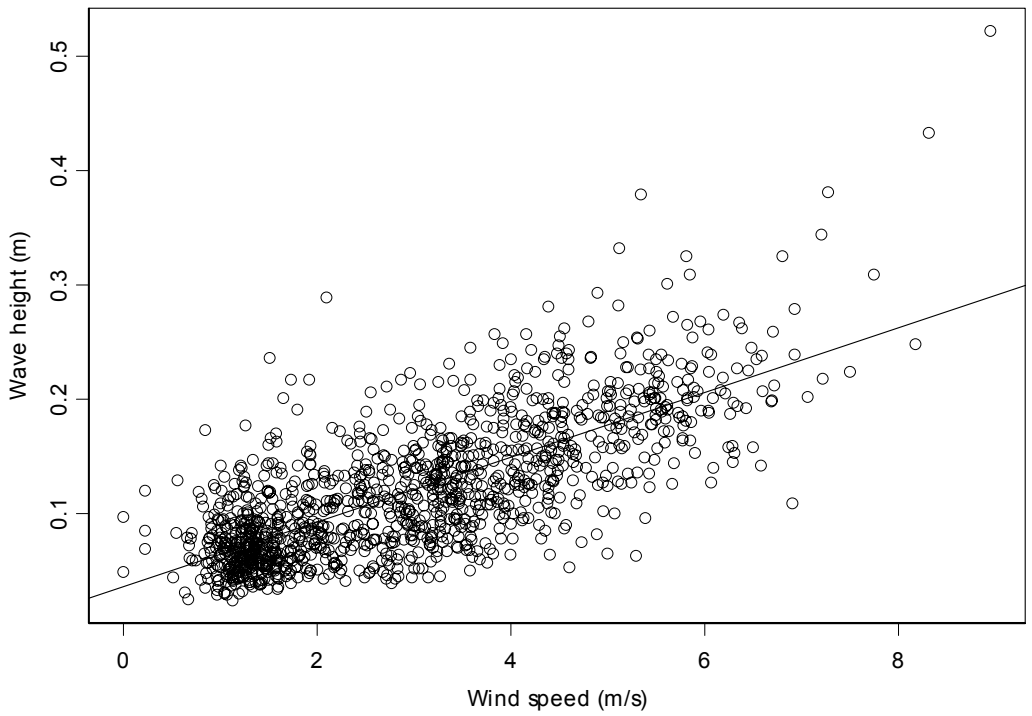

Figure 4-10. Comparison between wind speed and wave height for the Thunderbird Lodge location, R^2=0.74.

A comparison between winds and waves recorded at Thunderbird Lodge show a strong correlation (Fig. 4-10), which suggests that the winds at this location could be used to predict wave height. Scatter in this plot is attributed to the fact that even though winds were recorded from all directions (Fig. 4-9), waves only arrive from the south through the north. A similar relationship exists (R^2=0.72) between winds recorded at Thunderbird and waves recorded at the Incline site, which is to be expected because of the similar locations of Thunderbird and Incline (Fig. 4-4).

Wave Energy and Total Swash Elevation

Wave energy at Lake Tahoe is clearly episodic, where long periods of calm are separated by relatively windy periods during which the waves grow to a size dictated by wind and fetch conditions (Figs. 4-6, 4-7, and 4-8). Now that we actually have wave records spanning a moderate amount of time, a preliminary assessment of the amount of wave

energy imparted at the shore can be made. The energy density (E) of waves is directly related to the wave height by the following equation from Komar (1998):

$$E = 1/8pgH^2 \quad \text{Eq. 4-1}$$

Where p = density of water (1000 kg/m^3), g = acceleration due to gravity (9.8 m/sec^2), H = wave height (m). The units for this equation are Newtons/m^2. As waves approach the shore and begin to break, energy density (E) varies because wave height changes during shoaling. However, the energy flux or wave power (P)—which is the rate at which energy density is carried along by the moving waves—remains approximately constant (Komar, 1998). Energy flux (P) is given by:

$$P = EC \quad \text{Eq. 4-2}$$

Where E = energy density and C = celerity (velocity) of individual waves. Wave power at a shore is a direct measurement of wave energy and can be used to assess the cumulative amount of energy imparted by relatively common, small waves as compared to the amount of energy carried by infrequent, large waves.

Wave energy is the driving force behind shorezone erosion; but it is not known whether high frequency, low magnitude wave events or low frequency, high magnitude wave events accomplish more geomorphic work over time. Put another way, we do not know whether infrequent, large storm events erode more of the shore through time or whether the near daily occurrence of relatively small waves does more to erode the shore. Consequently, understanding the amount of energy and how it is delivered to the shore by different-sized wave events is important to gaining a more complete understanding of erosion processes and how sediment and nutrients are introduced into the lake. DRI's wave monitoring efforts were well-equipped to measure wave characteristics and energy associated with relatively frequent wave sizes but may not have been sufficient to capture rare, large wave events with recurrence intervals measured in years or decades.

To explore potential effects of large waves, we employed the concept of the "design storm," which is used by TRPA to calculate wave run up heights for engineering applications at Tahoe. According to the definitions chapter in the TRPA Code of Ordinances, the design storm is defined as follows: "An extreme wind event is an 80 miles per hour onshore wind of one hour duration." The short time period was chosen by TRPA staff because of the generally fetch-limited conditions at Lake Tahoe. Given these wind conditions, however, waves would reach their maximum size within about 10 km and be considered duration-limited in areas with longer fetch. The general geometry of the lake dictates that waves reaching almost every part of the shore from an 80 mph wind blowing for one hour would be duration-limited but would still obtain significant wave heights of about 2.6 m with a peak spectral period of about 5 seconds. An exception is in Emerald Bay where fetch is limited to about 3 km and waves from the same storm would reach significant wave heights of about 1.6 m with a peak spectral period of about 3.5 seconds.

Using the Incline Village wave record as an example (Fig. 4-6), cumulative wave power for all waves arriving at Incline Village from JD 61 to JD 430 was approximately 1.41 x 10^9 Joules (J). In comparison, wave power arriving at Incline Village from a single design storm event (H = 2.6 m, T = 5 seconds) is about 1.16 x 10^8 J. In other words, significantly more wave energy was expended at Incline Village in just over one year due to frequent but relatively small wave events than would be the case during the single hour of the design storm. This comparison points to the contribution of relatively frequent wave events to shorezone erosion. Even moderate-sized waves can generate enough shear stress to transport coarse sand and gravel. Therefore, although large storm events are likely important to long-term erosion trends, smaller, more frequent waves can cause significant erosion on shores composed of relatively soft materials, particularly when lake levels are high.

In fact, lake level may be one of the prime indicators of whether or not shorezone erosion will occur for a given wave event. When lake level is low at Tahoe, beach areas are significantly larger than when the lake is high and can absorb much of the wave energy. When lake level is high, however, breaking waves can directly impact backshore areas and cause erosion.

When large storm waves break on a shore, the elevation to which the swash extends depends on wave set-up and wave run-up (Komar, 1998). Wave set-up is a rise in the mean water level above the still water elevation created by the breaking waves. According to laboratory measurements, set-up is confined to the surf zone shoreward of the initial breaking point and consists of an upward slope of the water toward the land. Wave set-up effectively deepens local water depths, allowing waves to break closer to shore. The onrush of water up the beach slope after the wave breaks is known as run-up. The following equation (Komar, 1998) is used to calculate total swash elevation (Wave set-up plus wave run-up):

$$R^T = 0.36 g^{0.5} S H^{0.5} T \qquad \text{Eq. 4-3}$$

Where g = acceleration due to gravity (980 cm/sec^2), S = beach gradient (dimensionless) H = deep water significant wave height, and T = wave period. This equation gives total elevation achieved by the swash of waves above still water level. Table 4-1 displays the total swash elevation for each of the wave transects shown in Fig. 4-4 under design storm conditions (80 mph for 1 hour). Even for more common waves (i.e., 0.5 m height with a 3 second period), total swash elevation can be significant in shorezone erosion (Table 4-2).

Total swash elevation at Lake Tahoe takes on greater significance when considered in relation to Lake Tahoe's legal limit, 1898.65 m (6229.1 ft). Local water elevations can be significantly higher than this still-water limit during storms (Tables 4-1 and 4-2). When water level along a shore is raised by storm waves, the energy of the waves can directly impact areas above the legal limit. This effect may contribute to rapid periods of erosion such as occurred in January 1997, particularly along shores composed of relatively soft material such as alluvial and lacustrine deposits.

Table 4-1**.** Total swash elevations for waves generated from the design storm (80 mph, 1 hour) at Lake Tahoe. Locations of wave transects are shown in Fig. 4-4.

Transect #	Fetch (km)	Gradient	Deep water wave height (cm)	Wave period (sec)	Total swash elevation (cm)
1	20.5	0.2084	260	5	189
2	22.5	0.1616	260	5	147
3	25.2	0.1226	260	5	111
4	33.4	0.0701	260	5	64
5	32.8	0.0452	260	5	41
6	32.5	0.0398	260	5	36
7	30.9	0.0433	260	5	39
8	26.9	0.0302	260	5	27
9	19.3	0.0328	260	5	30
10	17	0.0203	260	5	18
11	22.8	0.0518	260	5	47
12	24	0.0274	260	5	25
13	23.3	0.0231	260	5	21
14	17.7	0.0415	260	5	38
15	24.5	0.1132	260	5	103
16	29.5	0.0182	260	5	16
17	32	0.0140	260	5	13
18	32.4	0.0196	260	5	18
19	32.8	0.0186	260	5	17
20	32.7	0.0253	260	5	23
21	33.1	0.0283	260	5	26
22	33	0.0497	260	5	45
23	30.8	0.0883	260	5	80
24	28.7	0.3454	260	5	314
25	27.7	0.1430	260	5	130
26	27.1	0.0509	260	5	46
27	21.4	0.0307	260	5	28
28	21.5	0.2997	260	5	272
29	15.1	0.1367	260	5	124
30	16.2	0.0466	260	5	42
31	23.4	0.0361	260	5	33
32	22.8	0.0441	260	5	40
33	22.7	0.0806	260	5	73
34	23.5	0.0562	260	5	51
35	23.7	0.2258	260	5	205
36	23.5	0.0877	260	5	80
37	23.3	0.0709	260	5	64
38	22.5	0.1185	260	5	108
39	22	0.0683	260	5	62
40	21.9	0.2674	260	5	243
41	24.8	0.1641	260	5	149
42	24.6	0.1065	260	5	97

Table 4-1 (cont.)

43	24.8	0.1225	260	5	111
44	25.6	0.1330	260	5	121
45	25.7	0.0415	260	5	38
46	26.3	0.0302	260	5	27
47	27.8	0.0072	260	5	7
48	28	0.0055	260	5	5
49	27.8	0.0055	260	5	5
50	26.7	0.0934	260	5	85
51	29.9	0.0512	260	5	47
52	30.8	0.0791	260	5	72
53	31.4	0.0334	260	5	30
54	31.4	0.0900	260	5	82
55	32	0.0226	260	5	20
56	32	0.0175	260	5	16
57	31.5	0.0155	260	5	14
58	30.4	0.0218	260	5	20

Table 4-2. Total swash elevations for relatively common waves at Lake Tahoe. Locations of wave transects are shown in Fig. 4-4.

Transect #	Fetch (km)	Gradient	Deep water wave height (cm)	Wave period (sec)	Total swash elevation (cm)
1	20.5	0.2084	50	3	50
2	22.5	0.1616	50	3	39
3	25.2	0.1226	50	3	29
4	33.4	0.0701	50	3	17
5	32.8	0.0452	50	3	11
6	32.5	0.0398	50	3	10
7	30.9	0.0433	50	3	10
8	26.9	0.0302	50	3	7
9	19.3	0.0328	50	3	8
10	17	0.0203	50	3	5
11	22.8	0.0518	50	3	12
12	24	0.0274	50	3	7
13	23.3	0.0231	50	3	6
14	17.7	0.0415	50	3	10
15	24.5	0.1132	50	3	27
16	29.5	0.0182	50	3	4
17	32	0.0140	50	3	3
18	32.4	0.0196	50	3	5
19	32.8	0.0186	50	3	4
20	32.7	0.0253	50	3	6
21	33.1	0.0283	50	3	7
22	33	0.0497	50	3	12
23	30.8	0.0883	50	3	21

Table 4-2 (cont.)

24	28.7	0.3454	50	3	83
25	27.7	0.1430	50	3	34
26	27.1	0.0509	50	3	12
27	21.4	0.0307	50	3	7
28	21.5	0.2997	50	3	72
29	15.1	0.1367	50	3	33
30	16.2	0.0466	50	3	11
31	23.4	0.0361	50	3	9
32	22.8	0.0441	50	3	11
33	22.7	0.0806	50	3	19
34	23.5	0.0562	50	3	13
35	23.7	0.2258	50	3	54
36	23.5	0.0877	50	3	21
37	23.3	0.0709	50	3	17
38	22.5	0.1185	50	3	28
39	22	0.0683	50	3	16
40	21.9	0.2674	50	3	64
41	24.8	0.1641	50	3	39
42	24.6	0.1065	50	3	25
43	24.8	0.1225	50	3	29
44	25.6	0.1330	50	3	32
45	25.7	0.0415	50	3	10
46	26.3	0.0302	50	3	7
47	27.8	0.0072	50	3	2
48	28	0.0055	50	3	1
49	27.8	0.0055	50	3	1
50	26.7	0.0934	50	3	22
51	29.9	0.0512	50	3	12
52	30.8	0.0791	50	3	19
53	31.4	0.0334	50	3	8
54	31.4	0.0900	50	3	22
55	32	0.0226	50	3	5
56	32	0.0175	50	3	4
57	31.5	0.0155	50	3	4
58	30.4	0.0218	50	3	5

Chapter 5
Modeling Shorezone Erosion at Lake Tahoe

Anna K. Panorska
Kenneth D. Adams

Introduction

Shorezone erosion has negative effects on the water quality of Lake Tahoe due to the introduction of fine sediment and nutrients (Reuter and Miller, 2000). In addition to introducing sediment and nutrients into the lake, shorezone erosion also results in direct losses of land in backshore areas. Many factors affect the locations, rates, and amounts of erosion making prediction a challenging task. During the last four years, studies of the Lake Tahoe shorezone have focused on documenting physical characteristics (Chapter 2), delineating where erosion has occurred historically (Chapter 3; Adams and Minor, 2002), and collecting hourly wind and wave data to characterize driving forces (Chapter 4). The next logical step is to incorporate these observations and data into a framework that attempts to predict where, how much, and under what conditions shorezone erosion will occur.

In this chapter, we use data and knowledge gained in our studies thus far to develop a series of stochastic models of shorezone erosion. We start with a model of erosion occurrenc, which connects the probability of erosion with environmental characteristics. We then present a model for (conditional) distribution of the amount of erosion, given that erosion occurred. In combination, these approaches provide valuable information on where, how much, and under what conditions shorezone erosion will occur by considering lake-level fluctuations, material properties of the shorezone, wind and wave climate at Lake Tahoe, and local shorezone conditions. This chapter is presented in two parts. The first section develops and describes stochastic methods to predict whether or not erosion will occur at a particular place, and the second section presents techniques to determine how much erosion will occur at a location.

Modeling the Occurrence of Erosion

We used a generalized linear model, logistic regression, to build a model for erosion occurrence. Because we wanted to model a binary variable (erosion or no erosion), we chose a tool built for binary response modeling. Additionally, logistic regression is available in most professional statistical software programs and is optimized (parameterized) automatically according to well-defined statistical principles.

Logistic Regression Model

We used the techniques of McCullagh and Nelder (1989) to provide an estimate of a function of the response variable (erosion or no erosion) as a linear function of the predictor variables. In logistic regression, the response variable is binomial. That is, the variable has only two possible values: erosion occurred (1) or no erosion occurred (0) with probability of success (erosion) given as p. The logistic regression equation connects

a function *L* of *p* (the link function) with the linear function of the predictor variables. The link function is the logit function: L(p)=ln(p/(1-p)). In mathematical terms:

$$L(p) = ln\frac{p}{1-p} = \beta_o + \sum_{i=1}^{n}\beta_i x_i + \sum_{i,j}\beta_{ij} x_i * x_j, \quad i,j=1, \ldots, k \qquad \text{Eq. 5-1}$$

where the β's are real coefficients (parameters of the model), and x_i's are the *k* explanatory variables. The terms $\beta_{ij} x_i * x_j$ are called "interaction" terms. Once the model is parameterized, *p*'s are computed from the values of L(p) for each observation using an inverse logit function:

$$p = \frac{e^L}{1+e^L} \qquad \text{Eq. 5-2}$$

The inverse logit function is closely connected with logistic distribution, which is why this regression technique is called *logistic* regression. The model is parameterized to the data with maximum likelihood estimates of β_i's. These are computed using an iterative optimization procedure called iterative reweighted least squares (IRLS). For details on the IRLS procedures and generalized linear models, see McCullagh and Nelder (1989). All computations were made using an Splus procedure *glm*. The logistic regression model assigns an estimated probability of erosion to each shoreline segment.

Variables Influencing Erosion

To assess the impact of individual land, shore, and meteorological characteristics on the probability of erosion, we employed analysis of deviance and the Cp statistic criterion. For analysis of deviance (McCullagh and Nelder, 1983), we used a sequential chi-square test for significance of sequential addition of individual variables to the null model (model with only a constant term). The Cp statistics (McCullagh and Nelder, 1983; Akaike, 1973) were used to approximate the relative importance of each variable (or its smoothed value) to the response. The smaller the Cp statistics, the more "influential" the corresponding explanatory variable.

Goodness-of-Fit Techniques

In any statistical modeling problem, we have a choice of measures for goodness of fit. They always depend on the questions we want to answer and the cost of erroneous predictions with the model. In this project, we felt that it was most important that the models classify observations correctly (i.e., that the agreement between the shoreline segments observed as eroded or not eroded and classified by the model as eroded or not eroded is reasonable). To quantify the goodness of fit, we used traditional, and new, perhaps more intuitive measures of fit.

The traditional measure of fit is a chi-square test for independence between observations and model predictions. The chi-square test (Hosmer and Lemeshow, 1989) provides a means for assessing classification accuracy by testing independence between the

observed and model-predicted observations. We classified observations as eroded (E) or not eroded (NE) based on the probability of erosion estimated by the model. This required choosing a cutoff for probability of erosion that would classify a segment as E or NE. We chose a cutoff of 0.62, which optimized all conditional probabilities of match between the model and data. Other methods of choosing cutoff probability can be used, depending on user preferences and needs.

Another look at fit can be provided by analysis of model deviance. Deviance or residual deviance[1] of a logistic regression model is defined as:

$$\textit{Residual deviance} = -2 \times \ln(F) \qquad \text{Eq. 5-3}$$

where F is the likelihood function. That is, the residual deviance is the familiar "*–2**loglikelihood function*"*. The likelihood function (in logistic regression) gives the probability of observing the observed data under a logistic regression model. That is, F is the probability of observing the data we actually observed computed using the probabilities of erosion estimated by the model. In mathematical terms:

$$F = \prod_{i=1}^{n} \pi_i^{E_i} (1-\pi_i)^{1-E_i} \qquad \text{Eq. 5-4}$$

where every $\pi_i = P(E_i = 1)$ is the probability of erosion of the *ith* shoreline segment estimated by the model, and *n* is the total number of observations. The common interpretation of the likelihood function is having two models that give two sets of probabilities of erosion for every segment (the one with larger likelihood F is better). Thus, the model with smaller residual deviance is better. We would like to note that although the definition of residual deviance is very different from the definition of the error (residual) sum of squares in the familiar linear regression, their use for assessing regression model fit is similar. For linear regression, we seek a model with minimal error sum of squares; for logistic regression, we seek a model with minimal residual deviance. We can test if the difference between two models is significant using a chi-square test based on the difference between the residual deviances of the models (McCullagh and Nelder, 1983).

Another, perhaps more informative use of residual deviance is computation of n^{th} *root* of the likelihood function for a given model, that is $\sqrt[n]{F}$. Mathematically, $\sqrt[n]{F}$ is the *geometric* average probability of modeling what was actually observed (per segment). Averaging is with respect to the number of observations. A geometric average is a more suitable estimate of an average term in a product (F is a product) than the arithmetic average. With the residual deviance computed for a model, it is easy to compute $\sqrt[n]{F}$.

[1] We use the term "residual deviance" to be consistent with the familiar notion of residual sum of squares for linear models.

Namely,

$$\sqrt[n]{F} = exp(-Residual\ deviance / 2n) \quad \text{Eq. 5-5}$$

where n is the number of observations in the data set. Again, a successful model will simulate with a high *average* probability (per segment) what was actually observed.

New, intuitive measures of fit include conditional probabilities of match between observations and model predictions. A good model should predict erosion with reasonable accuracy, but accuracy measures need to be defined. An intuitive approach is to examine the four combinations of model predictions coupled with observations. We have two outcomes from the model: erosion (1) or no erosion (0). The observations also were partitioned into eroded (1) and non-eroded segments (0). When we couple model predictions with observations, we can calculate the probabilities of the model correctly predicting what was observed. More precisely, we examined the following conditional probabilities:

1. P(o1|p1), the probability of observing erosion (o1) given (|) that the model predicted erosion (p1)
2. P(o0|p0), the probability of observing no erosion (o0) given that the model predicted no erosion (p0)
3. P(p1|o1), the probability of predicting erosion (p1) given that erosion occurred (o1)
4. P(p0|o0), the probability of the model predicting no erosion (p0) given that no erosion occurred (o0)

We will refer to these probabilities as measures of fit. The choice of a particular measure of fit should be left to the user, although we estimated all of them.

In order to estimate measures of fit, we classified the probabilities of erosion returned by the models into two categories: erosion or no erosion. This step required choosing a cutoff point for the probabilities of erosion. All probabilities less than the cutoff were classified as prediction of no erosion. All of those equal to or greater than the cutoff were classified as predicted erosion. For every model, we explored a range of cutoffs. As expected, a given cutoff does not maximize all measures of fit at the same time.

Conditional probabilities of fit were estimated as relative frequencies. For example, the conditional probability of observed erosion given predicted erosion was computed as:

P(o1|p1) = P(o1 and p1)/P(p1) ≈ (the number of segments with observed and predicted erosion)/(the number of segments with predicted erosion).

Results

Variables influencing erosion. Explanatory variables considered in the logistic regression models included the type of feature, slope, normalized height of shoreline

feature, material, aspect, and wind station location. Some of these variables were qualitative (type of feature, material, and wind station location) and some quantitative (slope, normalized height, and aspect).

Below, we present results of sequential chi-square tests for significance for all variables added sequentially (first-top to last-bottom) to the model (Table 5-1). This analysis, with a mix of qualitative and quantitative variables in a logistic regression model, corresponds to the familiar analysis of covariance in the multivariate regression. The first column lists all explanatory variables in the order they were added to the model. The second column provides residual deviance of the sequentially upgraded models. The last column contains p-values of the sequential chi-square tests. The last line of Table 5-1 corresponds to the model with all explanatory variables. The NULL model includes an intercept but no explanatory variables.

Table 5-1. Results of first test on all explanatory variables with no interaction terms. Terms added sequentially (first to last).

	Residual Deviance	P-value
NULL model	87.32067	
Feature	78.06127	0.0097577
Slope	72.74613	0.0211409
Normalized height	72.57669	0.6806083
Material	62.82363	0.0207862
Aspect	62.61548	0.6482209
Wind	62.18464	0.5115794

The chi-square test suggested that feature, slope, and material were significant explanatory variables. Next, we repeated this test with several interaction terms involving significant variables. We present results of the final model tests with two significant interactions (slope*material and slope*wind) in Table 5-2. In the final model, we used the three individual variables that were significant in the no-interaction model and two interactions. Since the interaction between wind and slope is significant, we included wind itself as an explanatory variable in the final model.

Table 5-2. Results of final model tests with two significant interaction terms. Terms added sequentially (first to last).

	Residual deviance	Pr(Chi)
NULL model	87.32067	
Feature	78.06127	0.0097577
Slope	72.74613	0.0211409
Material	62.88530	0.0197869
Wind	62.37638	0.4756064
Slope*material	50.01642	0.0062465
Slope*wind	46.19912	0.0507260

The sequential chi-square tests were significant for feature, slope, material, and the interactions of slope*material and slope*wind. Additionally, we tested the model with interactions for significant improvement over the model without interaction terms. The test showed significant improvement after adding two interaction terms.

Finally, we computed Cp statistics for all models that included only one explanatory variable. The Cp statistical values for the NULL and all one-variable models are provided in Table 5-3. The lower the Cp statistics are, the more "influential" the variable. The NULL model includes an intercept but no explanatory variables.

Table 5-3. Cp statistical values for the NULL and one-variable models.

	Cp
NULL model	65.03226
Feature	61.35856
Slope	60.16785
Normalized height	66.93348
Material	52.57659
Aspect	62.42300
Wind	52.91893

The Cp statistics roughly confirm results of the chi-square analysis. Since feature and two interaction terms were found significant in the sequential chi-square test, we selected the model with feature, slope, material, and the interactions of slope*material and slope*wind as explanatory variables.

Goodness-of-Fit Analysis

We computed all measures of fit (conditional probabilities of matches between observed and predicted erosion) as well as performed chi-square tests of independence and analysis of deviance described above.

Measures of fit. Starting with results on the conditional probabilities of fit, the logistic regression model was fit to the data, and the probabilities of erosion were computed for each segment. In order to compute conditional probabilities of fit, we had to choose a cut-off value for the model-predicted probability of erosion. Any observation with the estimated probability of erosion below the cutoff value was classified as having no erosion; otherwise it was classified as eroded. Then, the conditional probabilities of match between observed and predicted erosion were computed (see *Goodness-of-fit techniques*).

Figure 5-1 presents estimated conditional probabilities of fit (match) as functions of the cutoff value. Two conditional probabilities [P(o1|P1) and P(p0|o0)] are increasing and two are decreasing [P(o0|P0) and P(p1|o1)] functions of the cutoff value. Fortunately, the curves intersect at roughly one point with a cutoff value of about 0.62. This means that 0.62 is an optimal cutoff. Overall, we were positively impressed with the fit of the model. For cutoff 0.62, all probabilities of match are about 0.8.

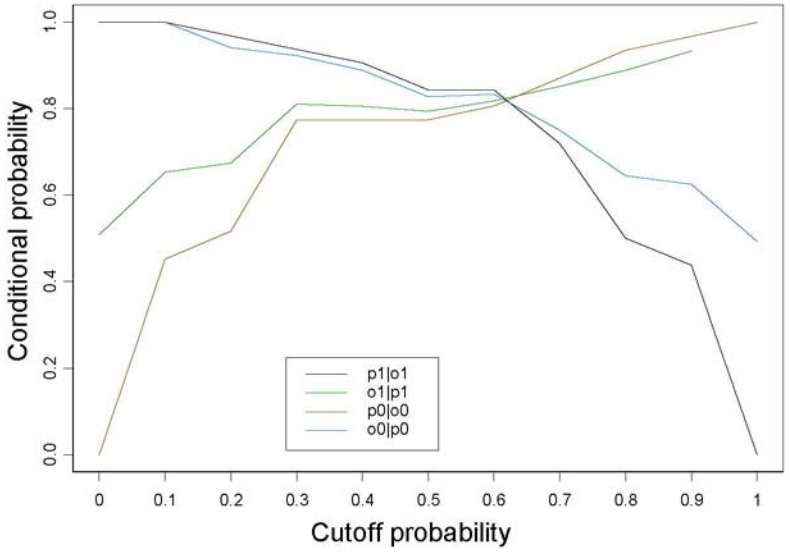

Figure 5-1. Estimated conditional probabilities of fit as a function of the cutoff value

Chi-square goodness-of-fit analysis. We also tested fit using the more conventional method of a chi-square test for independence between observed and model-predicted erosion. The tests showed dependence between observed and predicted erosion (p-values = 0).

Analysis of deviance. Estimates of geometric mean probabilities of modeling the data that was actually observed are as follows: NULL model (no explanatory variables) 0.5; fitted model: 0.69. The increase from 0.5 to about 0.7 is practically very significant.

MODELING THE AMOUNT OF EROSION

This section describes development of a stochastic model that predicts the amount of shorezone erosion at a location, given that erosion will occur. There were two main objectives for this part of the study:

1. Identifying a suite of explanatory variables necessary and significant for explaining and forecasting the amount of erosion on a lakeshore
2. Evaluating performance of different statistical models and choosing the model with the best predictive power.

Objective 1. Identifying a suite of explanatory variables necessary and significant for explaining and forecasting the amount of erosion on a lakeshore.

Adams and Minor (2002) defined 22 areas of the Lake Tahoe shorezone that have undergone erosion during the last 60 years (see Chapter 3). These areas were defined from a time-series of georectified air photos spanning the period from 1938 to 1998. The images were incorporated into an ArcView database for analysis. We used the 22 eroded shore segments as our study areas. For each of these segments, we compiled the following data: length, estimated eroded area and volume (Adams and Minor, 2002), soil material, slope, and total swash elevation for waves of a given height. We chose the estimated eroded area as the response variable describing the "amount" of erosion. We then analyzed wind and wave records looking for relationships with erosion. Our initial work focused on relationships between wind and wave statistics. The second step was exploration of the correlation between regional wind records from the National Oceanic and Atmospheric Administration (NOAA) Upper Air Archives (Oakland, California) and the local wind records at three sites around Lake Tahoe. Our objective for the wind data work was to explore the relationship between strong wind events causing high wave activity and erosion patterns around the lake.

Objective 2. Evaluating performance of different statistical models and choosing the model with the best predictive power.

We evaluated three types of models of erosion (linear, additive, and tree) as a function of the explanatory variables. We chose residual analysis and correlation between observed and model-predicted erosion as indicators of fit (or lack thereof).

Results

Variables for the model. As expected, the initial set of explanatory variables was successful in explaining variability in the amount of erosion at each of the sites (the variables were selected on the basis of their physical connections to erosion). Total swash elevation (TSE) reflects the lake level for any given wave energy and slope. TSE represents total elevation achieved by the swash of the waves above still water level (Komar, 1998). It is a linear function of slope, so the models with slope as an explanatory variable are equivalent to those with TSE. The reason for including TSE in the suite of explanatory variables was to make a connection between lake level and the amount of erosion. Although that connection is not direct, it is the only one we found significant in the models. We evaluated the usefulness of each variable in explaining the erosion amount by including that variable in the model and checking its contribution to variability in the erosion amount. Note that some of the explanatory variables are continuous (erosion area, TSE) and some are discrete (soil material-five levels)—implying that we use analysis of covariance as our tool.

We also explored a wide range of wind statistics as explanatory variables. These included maximum and average of local winds as well as the percent of time and number of hours the wind direction was within 30° of the aspect of a given segment. None of the wind statistics proved significant in modeling erosion. A discrete variable grouping eroded areas by the location of the closest wind station (wind location – 3 levels) proved significant, however. We are not sure why and will explore this question in future

research. The final set of explanatory variables included TSE50 (TSE with a common deep-water wave height of 50 cm), soil material, and wind direction.

Relationship between winds and waves. Wave records were combined with local wind records for this analysis. Both wind and wave records were summarized to hourly averages for the time period when both records were available (3/2/01–8/31/01). Wave records were from three wave stations: Incline Village (IV), Thunderbird Lodge (TB) and Meeks Bay (MB). The wind records were from three wind stations: TB, D.L. Bliss State Park (DLB), and South Lake Tahoe Blvd (SLT) (Fig. 4-4). Wind records corresponding to wave records were chosen by proximity. The wave records from IV and TB were paired with the wind record at TB. The wave record at MB was paired with DLB wind data. As expected, we found that significant wave height is closely correlated with wind speed (Fig. 4-10). This correlation depended on the site, however. Correlations between significant wave height and wind speed ranged from 0.75 at TB and 0.72 at IV to only 0.26 at MB. Our explanation is that the MB station is in a relatively sheltered location, and the direction of the winds is variable around that location because of the rugged terrain. This variability in wind direction may be one important factor diminishing the correlation between wind speed and wave height. Differences between distributions of wind direction and speed for the two wind records sites (DLB and TB) paired with the wave data are evident in the boxplots presented in Figs. 5-2 and 5-3.

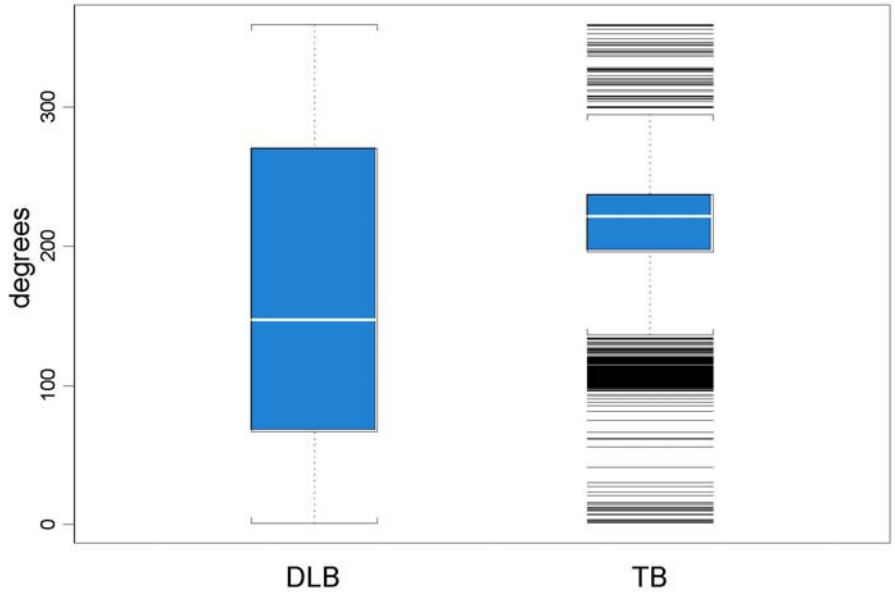

Figure 5-2. Boxplot showing the distribution of wind directions at the DLB and TB sites. Distribution of the wind direction at DLB shows much more dispersion than at TB. In fact, the standard deviation (in degrees) of wind direction at TB (53) is about half of the standard deviation of the wind direction at DLB (114).

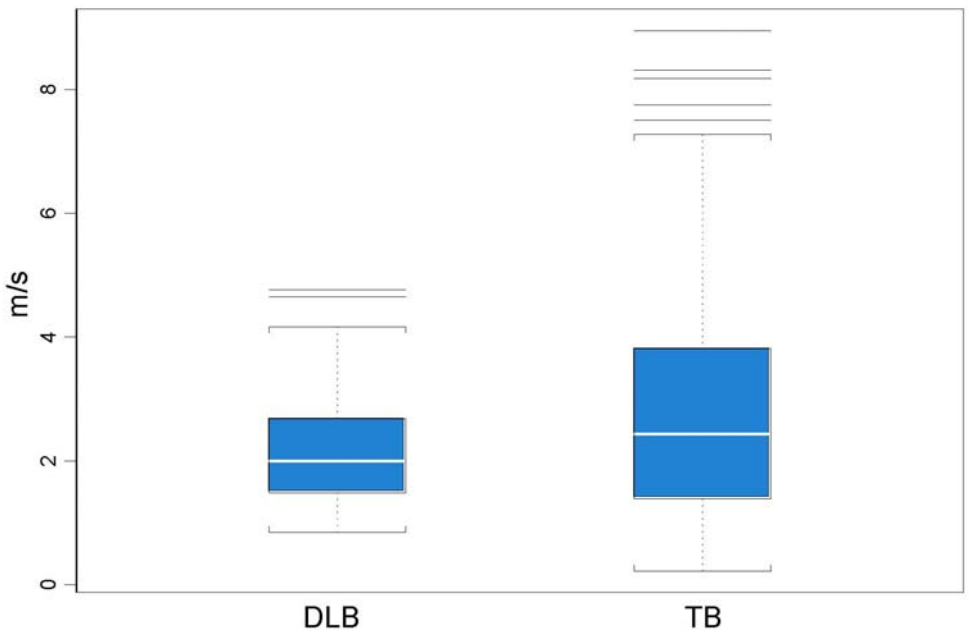

Figure 5-3. Boxplot showing distributions of hourly wind speeds at the DLB and TB sites. The wind speed at DLB is generally lower and less variable than at TB.

An exploratory step was taken by modeling wind speed at one lake location using speed at another as proxy. This analysis used wind data summarized to daily averages at the three stations for the period from 9/1/98 to 8/31/01. Wind speeds were smoothed to reduce variability, and then linear and polynomial models were fit to the smoothed, paired wind records. Correlations were computed between modeled and observed wind speeds. These ranged from 0.47 (LTB and DLB–linear model) to 0.70 (LTB and TB–polynomial model) to 0.75 (DLB and TB–polynomial model). It seems that future modeling should be done piecewise (i.e., using different models for high and low wind speeds).

Relationships of local and regional wind records. We also studied relationships between regional wind records from NOAA Upper Air Archives and local wind records from the three wind record sites around Lake Tahoe. This was undertaken to extend a proxy wind record for the Tahoe Basin back to the 1940s, the period of record for the Upper Air Archives. We summarized the local data sets from hourly to twice-daily wind statistics because the Oakland data recorded wind characteristics around noon and midnight. Local data between 6 a.m. and 5 p.m. were summarized (min, max, average, median) to correspond to the noon sampling in Oakland. The rest of the local data were summarized to correspond to the midnight sampling in Oakland. Our analysis focused on identifying

patterns linking the Oakland data to local wind records. No definite pattern was found. Correlations between wind speed and direction at Oakland and locally at Lake Tahoe were very low (below 0.3 in all cases). No transformation of variables helped. We concluded that the two records are not closely related and that there is little information about the local wind climate at Lake Tahoe that can be gained from the upper air records in Oakland.

Modeling erosion. We explored several statistical approaches to modeling erosion: linear, additive, and tree. We used residual analysis and correlation between observed and model-predicted erosion as indicators of fit. The best in terms of these measures of fit was the linear model. Since explanatory variables were mixed, continuous, and discrete, the model had to be fitted to the data using a "dummy variables" technique. The technique accounts for each level (value) of each discrete variable by assigning a coefficient to the indicator of that variable.

The data set used for modeling is included as Table 5-1. The five levels of soil material were coded as: old granitic beach sand (ogbs), granitic beach sand (gbs), gravelly silt (gs), glacial till (gt), and volcanic beach sand (vbs). The three levels of the wind data variable correspond to the locations of the wind stations closest to the shore segment. The resulting linear model was:

$$\text{Eroded area} = 6701.9 - 9586.7*I(gbs) - 7958.1*I(gs) - 1257.1*I(gt) + 72.3*I(ogbs) + 222.66*TSE50 + 2688.3*I(Bliss) - 2547.3*I(LTB) \quad \text{Eq. 5-6}$$

where I(x) is the indicator function. I(x) is 1 when its argument is equal to x, otherwise it is 0.

The multiple R^2 for this model is 0.738, and the correlation between the observed and model-predicted amount of erosion was 0.86. The observed and predicted erosion areas together with 95% pointwise prediction intervals are plotted in Fig. 5-4.

Table 5-4. Dataset for modeling the amount of shorezone erosion.

Location	Soil material	Eroded area	Tse50	Wind data	Predicted eroded area
NevadaBeach	ogbs	21898	22.71	LTB	13150.75
Stateline	ogbs	361	4.62	LTB	9122.98
BijouPark	ogbs	11644	3.19	LTB	8803.60
AlTahoe	ogbs	11275	3.19	LTB	8803.60
UpperTruckee	gbs	31643	4.38	LTB	31643.00
TahoeKeys	ogbs	1234	5.58	LTB	9335.90
KivaBeach	ogbs	10272	8.77	LTB	10045.64
BaldwinBeach	ogbs	13600	13.15	LTB	11021.53
SEEmeraldBay	gt	15544	117.14	Bliss	17912.42
EmeraldBayVikingsholm	gt	8304	63.35	Bliss	5935.58
MeeksBay	ogbs	6996	41.04	Bliss	11855.14
SugarPinePoint	ogbs	4008	11.16	Bliss	5201.35
Homewood	vbs	18813	31.08	Bliss	13769.91
TahoeTavern	vbs	9545	7.57	Bliss	8535.59
LakeForest	gs	1962	3.59	Tbird	1962.00
CarnelianBay	vbs	8160	17.93	Tbird	5888.74
AgateBay	vbs	4562	20.32	Tbird	6421.04
TahoeVista	vbs	3449	10.36	Tbird	4203.11
Brockway	ogbs	1190	6.77	Tbird	-728.05
KingsBeachwest	vbs	728	6.77	Tbird	3404.65
KingsBeacheast	vbs	903	9.16	Tbird	3936.96
Glenbrook	ogbs	4471	11.55	Tbird	336.56

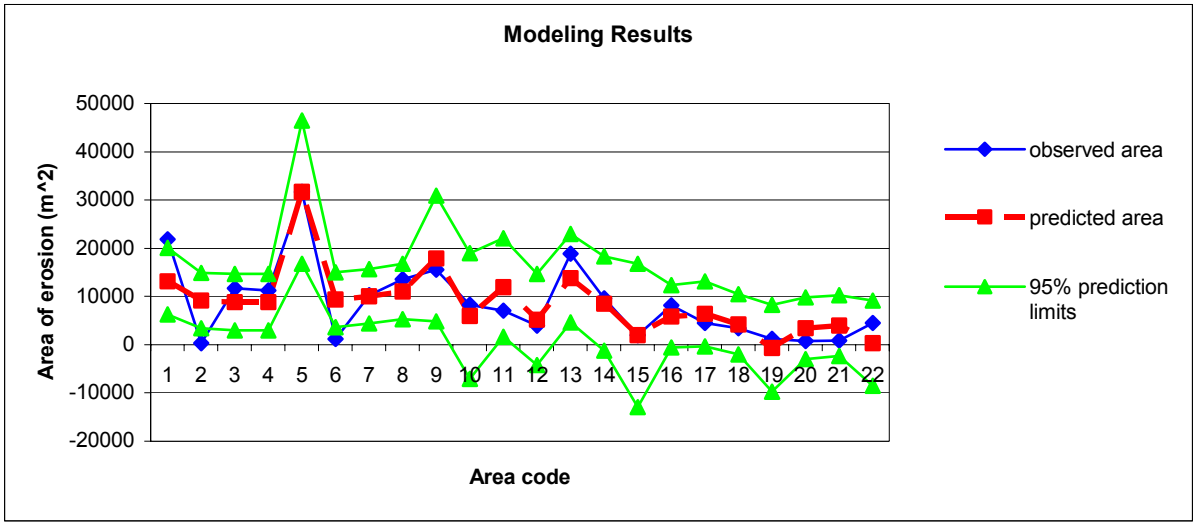

Figure 5-4. Plot of modeling results showing the predicted areas of erosion compared to the observed area and the 95% pointwise prediction limits.

All variables in the model are statistically significant on a 5% significance level (Table 5-5). The residuals for this model have the following statistics:

Table 5-5. Statistics of the residuals for shoreline erosion model.

Statistics of the residuals					
Minimum	1st Quartile	Mean	Median	3rd Quartile	Maximum
-8761.98	-2241.07	0.00	113.18	2445.65	8747.25

Distribution is fairly symmetric around zero and does not change much with the increase in predicted values. Thus, we conclude that our model, although simple, is a good working model. We believe that although the variables in the model were predictable (i.e., chosen because they should influence erosion), the value of this work lies in quantification of the amount of erosion.

Conclusions

In this paper we developed a series of stochastic models that predict where, how much, and under what conditions shorezone erosion will occur at Lake Tahoe. These models consider environmental factors such as lake-level fluctuations, material properties of the shorezone, and the wind and wave climate at Lake Tahoe. They do not, however, account for the effects of shorezone protective structures. Therefore, when applying these models, local shorezone conditions must be taken into account. The approaches and models developed herein should be adaptable to other large lakes if the contributing parameters are known or can be measured.

Chapter 6
Effect of Different Lake-Level Scenarios on Shorezone Erosion

Kenneth D. Adams
Anna K. Panorska

Introduction

The amount of shorezone erosion that has occurred, or has the potential to occur, at any particular location around Lake Tahoe is directly related to material properties of the shorezone, wave activity, and fluctuating water levels (Chapter 3; Adams and Minor, 2002). More specifically, shorezone erosion typically is caused by waves breaking at the bases of easily eroded bluffs when lake level is high. Both the direct impact of waves on the bluffs and the onrush of wave swash up the beach are capable of erosion and sediment transport. When lake level is low, wave energy is expended on the beaches and does not impact long-term shore erosion.

The natural spill point for Lake Tahoe is at about 1897 m (6223 ft). Since the 1880s, a series of dams at the outlet have increased lake level to as high as 1899.2 m (6231 ft) resulting in large amounts of shorezone erosion. The Lake Tahoe dam is now operated under the Truckee River Agreement (TRA), which has been in place since 1935. Under this management scheme, lake level is mandated to not exceed 1898.65 m (6229.1 ft), and water is managed for flood control and to satisfy water rights. A new management scheme, the Truckee River Operating Agreement (TROA), is currently under consideration to replace the existing management scheme for dam operations. Under TROA, the dam would continue to be operated for flood control and to satisfy water rights, but also would provide for enhancement of spawning flows in the lower Truckee River. Because projected lake levels under TROA would be slightly different than under the TRA, concerns have been raised about how TROA, if implemented, might affect shorezone erosion at Lake Tahoe. In this chapter, we address the question of whether or not lake levels under TROA would significantly affect shorezone erosion.

Observations of the Heights of Shoreline Angles and Beach Ridges

A record of past erosive events at Lake Tahoe is preserved by shoreline angles, which are formed by erosion and sediment transport during wave breaking and run up. Shoreline angles are defined by an abrupt change in slope found at the upper edges of beaches and at the bases of wave cut escarpments. These angles represent the minimum height of maximum wave run up (Fig. 6-1). Another measure of the height to which waves can reach is the crest of beach ridges, which commonly form on lower gradient slopes with an abundant sediment supply. Variations in the heights of both types of features provide a measure of how much shorezone erosion has occurred at a site in the past, and more importantly, the potential for further erosion in the future.

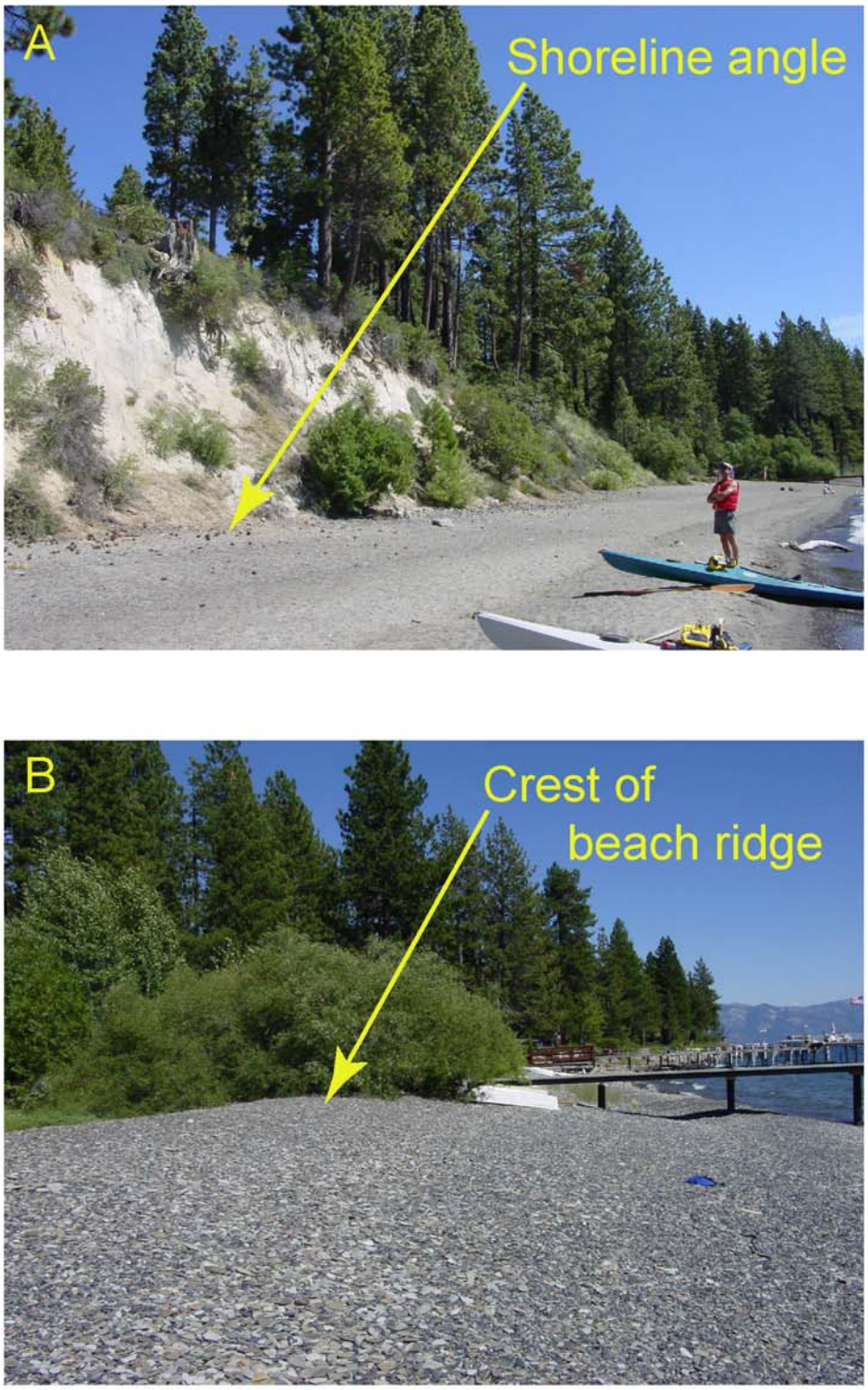

Figure 6-1. Photographs of features reflecting the height of modern wave runup. A) Shoreline angle formed at the top of the beach and at the base of a wave-eroded bluff. B) Coarse gravel beach ridge formed from wave run up.

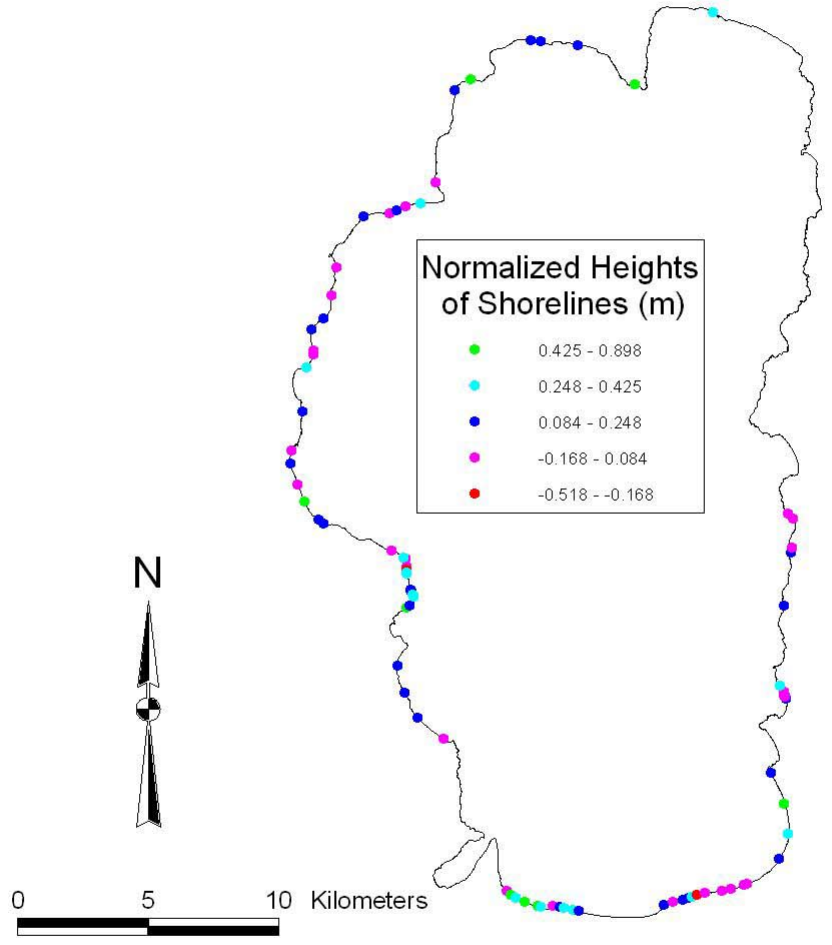

Figure 6-2. Map of the locations of shoreline angle and beach ridge measurements and their heights relative to the maximum lake level of 1898.65 m (6229.1 ft).

We made 90 elevation measurements of shoreline angles and the crests of beach ridges along most parts of the shore capable of erosion (Fig. 6-2 and Table 6-1). In Figure 6-2, the height of the shore features is plotted with respect to the maximum lake level of

1898.65 m (6229.1 ft); positive numbers indicate features above maximum lake level, while negative numbers indicate features below maximum lake level. Elevations were measured with a hand level and survey staff, using the surface of the lake as a known datum. Elevations of shoreline angles and beach ridges vary by as much as 1.4 m, which is in part a reflection of the variation in the height of wave run up at different locations around the lake. In general, elevations of beach ridge crests are higher than nearby shoreline angles, an observation consistent with Pleistocene beach features in the Lahontan basin (Adams and Wesnousky, 1998). For about 20% of the locations measured, the elevation of the shoreline angle is actually lower than the maximum lake level of 1898.65 m (6229.1 ft) (Table 6-1). This means that when the lake is at full pool, the still-water level is at or above the elevation of the shoreline angle and that waves will directly impact the bluff (see Fig. 2-5). The fact that there are a significant number of locations with shoreline angles lower than the maximum lake level is further proof that the shorezone system of Lake Tahoe is not yet in equilibrium and that erosion will continue to occur when lake levels are high.

Table 6-1. Locations and heights of features reflecting the modern wave climate at Lake Tahoe. SL angle = shoreline angle. Normalized height is the height of the feature minus the legal high limit of Lake Tahoe (1898.65 m). Coordinate system is UTM Zone 10, NAD 27.

	Easting	Northing	Feature	Height of feature (m)	Normalized height (m)
1	749818	4325595	beach ridge	1899.18	0.5285
2	749692	4327507	SL angle	1899.13	0.4785
3	749729	4327475	SL angle	1898.93	0.2785
4	749765	4327442	SL angle	1898.63	-0.0215
5	749834	4327167	SL angle	1898.78	0.1285
6	749836	4327140	SL angle	1898.53	-0.1215
7	749819	4327096	SL angle	1898.73	0.0785
8	749821	4327056	SL angle	1898.33	-0.3215
9	749815	4326989	SL angle	1898.38	-0.2715
10	749810	4326951	SL angle	1898.48	-0.1715
11	749809	4326922	SL angle	1898.98	0.3285
12	749810	4326874	SL angle	1898.98	0.3285
13	749957	4326279	SL angle	1898.83	0.1785
14	749981	4326228	SL angle	1898.83	0.1785
15	750001	4326195	SL angle	1898.88	0.2285
16	750013	4326153	SL angle	1898.83	0.1785
17	750034	4326096	SL angle	1898.98	0.3285
18	750073	4326030	SL angle	1898.98	0.3285
19	750095	4326006	SL angle	1898.98	0.3285
20	749926	4325665	SL angle	1898.88	0.2285
21	753637	4314771	SL angle	1898.53	-0.1184
22	753793	4314630	beach ridge	1899.33	0.6816
23	753975	4314530	beach ridge	1898.93	0.2816
24	754320	4314359	beach ridge	1899.28	0.6316

Table 6-1 (cont.)

25	754809	4314188	beach ridge	1899.13	0.4816
26	754946	4314156	beach ridge	1899.03	0.3816
27	755380	4314218	SL angle	1898.58	-0.0684
28	755651	4314171	SL angle	1898.88	0.2316
29	755806	4314131	SL angle	1898.98	0.3316
30	756148	4314042	SL angle	1898.93	0.2816
31	756383	4314003	SL angle	1898.78	0.1316
32	759651	4314232	SL angle	1898.83	0.1816
33	759996	4314378	SL angle	1898.58	-0.0684
34	760363	4314440	beach ridge	1898.83	0.1816
35	760578	4314526	beach ridge	1898.78	0.1316
36	760687	4314541	beach ridge	1899.03	0.3816
37	760902	4314633	SL angle	1898.13	-0.5184
38	761200	4314707	SL angle	1898.48	-0.1684
39	761833	4314795	SL angle	1898.63	-0.0184
40	762209	4314854	SL angle	1898.68	0.0316
41	762699	4315017	SL angle	1898.68	0.0316
42	762796	4315054	SL angle	1898.63	-0.0184
43	764234	4318118	beach ridge	1899.13	0.4785
44	764378	4316957	SL angle	1898.93	0.2785
45	764010	4315990	SL angle	1898.83	0.1785
46	763710	4319290	SL angle	1898.83	0.1785
47	745841	4333076	SL angle	1898.84	0.1834
48	745431	4331603	SL angle	1898.69	0.0334
49	745378	4331073	SL angle	1898.79	0.1334
50	745666	4330290	SL angle	1898.74	0.0834
51	745920	4329647	SL angle	1899.14	0.4834
52	746441	4328952	SL angle	1898.84	0.1834
53	746631	4328787	SL angle	1898.84	0.1834
54	749259	4327770	SL angle	1898.69	0.0334
55	749693	4327516	SL angle	1899.04	0.3834
56	746000	4334744	beach ridge	1898.99	0.3335
57	746273	4335259	SL angle	1898.59	-0.0665
58	746273	4335413	SL angle	1898.64	-0.0165
59	746200	4336210	SL angle	1898.89	0.2335
60	746656	4336629	SL angle	1898.74	0.0835
61	746949	4337495	SL angle	1898.69	0.0335
62	747133	4338565	SL angle	1898.69	0.0335
63	748166	4340504	SL angle	1898.74	0.0835
64	749458	4323365	SL angle	1898.78	0.1255
65	749726	4322339	SL angle	1898.88	0.2255
66	751248	4320567	SL angle	1898.58	-0.0745
67	750243	4321404	SL angle	1898.78	0.1255
68	764477	4327693	SL angle	1898.77	0.1133
69	764529	4327899	SL angle	1898.67	0.0133

Table 6-1 (cont.)

70	764574	4328969	SL angle	1898.72	0.0633
71	764376	4329197	SL angle	1898.67	0.0133
72	764222	4325661	SL angle	1898.77	0.1133
73	749161	4340634	SL angle	1898.55	-0.1019
74	749436	4340744	SL angle	1898.85	0.1981
75	749774	4340910	SL angle	1898.55	-0.1019
76	750360	4341034	SL angle	1898.90	0.2481
77	750923	4341830	SL angle	1898.60	-0.0519
78	751657	4345319	SL angle	1898.75	0.0981
79	752272	4345755	beach ridge	1899.55	0.8981
80	754565	4347239	SL angle	1898.83	0.1749
81	754952	4347210	SL angle	1898.88	0.2249
82	756345	4347036	SL angle	1898.78	0.1249
83	758514	4345579	SL angle	1899.08	0.4249
84	761495	4348327	SL angle	1898.98	0.3249
85	764297	4322109	SL angle	1898.82	0.1652
86	764262	4322179	SL angle	1898.72	0.0652
87	764247	4322214	SL angle	1898.72	0.0652
88	764221	4322240	SL angle	1898.72	0.0652
89	764205	4322375	SL angle	1898.72	0.0652
90	764082	4322615	SL angle	1898.92	0.2652

Modeling of Wave Run up

To address the question of whether TROA will significantly affect shorezone erosion, we need to define what "affect" means in this context. In order for the shorezone to erode, waves need to reach the shoreline angle, either by directly breaking on the bluff itself or by the swash of the breaking waves rushing up the beach and reaching the base of the bluff. The impact of waves at the bases of wave-cut escarpments results in undercutting and shoreward retreat of the bluff, which typically occurs when lake level is high. If wave run up does not reach the base of a bluff, then erosion likely will not occur. Similarly, shore retreat can occur if wave swash overtops active beach ridges, eroding material from the front of the beach ridge and depositing it on the shoreward side of the ridge, causing the ridge to migrate landward (Adams and Wesnousky, 1998).

Lake Tahoe typically fluctuates between its maximum lake level of 1898.65 m (6229.1 ft) and its natural rim elevation of about 1897 m (6223 ft) (Fig. 1-2), although sometimes the lake drops below its natural rim. It is reasonable to assume that shorezone erosion only occurs when lake level is high. The question then becomes, at what lake-surface elevation does shorezone erosion potentially become significant?

To address this question, we used observations of elevations of shoreline angles and beach ridges (Table 6-1) compared to modeled elevations of wave run up for a variety of wave parameters and lake levels. The maximum wave run up height above still-water

level is known as total swash elevation (TSE), which is linearly dependent on the local slope and wave period:

$$\text{Total swash elevation} = 0.36 g^{0.5} S H^{0.5} T \qquad \text{Eq. 6-1}$$

where g = 9.81 msec^{-2}, S = slope, H = deep-water significant wave height, and T = wave period (Komar, 1998). This equation predicts the height above still-water level that swash from waves of given parameters will reach upon breaking. Modeled lake levels for Lake Tahoe under current operating conditions were used in this analysis (Table 6-2), along with the wave parameters outlined in Table 6-3.

Table 6-2. Average annual lake levels for the water year under current conditions.

Exceedence values	Lake level (ft)	Lake level (m)
Maximum	6228.74	1898.54
5%	6228.45	1898.45
10%	6228.37	1898.43
20%	6228.24	1898.39
30%	6228.11	1898.35
40%	6227.89	1898.29
Median (50%)	6227.63	1898.20
60%	6226.90	1897.98
70%	6226.16	1897.76
80%	6224.92	1897.38
90%	6223.55	1896.96
95%	6222.86	1896.75
Minimum	6221.49	1896.33

Table 6-3. Wave parameters used in this analysis.

Wave height (m)	Wave period (sec)
0.5	3
1	4
2	5

We first modeled the TSE at each of the 90 shoreline measurement locations (Table 6-1), given the three sets of wave parameters in Table 6-3. Slope was calculated from high-resolution LIDAR bathymetry. We then added the TSE values for the three types of waves to the lake levels associated with each of the exceedence frequencies (Table 6-2) to determine the absolute height that the TSE would reach. These elevations were then compared to elevations of the shoreline angles and beach ridges (Table 6-1). If the TSE at a particular site reached the elevation of the shoreline angle or the crest of a beach ridge, then we concluded that shorezone erosion is possible at that location, for those conditions.

For the smallest waves (0.5 m, 3 sec), shoreline angles and beach ridges are not impacted at any of the 90 sites when lake level is at 1898.01 m (6227 ft) or lower. For the next larger waves (1 m, 4 sec), just one shoreline angle and no beach ridges are impacted when lake level is at 1898.01 m (6227 ft) or lower. For the largest waves (2 m, 5 sec), shoreline angles are impacted at four of the 90 sites when lake level is at 1898.01 m (6227 ft) or lower. Therefore, 1898.01 m (6227 ft) is a reasonable cutoff lake surface elevation to choose when discussing lake level as it relates to shorezone erosion.

Changing Water Levels Under TROA

In order to assess how much erosion is possible at any given location around Lake Tahoe and how changing lake levels under TROA might affect shorezone erosion, we must make several assumptions. We first assume that this assessment only applies to shorezones capable of erosion, which generally excludes bedrock shores and shores with significant and effective shore protective structures. Next, we assume that lake level will never rise above the maximum legal level of 1898.65 m (6229.1 ft). Given this constraint, there is a maximum run up elevation for every shore location based on the maximum size waves possible for that location and local conditions such as slope. Given enough time, the maximum size waves possible at any given location will occur at that location. The amount of time that it will take for the Lake Tahoe shorezone to reach equilibrium (i.e., when shorezone erosion no longer occurs) is unknown. It is likely, however, that the rate of change will decrease through time as more and more storms impact various parts of the shore when lake level is high. Recall that the natural rim of Lake Tahoe is at approximately 1897 m (6223 ft), so waves have only been acting on the shorezone being formed at 1898.65 m (6229.1 ft) for some fraction of the 120 years or so when the first dam was installed. Because TROA will not alter the maximum legal limit of Lake Tahoe, this proposed agreement should have no impact on the total, long-term amount of shorezone erosion. TROA may, however, affect the rate of shorezone erosion in the shorter term because it will affect lake levels below the maximum limit.

The concern that TROA will increase shorezone erosion is primarily related to the fact that lake levels would be altered from those under different lake-level management scenarios, including the existing scheme. In this analysis, three different lake level scenarios are compared to TROA, including Current, No Action, and Local Water Supply options. The U.S. Bureau of Reclamation supplied modeling data for each of these scenarios. If lake levels are the same or lower than under TROA in these comparisons, then no increases in shorezone erosion are expected. If lake levels are higher under TROA, then there is a potential for increased shorezone erosion.

The first step to evaluate potential effects of different lake-level scenarios on future shorezone erosion is to calculate the difference in lake levels from each of the four different scenarios. In this study, the 5% exceedence lake levels (wet conditions) (Table 6-4) and 50% exceedence lake levels (moderately wet conditions) (Table 6-5) were used for each calendar month for comparisons. The order of comparison is Current vs. No Action, Current vs. Local Water Supply, Current vs. TROA, No Action vs. TROA, and No Action vs. Local Water Supply.

Table 6-4**.** Comparison of lake level changes (5% exceedence values) between Current vs. No Action, Current vs. Local Water Supply, Current vs. TROA, No Action vs. TROA, and No Action vs. Local Water Supply. Green-shaded boxes are those that have positive lake-level changes under TROA. Units are in meters.

	OCT	NOV	DEC	JAN	FEB	MAR	APR	MAY	JUN	JUL	AUG	SEP
Current	1898.439	1898.409	1898.427	1898.452	1898.470	1898.528	1898.546	1898.622	1898.622	1898.622	1898.558	1898.479
vs.												
No Action	1898.430	1898.409	1898.421	1898.452	1898.467	1898.516	1898.546	1898.622	1898.622	1898.622	1898.558	1898.473
Differences	-0.009	0.000	-0.006	0.000	-0.003	-0.012	0.000	0.000	0.000	0.000	0.000	-0.006
Current	1898.439	1898.409	1898.427	1898.452	1898.470	1898.528	1898.546	1898.622	1898.622	1898.622	1898.558	1898.479
vs.												
Local Water Supply	1898.430	1898.409	1898.421	1898.452	1898.467	1898.516	1898.546	1898.622	1898.622	1898.622	1898.558	1898.473
Differences	-0.009	0.000	-0.006	0.000	-0.003	-0.012	0.000	0.000	0.000	0.000	0.000	-0.006
Current	1898.439	1898.409	1898.427	1898.452	1898.470	1898.528	1898.546	1898.622	1898.622	1898.622	1898.558	1898.479
vs.												
TROA	1898.427	1898.403	1898.421	1898.455	1898.473	1898.528	1898.546	1898.622	1898.622	1898.622	1898.552	1898.470
Differences	-0.012	-0.006	-0.006	0.003	0.003	0.000	0.000	0.000	0.000	0.000	-0.006	-0.009
No Action	1898.430	1898.409	1898.421	1898.452	1898.467	1898.516	1898.546	1898.622	1898.622	1898.622	1898.558	1898.473
vs.												
TROA	1898.427	1898.403	1898.421	1898.455	1898.473	1898.528	1898.546	1898.622	1898.622	1898.622	1898.552	1898.470
Differences	-0.003	-0.006	0.000	0.003	0.006	0.012	0.000	0.000	0.000	0.000	-0.006	-0.003
No Action	1898.430	1898.409	1898.421	1898.452	1898.467	1898.516	1898.546	1898.622	1898.622	1898.622	1898.558	1898.473
vs.												
Local Water Supply	1898.430	1898.409	1898.421	1898.452	1898.467	1898.516	1898.546	1898.622	1898.622	1898.622	1898.558	1898.473
Differences	0.000	0.000	0.000	0.000	0.000	0.000	0.000	0.000	0.000	0.000	0.000	0.000

Table 6-5**.** Comparison of lake level changes (50% exceedence values) between Current vs. No Action, Current vs. Local Water Supply, Current vs. TROA, No Action vs. TROA, and No Action vs. Local Water Supply. Green-shaded boxes are those that have positive lake-level changes under TROA. Units are in meters.

	OCT	NOV	DEC	JAN	FEB	MAR	APR	MAY	JUN	JUL	AUG	SEP
Current	1898.022	1898.010	1898.000	1898.107	1898.110	1898.122	1898.144	1898.342	1898.479	1898.421	1898.314	1898.180
vs.												
No Action	1898.010	1897.994	1897.985	1898.077	1898.089	1898.116	1898.135	1898.339	1898.467	1898.409	1898.299	1898.171
Differences	-0.012	-0.015	-0.015	-0.030	-0.021	-0.006	-0.009	-0.003	-0.012	-0.012	-0.015	-0.009
Current	1898.022	1898.010	1898.000	1898.107	1898.110	1898.122	1898.144	1898.342	1898.479	1898.421	1898.314	1898.180
vs.												
Local Water Supply	1898.007	1897.994	1897.985	1898.077	1898.089	1898.113	1898.135	1898.339	1898.464	1898.409	1898.299	1898.171
Differences	-0.015	-0.015	-0.015	-0.030	-0.021	-0.009	-0.009	-0.003	-0.015	-0.012	-0.015	-0.009
Current	1898.022	1898.010	1898.000	1898.107	1898.110	1898.122	1898.144	1898.342	1898.479	1898.421	1898.314	1898.180
vs.												
TROA	1898.061	1898.058	1898.049	1898.107	1898.132	1898.138	1898.171	1898.351	1898.476	1898.418	1898.305	1898.199
Differences	0.040	0.049	0.049	0.000	0.021	0.015	0.027	0.009	-0.003	-0.003	-0.009	0.018
No Action	1898.010	1897.994	1897.985	1898.077	1898.089	1898.116	1898.135	1898.339	1898.467	1898.409	1898.299	1898.171
vs.												
TROA	1898.061	1898.058	1898.049	1898.107	1898.132	1898.138	1898.171	1898.351	1898.476	1898.418	1898.305	1898.199
Differences	0.052	0.064	0.064	0.030	0.043	0.021	0.037	0.012	0.009	0.009	0.006	0.027
No Action	1898.010	1897.994	1897.985	1898.077	1898.089	1898.116	1898.135	1898.339	1898.467	1898.409	1898.299	1898.171
vs.												
Local Water Supply	1898.007	1897.994	1897.985	1898.077	1898.089	1898.113	1898.135	1898.339	1898.464	1898.409	1898.299	1898.171
Differences	-0.003	0.000	0.000	0.000	0.000	-0.003	0.000	0.000	-0.003	0.000	0.000	0.000

In examining Table 6-4 (5% exceedence values), most of the comparisons yield no change or a negative number, which indicates that lake level would actually be lowered in those cases. If lake level does not change or is lowered, then there is no increased potential for shorezone erosion. Therefore, in the scenario comparisons of Current vs. No Action, Current vs. Local Water Supply, and No Action vs. Local Water Supply (Table 6-4), shorezone erosion will not be affected. In both the Current vs. TROA and No Action vs. TROA scenario comparisons, lake level would be slightly increased for a period of two to three months each year (Table 6-4). The magnitude of lake-level change under TROA, compared to Current and No Action alternatives for the 5% exceedence values, would range from 0.3 to 1.2 cm (0.01 to 0.04 feet; 0.12 to 0.48 inches).

For the 50% exceedence values (Table 6-5), most of the comparisons also yield no change or a negative change. In particular, for the scenario comparisons of Current vs. No Action, Current vs. Local Water Supply, and No Action vs. Local Water Supply (Table 6-5), shorezone erosion will not be affected. In the Current vs. TROA comparison, lake level would be increased by as much as 4.9 cm (0.16 feet; 1.92 inches) in November and December and lesser amounts during other times of the year. For the TROA vs. No Action comparison, lake level would be increased during all months of the year by 0.6 to 6.4 cm (0.2 to 0.21 feet; 0.24 to 2.52 inches) (Table 6-5).

To evaluate whether or not these magnitudes of lake-level change (for both the 5% and 50% exceedence values) would influence shorezone erosion, we used observations of the elevations of shoreline angles and beach ridges combined with analytical modeling of wave run up processes and a statistical procedure to determine significance.

Stochastic Model

Our procedure was to evaluate the probability of whether shoreline angles and beach ridge crests (Table 6-1) would be reached by run up from different wave sizes under several lake-level scenarios. Given a lake level, we estimated the proportion of the 90 shoreline segments where the waves would have TSE large enough to reach the shoreline angle. That proportion would indicate the probability of erosion of a segment. Further, given two lake levels and wave parameters, we estimated the difference in the proportion of segments for which the waves reached the shoreline angle. Using stochastic techniques, we estimated that difference and tested its significance. If the difference was not significantly different from zero, we concluded that the two lake levels were no different in their erosive potential. If the difference was significantly different from zero, we concluded that the higher lake level had significant potential for causing more erosion. For this analysis, we used several combinations of wave height and period that are common or possible for Lake Tahoe (Table 6-3).

For a higher lake level, we let X_i, i=1, …, 90 be independent and identically distributed random variables indicating erosion potential (i.e., let X_i=1 for the i^{th} segment if the total swash elevation is greater than the elevation of the shoreline angle of that segment). This implies that waves will impact the shoreline angle and potentially cause erosion of that segment otherwise, we let X_i=0 (no erosion for given waves).

For the lower lake level, we let Y_i correspond to X_i's (i.e., Y_i has the same interpretation for each of the 90 shoreline segments).

Next, we let $p_x = (1/90)\Sigma_{i=1}^{90} X_i$ and $p_y = (1/90)\Sigma_{i=1}^{90} Y_i$ [i.e., p_x (p_y) is the proportion of the segments that have potential for erosion under higher (lower) lake level]. The difference between the proportions of areas (segments) that have potential for erosion under two lake levels is estimated by $d = p_x - p_y$. We wanted to test if d were significantly greater than zero. If $d>0$, then the proportion of segments with potential for erosion would be larger under the higher lake level.

Because random variables X_i and Y_i are dependent (computed for the same shoreline segments), the proportions p_x and p_y are also dependent. Thus, traditional tests for difference of proportions do not apply. Instead, we used tests for dependent proportions or matched pairs (Agresti, 2002). The null hypothesis in all cases was Ho: $d=0$ and was tested against the alternative H_1: $d>0$. Rejection of the null hypothesis means that the higher lake level would yield a significantly larger number of areas subject to erosion.

Assumptions under which this methodology works include identical distribution of the X_i's (Y_i's). We think of the shoreline of the lake as an infinite or very large collection of short segments. The true probability of erosion p is the probability that a segment will erode for a given set of wave and geological conditions. We also can think of p as the proportion of the total shoreline that has potential for erosion under certain types of wave conditions. Then, p is the true proportion of (potentially) eroded segments. We think of the sample of 90 segments as a random sample from the much larger population of shoreline segments. X_i's (Y_i's) indicate erosion for each segment in the sample. The probability that each X_i (Y_i) is 1 (erosion occurs) is p, the same for each sample segment. Thus, we may think of X_i's (Y_i's) as identically distributed.

Results

Lake-Level Scenarios in Table 6-4 (5% Exceedence Values)

There were no significant differences in the proportions of (potentially) eroded shoreline segments for any lake levels and wave characteristics (5% significance level).

Lake-Level Scenarios in Table 6-5 (50% Exceedence Values)

Each of the positive-value comparisons in Table 6-5 were analyzed for each of the wave types in Table 6-3 to test if significantly more shoreline angles were impacted by the TSE for the increased lake level.

For the smallest types of waves (H = 0.5 m, t = 3 sec), there were no significant differences in the proportions of impacted shoreline angles for any lake levels (5% significance level).

For moderate-sized waves (H = 1 m, t = 4 sec), only one comparison yielded a significant difference in the proportions of impacted shoreline angles. Lake levels during the month

of June under the No Action vs. TROA comparison would be increased from 1898.467 m to 1898.476 m, a difference of 0.009 m. The sample proportion of nonimpacted shoreline angles under the No Action lake level (LL1) is 0.7444 but is 0.7 under TROA (LL2). The observed difference of 0.0444 has a p-value of 0.0455 and is therefore significant.

For the largest waves (H = 2 m, t = 5 sec), three of the comparisons yielded significant differences in the proportions of impacted shoreline angles. Table 6-6 outlines the specific comparisons that yielded the significant differences.

Table 6-6. Comparisons yielding significant differences in proportions of impacted shoreline angles under two lake levels. Lake levels are in meters.

Comparison	Month	LL1	LL2	Lake-level difference	Proportion non impacted for LL1	Proportion non impacted for LL2	Difference	P-value
Current vs. TROA	OCT	1898.022	1898.061	0.040	0.9556	0.9111	0.0444	0.0455
No Action vs. TROA	OCT	1898.010	1898.061	0.052	0.9556	0.9111	0.0444	0.0455
No Action vs. TROA	FEB	1898.089	1898.132	0.043	0.9000	0.8444	0.0556	0.0253

Our next step was to determine how much lake level would need to be increased to produce a significantly larger proportion of impacted shoreline angles for each of the positive value comparisons listed in Tables 6-5 and 6-6. For this analysis, we started with the lower lake level (LL1) and increased it by 0.001 m increments until the proportion of nonimpacted shoreline angles under the higher lake level (LL2) was significantly greater than under the starting lake level. We chose a significance level of 5%. Results of this analysis are shown in Table 6-7.

The magnitude of lake level increase required to cause a significant increase in the number of impacted shoreline sites ranged from several millimeters up to about thirty centimeters (Table 6-7). In general, the largest increases are associated with the smallest wave types (H = 0.5 m, t = 3 sec), but the trends are not very well defined.

Table 6-7. Results from the analysis to determine magnitude of lake level changes necessary to significantly increase shorezone erosion under different wave conditions and starting lake levels. The columns for this table are as follows: h=wave height, t=wave period, LL1=lake level 1 (starting lake level), LL2=lake level 2=first lake level higher than LL1 with significantly larger proportion of nonimpacted shoreline angles, p1p=proportion of nonimpacted shoreline angles under LL1, pp1=proportion of nonimpacted shoreline angles under LL2 (should be smaller than p1p), d=difference=p1p-pp1, L=lower end of the 95% CI for d, U=upper end of the 95% CI for d, p.value1=p-value for testing hypotheses: H_0: d=0 versus H_A: d>0. All values of p-value1 are less than 5% by design.

h	t	LL1	LL2	p1p	pp1	d	L	U	p.value1
0.5	3	1898.452	1898.503	0.8889	0.8556	0.0333	-0.0038	0.0704	0.0416
0.5	3	1898.47	1898.503	0.8889	0.8556	0.0333	-0.0038	0.0704	0.0416
0.5	3	1898.467	1898.503	0.8889	0.8556	0.0333	-0.0038	0.0704	0.0416
0.5	3	1898.516	1898.551	0.8333	0.8	0.0333	-0.0038	0.0704	0.0416
1	4	1898.452	1898.467	0.7778	0.7444	0.0333	-0.0038	0.0704	0.0416
1	4	1898.47	1898.475	0.7333	0.7	0.0333	-0.0038	0.0704	0.0416
1	4	1898.467	1898.474	0.7444	0.7111	0.0333	-0.0038	0.0704	0.0416
1	4	1898.516	1898.54	0.6667	0.6333	0.0333	-0.0038	0.0704	0.0416
2	5	1898.47	1898.492	0.5444	0.5111	0.0333	-0.0038	0.0704	0.0416
2	5	1898.467	1898.492	0.5444	0.5111	0.0333	-0.0038	0.0704	0.0416
2	5	1898.516	1898.54	0.4778	0.4444	0.0333	-0.0038	0.0704	0.0416
0.5	3	1898.022	1898.288	1	0.9667	0.0333	-0.0038	0.0704	0.0416
0.5	3	1898.01	1898.288	1	0.9667	0.0333	-0.0038	0.0704	0.0416
0.5	3	1898	1898.288	1	0.9667	0.0333	-0.0038	0.0704	0.0416
0.5	3	1898.107	1898.288	1	0.9667	0.0333	-0.0038	0.0704	0.0416
0.5	3	1898.11	1898.288	1	0.9667	0.0333	-0.0038	0.0704	0.0416
0.5	3	1898.122	1898.288	1	0.9667	0.0333	-0.0038	0.0704	0.0416
0.5	3	1898.144	1898.299	0.9889	0.9556	0.0333	-0.0038	0.0704	0.0416
0.5	3	1898.342	1898.406	0.9556	0.9222	0.0333	-0.0038	0.0704	0.0416
0.5	3	1898.18	1898.299	0.9889	0.9556	0.0333	-0.0038	0.0704	0.0416
0.5	3	1898.01	1898.288	1	0.9667	0.0333	-0.0038	0.0704	0.0416
0.5	3	1897.994	1898.288	1	0.9667	0.0333	-0.0038	0.0704	0.0416
0.5	3	1897.985	1898.288	1	0.9667	0.0333	-0.0038	0.0704	0.0416
0.5	3	1898.077	1898.288	1	0.9667	0.0333	-0.0038	0.0704	0.0416
0.5	3	1898.089	1898.288	1	0.9667	0.0333	-0.0038	0.0704	0.0416
0.5	3	1898.116	1898.288	1	0.9667	0.0333	-0.0038	0.0704	0.0416
0.5	3	1898.135	1898.299	0.9889	0.9556	0.0333	-0.0038	0.0704	0.0416
0.5	3	1898.339	1898.406	0.9556	0.9222	0.0333	-0.0038	0.0704	0.0416
0.5	3	1898.467	1898.503	0.8889	0.8556	0.0333	-0.0038	0.0704	0.0416
0.5	3	1898.409	1898.449	0.9222	0.8889	0.0333	-0.0038	0.0704	0.0416
0.5	3	1898.299	1898.406	0.9556	0.9222	0.0333	-0.0038	0.0704	0.0416
0.5	3	1898.171	1898.299	0.9889	0.9556	0.0333	-0.0038	0.0704	0.0416
1	4	1898.022	1898.195	0.9889	0.9556	0.0333	-0.0038	0.0704	0.0416
1	4	1898.01	1898.195	0.9889	0.9556	0.0333	-0.0038	0.0704	0.0416
1	4	1898	1898.195	0.9889	0.9556	0.0333	-0.0038	0.0704	0.0416
1	4	1898.107	1898.195	0.9889	0.9556	0.0333	-0.0038	0.0704	0.0416

Table 6-7 (cont.)

1	4	1898.11	1898.195	0.9889	0.9556	0.0333	-0.0038	0.0704	0.0416
1	4	1898.122	1898.212	0.9778	0.9444	0.0333	-0.0038	0.0704	0.0416
1	4	1898.144	1898.212	0.9778	0.9444	0.0333	-0.0038	0.0704	0.0416
1	4	1898.342	1898.385	0.8889	0.8444	0.0444	0.0019	0.087	0.0228
1	4	1898.18	1898.212	0.9778	0.9444	0.0333	-0.0038	0.0704	0.0416
1	4	1898.01	1898.195	0.9889	0.9556	0.0333	-0.0038	0.0704	0.0416
1	4	1897.994	1898.195	0.9889	0.9556	0.0333	-0.0038	0.0704	0.0416
1	4	1897.985	1898.195	0.9889	0.9556	0.0333	-0.0038	0.0704	0.0416
1	4	1898.077	1898.195	0.9889	0.9556	0.0333	-0.0038	0.0704	0.0416
1	4	1898.089	1898.195	0.9889	0.9556	0.0333	-0.0038	0.0704	0.0416
1	4	1898.116	1898.195	0.9889	0.9556	0.0333	-0.0038	0.0704	0.0416
1	4	1898.135	1898.212	0.9778	0.9444	0.0333	-0.0038	0.0704	0.0416
1	4	1898.339	1898.385	0.8889	0.8444	0.0444	0.0019	0.087	0.0228
1	4	1898.467	1898.474	0.7444	0.7111	0.0333	-0.0038	0.0704	0.0416
1	4	1898.409	1898.449	0.8222	0.7889	0.0333	-0.0038	0.0704	0.0416
1	4	1898.299	1898.377	0.9	0.8667	0.0333	-0.0038	0.0704	0.0416
1	4	1898.171	1898.212	0.9778	0.9444	0.0333	-0.0038	0.0704	0.0416
2	5	1898.022	1898.061	0.9556	0.9111	0.0444	0.0019	0.087	0.0228
2	5	1898.01	1898.061	0.9556	0.9111	0.0444	0.0019	0.087	0.0228
2	5	1898	1898.061	0.9556	0.9111	0.0444	0.0019	0.087	0.0228
2	5	1898.107	1898.153	0.8667	0.8333	0.0333	-0.0038	0.0704	0.0416
2	5	1898.11	1898.193	0.8556	0.8222	0.0333	-0.0038	0.0704	0.0416
2	5	1898.122	1898.2	0.8444	0.8111	0.0333	-0.0038	0.0704	0.0416
2	5	1898.144	1898.2	0.8444	0.8111	0.0333	-0.0038	0.0704	0.0416
2	5	1898.342	1898.39	0.6667	0.6333	0.0333	-0.0038	0.0704	0.0416
2	5	1898.18	1898.212	0.8333	0.8	0.0333	-0.0038	0.0704	0.0416
2	5	1898.01	1898.061	0.9556	0.9111	0.0444	0.0019	0.087	0.0228
2	5	1897.994	1898.061	0.9556	0.9111	0.0444	0.0019	0.087	0.0228
2	5	1897.985	1898.061	0.9556	0.9111	0.0444	0.0019	0.087	0.0228
2	5	1898.077	1898.107	0.9	0.8667	0.0333	-0.0038	0.0704	0.0416
2	5	1898.089	1898.107	0.9	0.8667	0.0333	-0.0038	0.0704	0.0416
2	5	1898.116	1898.193	0.8556	0.8222	0.0333	-0.0038	0.0704	0.0416
2	5	1898.135	1898.2	0.8444	0.8111	0.0333	-0.0038	0.0704	0.0416
2	5	1898.339	1898.39	0.6667	0.6333	0.0333	-0.0038	0.0704	0.0416
2	5	1898.467	1898.492	0.5444	0.5111	0.0333	-0.0038	0.0704	0.0416
2	5	1898.409	1898.431	0.6222	0.5889	0.0333	-0.0038	0.0704	0.0416
2	5	1898.299	1898.373	0.6889	0.6556	0.0333	-0.0038	0.0704	0.0416
2	5	1898.171	1898.212	0.8333	0.8	0.0333	-0.0038	0.0704	0.0416

Discussion and Conclusions

Lake Levels and Erosion Potential

In the above analyses, our goal was to determine whether or not different lake-level management schemes for Lake Tahoe would significantly affect shorezone erosion. In particular, would implementation of TROA significantly increase shorezone erosion? Our

approach combined field measurements of the elevations of wave-formed geomorphic features (shoreline angles and beach ridges) (Table 6-1), analytical modeling of the wave run up process (TSE), and a statistical procedure to test for significance. In this approach, we assumed that further shorezone erosion would not occur if swash from waves did not reach the shoreline angle or the crest of a beach ridge. The converse, however, is not necessarily true. That is, if swash from waves does reach the shoreline angle or beach ridge crest, then the potential exists for further erosion, but this is not a certainty. Whether or not erosion actually occurs at a site will be dependent on a number of factors including the frequency, magnitude, and direction of wind events when water levels are high (which controls the amount of wave energy impacting a particular site) and the material properties of the shorezone.

For 5% exceedence values (wet conditions), there is no significant increase in erosion potential for any of the lake-level scenario comparisons (Table 6-4) under the three different wave types (Table 6-3). This means that when lake levels are at their highest, implementing TROA will not affect shorezone erosion at Lake Tahoe.

For 50% exceedence values (moderately wet conditions), three discrete lake-level comparisons produced significant differences in proportions of impacted shoreline angles under both lake level scenarios (Table 6-6). In each comparison, TROA levels would be higher by about 4 to 5 cm. Under TROA levels, however, we emphasize that from 84 to 91% of the measured shoreline angles and beach ridges would *not* be impacted. Under Current or No Action lake levels, from 90 to 96% of the sites would not be impacted. There is certainly a statistical difference in the number of sites impacted under the three comparisons in Table 6-6 (5% significance level), but how these statistical differences translate into real differences in shorezone erosion potential is not entirely clear. We suspect the impact to be minimal, however. Therefore, implementing TROA should have minor to no effect on shorezone erosion at Lake Tahoe.

Using the Appropriate Statistical Technique

The implications of incorrectly using the familiar method of comparing independent proportions can be alarming. The difference between the two methods is mainly manifested in different variances of the sample difference of proportions d [i.e., different Var(d)]. Suppose first that the two sample proportions are positively correlated (as they are in most problems). In our approach, this means that if a given segment has a high probability of erosion under one lake level, it also will have a high probability of erosion under another lake level. This is true because the probability of erosion depends on natural, environmental characteristics of the shoreline, which do not change with respect to lake level. Assuming that the correlation between sample proportions of nonimpacted shoreline angles is positive, Var(d) computed for dependent samples is smaller than Var(d) computed for independent samples. Thus, the paired design (in the case of positively correlated proportions) improves the precision of statistical inference. In fact, the p-value from independent sample analysis will be larger than for dependent sample analysis.

For example, consider the case of H=1, T=4, LL1= 1898.342, and LL2=1898.385. The sample proportion of nonimpacted segments under LL1 is 0.8889, and the sample proportion of nonimpacted segments under LL2 is 0.8444 giving a sample difference of d=0.0444. Dependent proportions analysis yields a p-value of 0.02, but incorrect independent sample analysis yields a p-value of 0.2553. Thus, on a 5% significance level, we get two contradictory conclusions. From the correct dependent samples analysis, we conclude that the difference in proportions of non-eroded segments is significant under the two lake-level scenarios. We get an insignificant result for the incorrect independent samples analysis, however. In the long run, assuming independent proportions will lead to fewer significant results. That is, we will classify the difference in lake level as insignificant when in fact it is significant.

In the second case, when sample proportions are negatively correlated, Var(d) computed for dependent samples is larger than Var(d) computed for independent samples. Then, the p-value from the independent sample analysis will be smaller than for the dependent sample analysis. As a result, we would reject the null hypothesis too often.

Comments on Earlier Modeling Efforts

In the two earlier models we developed, we studied the influence of environmental and geological factors on erosion potential (Chapter 5). One model used the amount of erosion and the other the probability of erosion as the response variables. The first was linear while the second was a logistic regression model. Both aimed at explaining the erosive climate of the Lake Tahoe shorezone. Lake level never entered the models as an explanatory variable, because it is the same for all segments around the lake. As such, it would be an inconsequential explanatory variable. In order for lake level to be a useful explanatory variable, we would need to have erosion measurements under two lake levels, which we do not have. Additionally, it is unclear whether such measurements could be gathered at all, given that the range of lake-level fluctuations from year to year is greater than the variation imposed under TROA. Our approach of computing the difference in proportions of potentially eroded areas under two lake-level scenarios captures the need for estimation of erosion potential without requiring direct observations of erosion occurring under two lake levels.

Acknowledgements

The authors would like to thank the U.S. Bureau of Reclamation (USBR), the Tahoe Regional Planning Agency (TRPA), the Center for Watersheds and Environmental Sustainability (CWES) at the Desert Research Institute, and the Nevada NSF-EPSCoR RING TRUE program for funding these studies. The U.S. Geological Survey generously provided SHOALS bathymetric data and the Lahontan Regional Water Quality Control Board provided access to shoreline erosion pin maps. The U.S. Forest Service provided access to some of the historic aerial photographs. The authors also would like to thank Brad Lyles for his technical expertise in installing the wave monitoring equipment and trouble shooting when necessary. The generosity of John Klacking, Don Davis, Phil Caterino, and the Thunderbird Lodge Preservation Society is greatly appreciated. By allowing the use of their private piers or facilities, they substantially contributed to this project. The help of Jamie McCaughey, Rick Walker, Gregg Lamorey, Eric Martin, Tom Sawyer, Sheryl Fontaine, and Annette Risley in completing various phases of the project is also appreciated. Roger Kreidberg provided detailed and helpful reviews of this manuscript.

References

Adams, K. D., and Minor, T. B., 2002, Historic shoreline change at Lake Tahoe from 1938 to 1998: implications for sediment and nutrient delivery: Journal of Coastal Research, v. 18, no. 4, p. 637-651.

Adams, K. D., and Wesnousky, S. G., 1998, Shoreline processes and the age of the Lake Lahontan highstand in the Jessup embayment, Nevada: Geological Society of America Bulletin, v. 110, no. 10, p. 1318-1332.

Agresti, A., 2002, Categorical Data Analysis: New Jersey, Wiley.

Akaike, H., 1973, Information Theory and an Extension of the Maximum Likelihood Principle, *in* Second International Symposium on Information Theory, Budapest, p. 267-281.

Birkeland, P. W., 1964, Pleistocene glaciation of the northern Sierra Nevada, north of Lake Tahoe, California: Journal of Geology, v. 72, p. 810-825.

Bruun, P., 1988, Rationalities of coastal protection: An example from Hilton Head Island, South Carolina: Journal of Coastal Research, v. 4, no. 1, p. 129-138.

Budlong, G. M., 1971, Processes of beach change at Tahoe Keys, California: An example of man and nature as geomorphological agents [Masters thesis]: Chico State College, 105 p.

Burnett, J. L., 1971, Geology of the Lake Tahoe Basin: California Geology, v. 7, p. 119-127.

Bursik, M. I., and Gillespie, A. R., 1993, Late Pleistocene glaciation of the Mono Basin, Califfornia: Quaternary Research, v. 39, p. 24-35.

Carter, R. W. G., 1988, Coastal Environments: San Diego, CA, Academic Press, 617 p.

CERC, 1984, Shore Protection Manual: Washington, D.C., U.S. Army Corps of Engineers, U.S. Govt. Printing Office, 607 p.

Davis, J. O., Elston, R., and Townsend, G., 1976, Coastal geomorphology of the south shore of Lake Tahoe; suggestion of an Altithermal lowstand, *in* Elston, R. G., ed., Holocene environmental change in the Great Basin, Nevada Archeological Survey Research Papers No. 6, p. 40-65.

Dolan, R., Hayden, B. P., May, P., and May, S., 1980, The reliability of shoreline change measurements from aerial photographs: Shore and Beach, v. 48, no. 4, p. 22-29.

Earle, M. D., McGehee, D., and Tubman, M., 1995, Field wave gaging program, wave data analysis standard: U.S. Army Corps of Engineers Instruction Report CERC-95-1.

Edelman, M. C., 1984, Petrographic and textural evidence for backshore and cliff derivation of littoral sand in Lake Tahoe [Masters thesis]: University of Southern California, 122 p.

Engstrom, W. N., 1978, The physical stability of the Lake Tahoe shoreline: Shore and Beach, v. 46, no. 4, p. 9-13.

Gardner, J. V., Dartnell, P., Mayer, L. A., and Clarke, J. E. H., 1999, Bathymetry and selected perspective views of Lake Tahoe, California and Nevada: U.S. Geological Survey, Water-Resources Investigation Report 99-4043, p. 2 plates.

Gardner, J. V., Mayer, L. A., and Hughs-Clarke, J. E., 2000, Morphology and processes in Lake Tahoe (California-Nevada): Geological Society of America Bulletin, v. 112, no. 5, p. 736-746.
Gaynor, J. M., 1984, Sources and transport of sand in the littoral zone of Lake Tahoe, California and Nevada: Fourier grain-shape analysis [Masters thesis]: University of Southern California, 112 p.
Griggs, G. B., and Fulton-Bennett, K., 1988, Rip rap revetments and seawalls and their effectiveness along the central California coast: Shore and Beach, v. 56, no. 2, p. 3-11.
Griggs, G. B., and Tait, J. F., 1988, The effects of coastal protection structures on beaches along northern Monterey Bay, California: Journal of Coastal Research, no. SI 4, p. 93-111.
Hands, E. B., 1983, The Great Lakes as a test model for profile responses to sea level change, *in* Komar, P. D., ed., CRC Handbook of Coastal Processes and Erosion: Boca Raton, FL, CRC Press, Inc., p. 167-189.
Hosmer, D. W., and Lemeshow, S., 1989, Applied Logistic Regression: New York, John Wiley and Sons, Inc., 307 p.
James, L. A., Harbor, J., Fabel, D., Dahms, D., and Elmore, D., 2002, Late Pleistocene glaciations in the northwestern Sierra Nevada, California: Quaternary Research, v. 57, p. 409-419.
Kent, G., Babcock, J., and Harding, A., 2000, The application of CHIRP technology to study Holocene tectonics, lake-level changes and sedimentation rates within the Lake Tahoe Basin: Geological Society of America Abstracts with Programs, v. 32, no. 7, p. A-244.
Kilroy, K., C., Lawrence, S. J., Lico, M. S., Bevans, H. E., and Watkins, S. A., 1997, Water-quality assessment of the Las Vegas Valley area and the Carson and Truckee river basins, Nevada and California-Nutrients, pesticides, and suspended sediment, October 1969-April 1990: U.S. Geological Survey Water Resources Investigations Report 97-4106, p. 144.
Komar, P. D., 1998, Beach processes and sedimentation: Upper Saddle River, NJ, Prentice Hall, 543 p.
Komar, P. D., and McDougal, W. G., 1988, Coastal erosion and engineering structures: The Oregon experience: Journal of Coastal Research, no. Special Issue 4, p. 77-92.
Kraus, N. C., 1988, The effects of seawalls on the beach: An extended literature review: Journal of Coastal Research, no. Special Issue 4, p. 1-28.
Kraus, N. C., and McDougal, W. G., 1996, The effects of seawalls on the beach: Part 1, an updated literature review: Journal of Coastal Research, v. 12, no. 3, p. 691-701.
LeConte, J., 1884, Physical studies of Lake Tahoe: The Overland Monthly, v. 3, no. 1, p. 41-46.
Lindstrom, S., 1990, Submerged tree stumps as indicators of mid-Holocene aridity in the Lake Tahoe region: Journal of California and Great Basin Anthropology, v. 12, no. 2, p. 146-157.
Lorang, M. S., 1992, Lake level regulation, shoreline erosion and shore protection: Flathead Lake, Montana [M.S. thesis]: Oregon State University, 148 p.

McCullagh, P., and Nelder, J. A., 1989, Generalized Linear Models: London, Chapman and Hall, 511 p.
McDougal, W. G., Sturtevant, M. A., and Komar, P. D., 1987, Laboratory and field investigations of the impact of shoreline stabilization structures on adjacent properties, *in* Coastal Sediments '87, p. 961-973.
McGarr, A., and Vorhis, R. C., 1968, Seismic seiches from the March 1964 Alaska earthquake: U.S. Geological Survey Professional Paper 544-E, p. 1-43.
Moore, L. J., 2000, Shoreline mapping techniques: Journal of Coastal Research, v. 16, no. 1, p. 111-124.
Moory, R. L., and Osborne, R. H., 1984, Structure and dynamics of the nearshore sedimentologic system in Lake Tahoe and the effects of man-made structures, *in* Lintz, J., ed., Western Geological Excursions: Reno, NV, Department of Geological Sciences, Mackay School of Mines, University of Nevada Reno, p. 96-105.
Morrison, R. B., 1991, Quaternary stratigraphic, hydrologic, and climatic history of the Great Basin, with emphasis on Lake Lahontan, Bonneville, and Tecopa, *in* Morrison, R. B., ed., Quaternary nonglacial geology; conterminous U.S.: Boulder, CO, United States, Geological Society of America, p. 283-320.
Mulberg, E. J., 1984, Lake Tahoe seasonal wind study: California Air Resources Board.
Murphy, D. D., and Knopp, C. M., 2000, Lake Tahoe watershed assessment, U.S. Department of Agriculture, Forest Service, Pacific Southwest Research Station, General Technical Report PSW-GTR-1751, p. 735.
Nolan, K. M., and Hill, B. R., 1991, Suspended-sediment budgets for four drainage basins tributary to Lake Tahoe, California and Nevada, 1984-87: U.S. Geological Survey Water-Resources Investigations Report 91-4054, p. 40.
Orme, A. R., 1971, The Shore-zone system for Lake Tahoe: Tahoe Regional Planning Agency, Project No. NEV P-30.
-, 1972, Toward a shore-zone plan for Lake Tahoe: Tahoe Regional Planning Agency, p. 52.
Osborne, R. H., Edelman, M. C., Gaynor, J. M., and Waldron, J. M., 1985, Sedimentology of the littoral zone in Lake Tahoe, California-Nevada, Planning and Environmental Coordination, California State Lands Commission, 88 p.
Phillips, F. M., Zreda, M. G., Smith, S. S., Elmore, D., Kubik, P. W., and Sharma, P., 1990, Cosmogenic Chlorine-36 chronology for glacial deposits at Bloody Canyon, eastern Sierra Nevada: Science, v. 248, p. 1529-1532.
Pilkey, O. H., and Wright, H. L., III, 1988, Seawalls versus beaches: Journal of Coastal Research, no. SI-4, p. 41-64.
Plant, N. G., and Griggs, G. B., 1992, Interactions between nearshore processes and beach morphology near a seawall: Journal of Coastal Research, v. 8, no. 1, p. 183-200.
Reuter, J. E., and Miller, W. W., 2000, Aquatic resources, water quality, and limnology of Lake Tahoe and its upland watershed, *in* Murphy, D. D., and Knopp, C. M., eds., Lake Tahoe Watershed Assessment: Albany, CA, U.S. Forest Service Pacific Southwest Research Station, p. 213-399.

Rodgers, J. H., 1974, Soil survey of the Tahoe Basin area, California and Nevada, United States Department of Agriculture, Soil Conservation Service, 84 p.
Rowe, T. G., and Allander, K. K., 2000, Surface- and ground-water characteristics in the Upper Truckee River and Trout Creek watersheds, South Lake Tahoe, California and Nevada, July-December 1996: U.S. Geological Survey Water-Resources Investigations Report 00-4001, p. 39.
T. R. P. A. Staff, 1971, Climate and air quality of the Lake Tahoe region, a guide to planning.
-, 1999, Lake Tahoe shorezone ordinances amendments, draft environmental impact statement: Tahoe Regional Planning Agency.
Taylor, J. R., 1997, An introduction to error analysis, the study of uncertainties in physical measurements: Sausalito, CA, University Science Books, 327 p.
Thieler, E. R., and Danforth, W. W., 1994, Historical shoreline mapping (I): improving techniques and reducing positioning errors: Journal of Coastal Research, v. 10, no. 3, p. 549-563.
Waldron, J. M., 1982, Sand transport and petrofacies of the Lake Tahoe littoral zone [Masters thesis]: University of Southern California, 83 p.
Weggel, J. R., 1988, Seawalls: The need for research, dimensional considerations and a suggested classification: Journal of Coastal Research, no. Special Issue 4, p. 29-39.
Wood, W. L., 1988, Effects of seawalls on profile adjustment along Great Lakes coastlines: Journal of Coastal Research, no. Special Issue 4, p. 135-146.